Regulation of the Cyclin-Dependent Kinase Inhibitor p21 by TBX3

Shannagh Hare

Supervised by Associate Professor Sharon Prince

Thesis presented for the degree of

Master of Science in Medicine

Cell Biology

Department of Human Biology

Faculty of Health Sciences

University of Cape Town

November 2013

Declaration

I, Shannagh Hare, hereby declare that the work on which this thesis is based is my original work and that neither the whole work nor any part of it has been, is being, or is to be submitted for another degree in this or any other University. I empower the University to reproduce for the purpose of research either the whole or any portion of the contents in any manner whatsoever.

November 2013

Acknowledgements

I am grateful to the following people for all of their support throughout the duration of this dissertation:

Associate Professor Sharon Prince for her continual support, guidance, knowledge and encouragement. I thank you for your enthusiasm for science and for being a wonderful mentor.

Aretha Cooper for all of her help in the laboratory. You are a wonderful and patient teacher and I value the friendship that we have developed over the past three years.

Many thanks to all the ***T-box lab members*** for their support and advice. You all contributed to a very pleasant working environment. To all members of the ***Kidson and Redox lab***, it was wonderful to work with all of you too.

My parents ***Julian*** **and** ***Sandy,*** as well as my sister ***Aimee***, whose continued love, guidance and support are deeply valued. To my partner ***Stuart*** for his endless encouragement and love.

I am particularly grateful to my ***friends*** for their support and understanding throughout the last two years. A special thanks to ***Hayley Tomes*** for her enthusiasm for all things Science and for always taking an interest in my project.

This work was kindly supported by the National Research Fund (NRF), Stella and Paul Loewenstein Trust and Cancer Research Initiative of South Africa (CARISA). I hereby acknowledge, with thanks, the financial help that I received from the Struwig-Germeshuysen-Kankernavorsingtrust (SGKN) (bursary) for the completion of my studies. Opinions that are expressed in this thesis and conclusions drawn are entirely those of the researcher and do not necessarily reflect those of the SGKN-Trust.

Table of Contents

List of Figures and Tables

Figures

Appendix Figures

Tables

Abstract

TBX3, a member of the T-box family of transcription factors, is essential in development and has emerged as an important player in the oncogenic process. It is vital for the development of the heart, breasts, limbs, teeth and genitalia and TBX3 mutations lead to Ulnar-Mammary Syndrome, which is characterised by malformations of these organs and body structures. TBX3 is overexpressed in several cancers and has been implicated in a number of oncogenic processes ranging from the bypass of senescence to the inhibition of apoptosis and more recently TBX3 has been shown to contribute directly to tumour formation, migration and invasion of melanoma and breast cancer cells. However, little is known about the molecular basis for its role in development and oncogenesis because there is a paucity of information regarding its target genes. Of interest to the current study, preliminary evidence suggest that TBX3 may repress the cyclin-dependent kinase inhibitor $p21^{WAF1}$, which has a role in a myriad of processes including cell cycle arrest, senescence, apoptosis, differentiation and DNA replication and repair. The current study therefore aimed to explore this possibility and to reveal a mechanism by which TBX3 regulates $p21^{WAF1}$. Results show, using luciferase reporter gene assays, that TBX3 is a potent transcriptional repressor of the $p21^{WAF1}$ promoter and that this repression is due to a direct interaction between TBX3 and the $p21^{WAF1}$ promoter via the TBX3 DNA-binding domain. This study also provides evidence that the ability of TBX3 to repress $p21^{WAF1}$ may require the TBX3 N-terminal repression domain. In addition, the site through which TBX3 acts to repress $p21^{WAF1}$ was identified close to the initiator of the $p21^{WAF1}$ promoter and TBX3 is shown to bind this site in vitro and in vivo. Furthermore, this study provides evidence that a serine proline motif (S190) located within the DNA-binding domain of TBX3, may play an important role in regulating the ability of TBX3 to transcriptionally repress $p21^{WAF1}$ by inhibiting binding. Lastly, the repression of $p21^{WAF1}$ by TBX3 is also shown to be biologically significant in TBX3 overexpression and knock down cell culture models. Results from this study provide a detailed mechanism of how TBX3 directly transcriptionally represses $p21^{WAF1}$ which adds to our understanding of how TBX3 may contribute to oncogenesis.

1. Introduction

The deregulation of developmental transcription factors has been shown to play an important role in oncogenesis (Darnell 2002; Matheu et al. 2012). The T-box family of transcription factors provide a good example of this because while they are well-known for the role that they play in embryonic development, their deregulation has been linked to the formation and progression of several cancers. The T-box factor TBX3 is necessary for the development of the limbs, heart, breasts, teeth and genitalia and mutations in this gene lead to the developmental disorder Ulnar-Mammary syndrome (Bamshad et al. 1997). There is also accumulating evidence to suggest that overexpression of TBX3 may lead to the formation of a number of different cancer types (Fan et al. 2004; Yarosh et al. 2008; Lomnytska et al. 2006; Renard et al. 2007). Transcription factors, like TBX3, are highly desirable candidates for therapeutic manipulation (Libermann & Zerbini 2006) and it is therefore important to explore the molecular mechanism(s) underpinning the role of TBX3 in cancer.

Despite the consequences of deregulated TBX3 expression, very little is known about its target genes and the mechanisms involved in its transcriptional activity. Preliminary evidence has suggested that TBX3 represses the cyclin-dependent kinase inhibitor $p21^{WAF1}$, but a full characterisation has not been reported and therefore forms the main objective of this dissertation. This introduction will highlight key areas of research that are relevant to the aims addressed in this project.

1.1. The T-box transcription factor family

Members of the T-box transcription factor family are defined by a conserved DNA-binding domain, the T-box (Kispert & Herrmann 1993; Pflugfelder et al. 1992), which allows specific binding to target gene promoter regions (Kispert et al. 1995). T-box factors are highly conserved in evolution and are expressed across a vast range of species including fruit flies, fish, frogs, mice, chickens and humans (Wilson & Conlon 2002). The classical and crucial roles played by these factors in embryonic development has been well described (Showell et al. 2004) and haploinsufficiency of certain members of the T-box family is responsible for a number of human developmental syndromes (Klopocki et al. 2006; Merscher et al. 2001; Basson et al. 1997; Braybrook et al. 2001). T-box factors play important roles in regulating cell proliferation and differentiation, tissue organisation and organogenesis (Naiche et al. 2005) and it is therefore not surprising that they have been implicated in the fields of cancer, stem cell biology and regenerative medicine (Takashima & Suzuki 2013).

The first member of the T-box family was identified in 1927 by the Russian surgeon and scientist Nadine Dobrovoskaia-Zavadskaia (**Figure 1.1.A**). While studying the influence of modifications produced by X-rays on gene inheritance in mice, Dobrovoskaia-Zavadskaia observed that while mice homozygous for a specific gene died in utero, heterozygous mice did not undergo complete tail development and consequently had a short tail (Dobrovolskaia-Zadvadskaia, 1927). Interestingly different allelic forms of this gene were shown to create a gradient in severity of the short tail phenotype, illustrating for the first time that T-box proteins exhibit dosage sensitivity (Macmurray & Shin 1988) (**Figure 1.1.B**). Dobrovoskaia-Zavadskaia named the gene *Brachyury*, from the Greek *brakhus* meaning short and *oura* meaning tail. This gene has also come to be known by the name *T,* for tail. The *Brachyury* gene was first cloned in 1990 by Herrmann et al. (1990) and subsequently homologues were found in several other species including *Danio rerio* (Schulte-Merker et al. 1992), *Xenopus laevis* (Smith et al. 1991) and *Drosophila melanogaster* (Pflugfelder et al. 1992). Extensive studies aimed at functional and structural characterisation of Brachyury found that it is a transcription factor (Kispert et al. 1995) and that the amino (N)-terminus region contains a novel DNA-binding domain called the T-box (Kispert & Herrmann 1993). It was later shown that a number of genes in different organisms carried this highly conserved domain (**Figure 1.1.C**) (Smith 1999) which confirmed the existence of a novel gene family called the T-box family. The origins of this gene family have also been analysed and traced back to a common ancestor which through gene duplication events further diverged along individual lineages (**Figure 1.1D**). Indeed, phylogenetic analysis show that the T-box gene family can be subdivided into 5 subfamilies namely TBX1, TBX2, TBX6, T and TBR1 (Agulnik et al. 1996). This has allowed different T-box family members to acquire unique functions and expression patterns, while retaining a conserved T-box domain (Agulnik et al. 1996; Minguillon & Logan 2003).

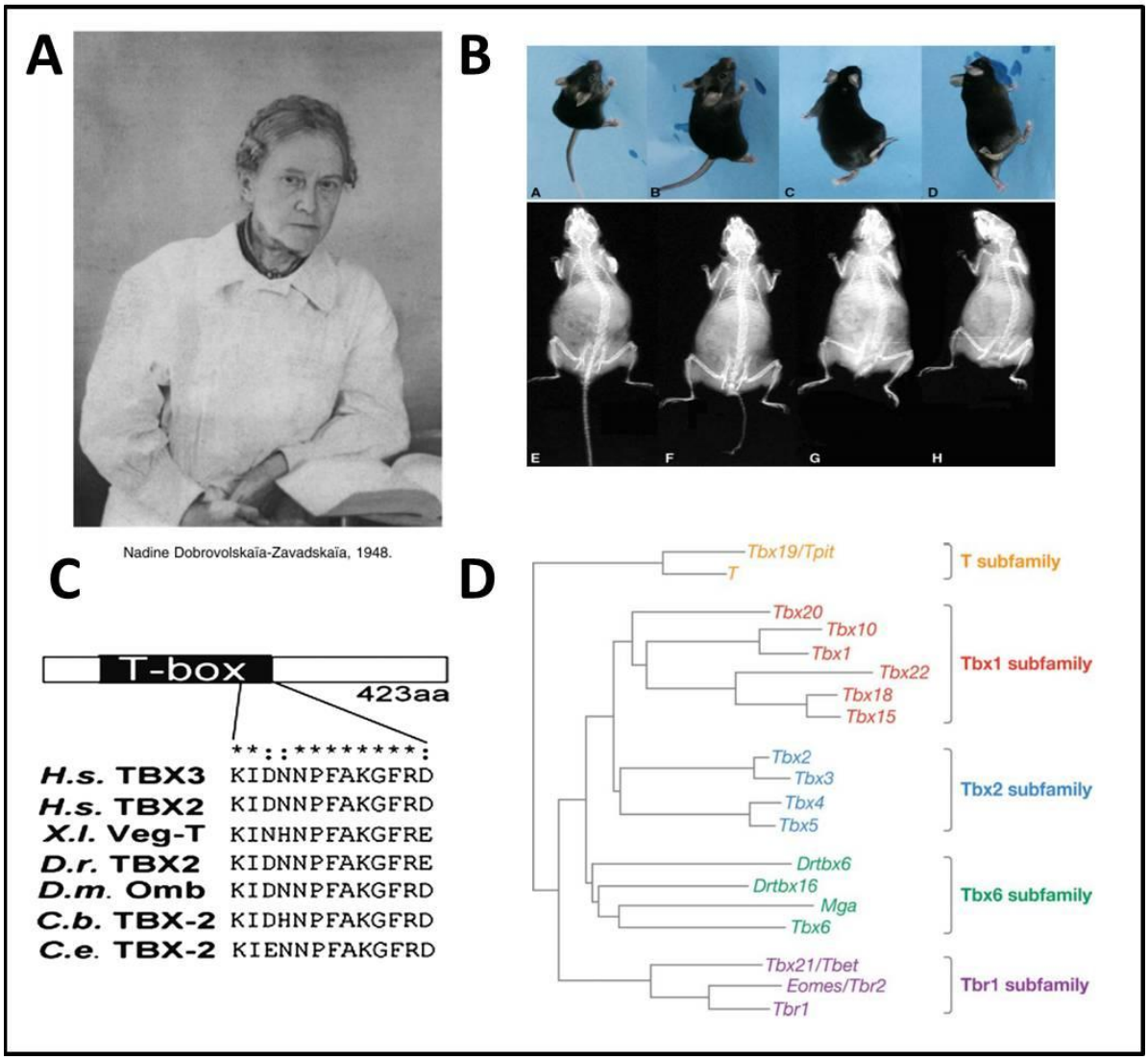

Figure 1.1. **The T-box factor family.**

A. Nadine Dobrovoskaia-Zavadskaia, 1948. Image sourced from Korzh & Grunwald (2001). **B**. The phenotypes of the short-tailed mouse. a, e Control mice. b, f Middle-length-tailed mouse. c, g Short-tailed mouse. d, h Mouse with tail bud. Image sourced from Wu et al. (2010). **C**. Conservation of the T-box across a number of different T-box factors and species. Image sourced from Singhvi et al. (2008). **D**. Phylogenetic tree of T-box genes. Image sourced from Naiche et al. (2005).

The T-box domain is unique as it is unusually large, consisting of approximately 200bp, and does not have any sequence similarities to any known transcription factor DNA-binding domain (Kispert & Herrmann 1993). Early studies using in vitro binding assays found the Brachyury protein to bind to the consensus palindromic sequence TTT(C/G)ACACCT AGGTGTGAAATT, as either a monomer or dimer. To date most T-box factors have been shown to bind in vitro as a monomer to the core sequence TCACACCT, also known as the T-element (Wilson & Conlon 2002). The T-element sequence has, however, been shown to be highly variable and degenerate in vivo (Lingbeek et al. 2002; Boogaard et al. 2012). To overcome this problem, Coll et al. (2002) suggested that the sequence 5'-xTxxCACxx-3' (where x = less conserved bases) should be used for the identification of T-box DNA-binding sites. In addition, Müller & Herrmann (1997) were able to show, using x-ray crystallography, that the Brachyury T-box domain interacts with both the major and minor groove of DNA. The other functional domains of the Brachyury protein were characterised using chloramphenicol acetyltransferase (CAT) reporter gene assays and alternating transactivation and repression domains were identified in the carboxy (C)-terminus of the protein, as well as a region thought to encode a nuclear localisation signal (NLS) (Kispert et al. 1995). Due to the high degree of homology within the T-box family much of this structural characterisation has been shown to be relevant to other T-box factors (Carlson et al. 2001).

T-box factors can function as transcriptional activators and/or repressors. For example Brachyury, TBX1, TBX5, TBX6, TBX19 and TBX20 have been shown to function as transcriptional activators, (Ataliotis et al. 2005; Zaragoza et al. 2004; Gonzalez et al. 2013; Maira et al. 2003; Lingbeek et al. 2002; Stennard et al. 2005; Casey et al. 1998) whereas TBX2, TBX3, TBX15, TBX18 and TBX22 demonstrate repressor activity (Prince et al. 2004; Jacobs et al. 2000; Andreou et al. 2007; Carlson et al. 2001; Farin et al. 2013). In addition, there is evidence that Brachyury, TBX2, TBX3, TBX5, TBX20 , TBX24 and Mga (MAX gene associated) can both activate and repress their targets (Carreira et al. 1998; Casey et al. 1998; Sakabe et al. 2012; Prince et al. 2004; Lu et al. 2011; Carlson et al. 2001; Takeuchi et al. 1999; Zaragoza et al. 2004; Stennard et al. 2005; Singh et al. 2005; Kawamura et al. 2008; Hurlin et al. 1999).

While all T-box factors tested to date can recognise and bind the same consensus T-element in vitro, their ability to recognise different targets and either transcriptionally activate or repress them suggests that co-factor interaction may be involved. Indeed, a number of co-factors have been identified to interact with T-box factors during embryonic development. Within the pituitary gland, activation of pro-opiomelanocortin (POMC) by TBX19 requires the binding of the homeoprotein Pitx

to a nearby site on the promoter (Lamolet et al. 2001), while the co-factor NK2 homeobox 5 (NKX2.5) interacts with TBX2 and TBX5 during heart chamber formation and cardiomyocyte differentiation, respectively (Habets et al. 2002; Hiroi et al. 2001). In addition, Sox4 binds with TBX3 to the first intron of the heart-specific *Gja1/connexion 43* gene in vivo to modulate connexion 43 expression (Boogerd et al. 2011). Furthermore, Murakami et al. (2005) showed that TAZ and TBX5 interact together with histone acetyltransferase p300 and p300/CBP-associated factor, thereby causing histone acetylation of a number of TBX5 target genes involved in cardiac and limb development. Lastly, both the Smad and Groucho protein families have been shown to interact and regulate the transcriptional activity of a number of T-box factors (Singh et al. 2009; Messenger et al. 2005; Miller & Okkema 2011; Kawamura et al. 2008; Farin et al. 2013). Despite these numerous studies only one cancer related T-box co-factor has been identified. A recent study showed that TBX2 recruits and interacts with early growth response 1 (EGR1) to target and repress the N-myc down-regulated gene 1 (NDRG1) promoter in breast cancer cells (Redmond et al. 2010).

T-box factors themselves can act as co-factors for other transcription factors, demonstrating that they do not always regulate genes by direct binding. For instance, binding of Brachyury, Eomes and TBX6 to the Mixl homeodomain transcription factor inhibits the ability of Mixl to activate the goosecoid and platelet derived growth factor receptor alpha promoters (Pereira et al. 2011). In addition, an interaction between TBX5 and Gata4 suggests that TBX5 could be a co-factor for Gata4 in heart development (Garg et al. 2003). Indeed, a mutation in *Gata4* was shown to cause a disruption in this interaction which led to cardiac septal defects. Lastly, TBX3 was shown to interact with the histone demethylase Jmjd3 at the enhancer of the *Eomes* gene (Kartikasari et al. 2013).

1.2. Developmental syndromes associated with T-box factors

The critical role played by T-box factors throughout development has been well described and documented (Naiche et al. 2005; Chapman et al. 1996). However, since this is not the focus of the current dissertation, this review will be limited to a description of some of the T-box factors directly linked to human developmental syndromes. These syndromes emphasize the severe consequences resulting from deregulated expression of T-box factors and also give insight into the vast number of developmental processes that T-box factors are involved in. Mutations in *TBX1*, *TBX3* and *TBX5* lead to haploinsufficiency, or decreased levels of functional protein, which is responsible for DiGeorge Syndrome, Ulnar-Mammary Syndrome and Holt-Oram Syndrome, respectively.

DiGeorge syndrome arises from a deletion or translocation of the 22q11 locus to which the *TBX1* gene maps (Scambler 2000). In addition, a genetic screen of 10 patients with DiGeorge Syndrome also revealed the presence of missense mutations and one truncating mutation in the *TBX1* gene (Yagi et al. 2003). While the missense mutations cause haploinsufficiency of TBX1, the truncation resulted in the loss of the TBX1 NLS (Stoller & Epstein 2005). The key features of DiGeorge syndrome include heart abnormalities, hearing problems, parathyroid deficiency, hypocalcemia and cranio-facial and palatal defects (Merscher et al. 2001; Vitelli et al. 2003; Jerome & Papaioannou 2001). These abnormalities are consistent with the important roles that TBX1 plays in the development of structures such as the outflow tract and aorto-pulmonary septum of the heart (Xu et al. 2004), in the development of the cochlea and the vestibulum of the inner ear (Vitelli et al. 2003) as well as in the thymus (Zhang et al. 2006) and parathyroid gland (Grigorieva & Thakker 2011).

Patients with mutations, including nonsense and missense mutations, in *TBX5* present with Holt-Oram syndrome which is characterised by both heart and upper limb abnormalities (Basson et al. 1997). This underscores the critical role that TBX5[1] has in the formation and the patterning of the developing heart (Bruneau et al. 2001), as well as in the outgrowth of the forelimb and in limb identity determination (Rodriguez-Esteban et al. 1999). In addition, TBX5 is also expressed in the developing lung and trachea where it interacts with TBX4 and Fgf10 during lung growth and lobe branching (Arora et al. 2012). Using a Tbx5 mutant mouse model Bruneau et al. (2001) showed that homozygous mice died early in embryogenesis and displayed gross changes in heart chamber development, while heterozygote mice had enlarged hearts, atrial septal defects and abnormalities in their cardiac conduction system. Both mutants also displayed upper limb malformation.

The rare autosomal dominant disorder, Ulnar-Mammary syndrome (UMS) results from mutations in the *TBX3* gene and will be discussed later under section 1.4.2 dealing with TBX3 in development.

1.3. T-box factors and cancer

A growing list of studies have reported deregulated levels of T-box factors in a number of different cancer types and inappropriate T-box factor expression has been directly linked to oncogenesis. Indeed, a number of T-box factors have been shown to possess tumour promoting properties and more recently tumour suppressor functions have also been revealed for some T-box factors. These T-box factors include Brachyury, Eomes, TBX1, TBX2, TBX3, TBX4, TBX5 and T-bet (TBX21) (He et al. 2002; Yu et al. 2010; Trempus et al. 2011; Atreya et al. 2007; Reinert et al. 2011; Park et al. 2008; Fernando et al. 2010; Yang et al. 2009; McCune et al. 2010).

[1] The accepted convention will be used for human, TBX5, and when referring to both mouse and human, Tbx5/TBX5 will be used.

While Brachyury was the first T-box factor to be discovered and identified as a critical developmental factor, more recent evidence suggests that it may also have tumour promoting and tumour suppressor properties. In a study by Palena et al. (2007), Brachyury overexpression was observed in several cell lines derived from cancers of the oesophagus, lung, stomach, small intestine, kidney, bladder, uterus and testis. Importantly, Fernando et al. (2010) demonstrated that when Brachyury was knocked down in lung cancer cells it decreased their invasive potential in nude mice. A number of studies have also highlighted the importance of Brachyury in the process of epithelial to mesenchymal transition (EMT) (Fernando et al. 2010; Shimoda et al. 2012; Imajyo et al. 2012; Palena et al. 2007) which is important for tumour progression and metastasis (Thiery 2002). In these studies the overexpression of Brachyury led to an increase in the expression of mesenchymal markers such as vimentin, N-cadherin and fibronectin and a decrease in the epithelial markers E-cadherin and plakoglobin. In addition, Shimoda et al. (2012) showed that when Brachyury is silenced in adenoid cystic carcinoma cells their sphere-forming ability, EMT characteristics and tumourigenicity were reversed. Lastly, duplication of the *Brachyury* gene has been associated with the rare bone cancer, chordoma (Yang et al. 2009). While the above observations provide compelling evidence that Brachyury is a tumour promoting factor, Park et al. (2008) suggest that it may also have a tumour suppressor function in non-small cell lung cancer. They showed using methylation sensitive microarray analysis, that Brachyury is epigenetically silenced in these cancer cells as compared to a normal lung cell line. While silencing of Brachyury correlated with the development of non-small cell lung cancer, it is however not known whether this is a cause or consequence of the oncogenic process.

Eomes, a member of the TBR1 subfamily, has also been implicated as a tumour suppressor. Eomes plays a critical role in immunity and defence by activating effector CD8+ T cells (Pearce et al. 2003) and evidence that these T cells play an important role in colorectal cancer and anti-tumour immunity (Dalerba et al. 2003) prompted investigations into the potential role of Eomes in colorectal cancer. Indeed, an inverse relationship between Eomes expression and the presence of lymph node metastases in colorectal cancer was observed (Atreya et al. 2007). In situ hybridisation and RT-PCR confirmed that this relationship was unique, as a similar correlation was not observed with any other transcription factor associated with CD8+ T cells. Lastly, the mechanism through which Eomes reduces lymph node metastasis was shown to involve the activation of CD8+ T cells via perforin induction.

TBX1[2] has been shown to be down-regulated in mouse skin tumours and it was therefore implicated as a negative regulator of these tumours (Trempus et al. 2011). To test this possibility, the authors ectopically expressed Tbx1 in a mouse spindle carcinoma cell line which does not express endogenous Tbx1 and which is highly tumourigenic. They then tested the tumour forming ability of the resulting cell lines in mice and they showed that Tbx1 expression significantly suppressed tumour growth. Furthermore, in culture, ectopic Tbx1 expression resulted in decreased cell growth and reduced development into multi-layered colonies compared to control cells. In addition, it was demonstrated using flow cytometry that cells transfected with TBX1 accumulated predominantly in G1 phase suggesting that TBX1-expressing cells tend to exhibit a senescent or quiescent cell cycle profile. Lastly Trempus et al. (2011) showed that contact inhibition could be restored by expressing TBX1, which caused a dose-dependent decrease in cell proliferation.

TBX2 is overexpressed in melanoma, breast, pancreatic, cervical, endometrial and ovarian cancers (Vance et al. 2005; Rodriguez et al. 2008; Hoek et al. 2004; Jacobs et al. 2000; Sinclair et al. 2002; Fan et al. 2004; Mahlamäki et al. 2002; Duo et al. 2009; Hansel et al. 2004; Cavard et al. 2009; Liu et al. 2010a; Liu et al. 2010b; Dimova et al. 2009) and there is a growing body of evidence to suggest that TBX2 plays a key role in the oncogenic process. Correlations have been made between TBX2 expression and tumour stage, differentiation (Chen et al. 2008) and metastasis of pancreatic tumours (Duo et al. 2009) and TBX2 overexpression has also been correlated with tumour stage in endometrial adenocarcinoma (Liu et al. 2010b) as well as poor survival in breast cancer (Wang et al. 2012). Interestingly, TBX2 was observed to be highly expressed in cervical squamous cell carcinomas which were human papilloma virus (HPV) 16 positive (Liu et al. 2010a). TBX2 was also demonstrated to be a co-factor of the HPV capsid protein L2, which performs multiple functions in the HPV viral lifecycle, and to repress the long coding region thereby regulating the HPV genes E6 and E7 (Schneider et al. 2013).

Numerous studies have demonstrated that TBX2 is required to maintain proliferation and suppress senescence, a protective barrier against cancer, in various cancer cell lines including breast cancer and melanoma (Jacobs et al. 2000; Vance et al. 2005; Prince et al. 2004; Peres et al. 2010; Redmond et al. 2010). TBX2 is able to maintain proliferation by avoiding senescence partly through its ability to repress the cell cycle regulator genes, mouse $p19^{ARF}$ (Jacobs et al. 2000) and $p21^{WAF1}$ (Prince et al. 2004). TBX2 was shown to repress human $p14^{ARF}$ by binding to a variant T-element in its promoter (Lingbeek et al. 2002) and to bind and repress $p21^{WAF1}$ via a T-element close to its initiator region in co-operation with histone deacetylase 1 (HDAC1) (Prince et al. 2004; Vance et al. 2005). In addition,

[2] The accepted convention will be used for human, TBX1, and when referring to both mouse and human, Tbx1/TBX1 will be used.

a recent study showed that TBX2 can interact with the pro-senescence factor, promyelocytic leukemia (PML) protein, in Wi38 primary human fibroblasts, which prevents the induction of senescence (Martin et al. 2012). Taken together, these studies illustrate the ability of TBX2 to induce a strong senescence bypass signal in cancer. Furthermore, a study by Redmond et al. (2010) demonstrated elegantly that TBX2 could promote proliferation of MCF-7 breast cancer cells by co-operating with EGR1 to repress the tumour suppressor NDRG1.

Another oncogenic role for TBX2 was revealed in a study by Davis et al. (2008) when they ectopically expressed TBX2 in transformed fibroblasts and melanoma cells that had low levels of endogenous TBX2. These stably transfected cells exhibited several mitotic defects and chromosomal instability, for example chromosome missegregation, chromosomal rearrangements and polyploidy. Chromosomal instability may drive key genomic alterations leading to tumourigenesis and is associated with drug resistance and a poor diagnosis (Lee et al. 2011; Hanahan & Weinberg 2011) Furthermore, ectopic expression of TBX2 in transformed fibroblasts was found to increase resistance to the chemotherapeutic agent cisplatin (Davis et al. 2008). The above studies demonstrated that TBX2 plays a pivotal role in the oncogenic process through its ability to control key cell cycle regulators. Interestingly, in a study by Ismail & Bateman (2009) the authors showed that overexpression of TBX2 in the p53-negative SW13 adrenocortical carcinoma cell line, which also has no detectable p21 expression, promoted anchorage-independent growth and cell survival in response to UV-induced apoptosis. Although these results could not be replicated in a p53-negative pancreatic cell line, they are interesting because they suggest that TBX2 may also contribute to carcinogenesis via mechanisms independent of p53 or cell cycle regulation.

A number of recent high-throughput studies have implicated TBX4 as a potential tumour suppressor. Increased TBX4 methylation was observed in the aggressive progressing non-muscle-invasive (Ta) urinary bladder tumours as compared to stable Ta tumours (Reinert et al. 2011). Using microarray analysis and validation of targets by PCR and bisulphite sequencing, TBX4 was highlighted as a good candidate marker for disease progression in bladder cancer. Furthermore, Zong et al. (2011) showed that low levels of TBX4 correlated with a decrease in the overall survival of pancreatic ductal cell adenocarcinoma patients. In addition, the authors demonstrated in another study that TBX4 can be used as a biomarker to predict the stage of intrahepatic cholangiocarcinoma tumours (Zong et al. 2013). Additional research is, however, needed in order to elucidate the molecular mechanisms by which TBX4 exerts its tumour suppressor activity.

Interestingly there is some data to suggest that, TBX5, the closely related family member of TBX4, also functions as a tumour suppressor. The ectopic expression of TBX5 in cells derived from a lung cancer and an osteosarcoma, led to an increase in apoptosis and a decrease in cell proliferation and colony formation (He et al. 2002). Using methylation-sensitive arbitrarily primed PCR, Yu et al. (2010) also showed that the TBX5 promoter was silenced by methylation in 7 out of 8 human colon cancer cell lines. Furthermore, when TBX5 levels were reintroduced in the colon cancer cells, either by ectopic expression or by treatment with a hypomethylating agent, a decrease in cell proliferation and migration and an increase in apoptosis were observed. The clinical significance was also examined and TBX5 promoter methylation was found to be associated with poor survival in colon cancer patients. This work has, however, subsequently been challenged as TBX5 has been shown to be involved in the activation of anti-apoptotic genes in a number of β-catenin driven cancer cell lines, including colon cancer (Rosenbluh et al. 2012). These conflicting studies highlight a need for more research into the role of TBX5 in cancer.

T-bet (TBX21), another example of a tumour promoting T-box factor, is overexpressed in a subset of estrogen receptor alpha (ERα) positive breast cancers (McCune et al. 2010). McCune et al. (2010) investigated the role that insulin may play in the hormonal network of ERα positive breast cancers and showed in MCF-7 breast cancer cells that insulin treatment led to the induction of T-bet. Increased expression of T-bet resulted in a disrupted estrogen receptor hormonal network leading to resistance to hormone therapy and an unfavourable prognosis. This network includes the transcription factors Gata3 and FoxA1 whose expression was found to be down-regulated following insulin treatment or stable overexpression of T-bet. Furthermore, T-bet overexpressing cells were also more resistant to tamoxifen therapy in the presence of insulin and displayed elevated ERK and AKT activation, which is associated with anti-estrogen resistance.

Several lines of evidence have also implicated TBX3 in cancer and since TBX3 is the major focus of this study a description of the gene and protein is provided before discussing its role in malignancy.

1.4. TBX3

1.4.1. Gene and protein

TBX3 is an interesting gene and protein to study due to its important role in development as well as its emerging role in cancer. The gene has been mapped to chromosome 12 at position 12q23-24.1 and is classified as a member of the TBX2 subfamily (Agulnik et al. 1996). While several TBX3 transcript variants exist due to alternative splicing (Bamshad et al. 1999), TBX3 and TBX3+2a are the most well studied and the ratio of their expression has been shown to be species and tissue specific (Fan et al. 2004). The dominant transcript TBX3 is approximately 5.2kb, contains seven exons (**Figure 1.2.A**) and encodes a protein of 723 amino acids. TBX3+2a arises from intronic splicing between exons 2 and 3 which results in an additional 20 amino acids within its DNA-binding domain or T-box. It is unclear whether this insertion affects TBX3+2a DNA-binding ability or target gene specificity and whether the two isoforms have different functions. Fan et al. (2004) showed that while TBX3 functions as an anti-senescence factor in mouse embryonic fibroblasts (MEFs) and can bind the consensus T-element in an oligonucleotide binding assay, TBX3+2a promotes senescence and cannot bind this site. On the other hand, Hoogaars et al. (2008) demonstrated that both isoforms bind and repress the $p21^{WAF1}$ and Nppa promoters in vitro and act similarly in an in vivo model. The functional role of TBX3 and TBX3+2a therefore remains to be resolved.

The functional domains of the TBX3 protein (**Figure 1.2.B**) were mapped by Carlson et al. (2001) using fusion proteins of a Gal4 binding domain fused to different regions of TBX3 on a luciferase reporter driven by four proximal promoter Gal4 binding sites. Constructs expressing either the full length TBX3 or regions 123-200 or 567-623 of the TBX3 protein led to a repression of relative luciferase activity. This indicated that TBX3 was a transcriptional repressor and identified regions 567-623 and 123-200 as repression domains, which the authors called R1 and R2, respectively. Indeed, TBX3 was subsequently shown to transcriptionally repress $p14^{ARF}$/$p19^{ARF}$, $p21^{WAF1}$, Nppa, E-cadherin and phosphatase and tensin homolog (PTEN) (Burgucu et al. 2012; Brummelkamp et al. 2002; Lingbeek et al. 2002; Rodriguez et al. 2008; Hoogaars et al. 2008) Furthermore, when R1 or R2 were fused to the VP16 (herpes simplex) activation domain and tested in similar experiments, R1 but not R2, was able to override the VP16 activation domain and to repress transcriptional activity. This led to the suggestion that R1, which resides in the C-terminal portion of TBX3, is the dominant repression domain. Interestingly, most UMS associated C-terminal mutants lack this domain and show increased rates of protein decay, suggesting that the TBX3 C-terminus is important for protein stability. A putative activation domain at amino acids 423-500

was also mapped and indeed TBX3 has been shown to activate Connexin43 (Boogerd et al. 2011) and Gata6 (Lu et al. 2011) which are both important in heart embryogenesis. Using electrophoretic mobility shift assays (EMSA) the DNA-binding region was found to be located in the N-terminus (position 105-287 (REFSEQ: accession NM 005996.3)) and a NLS was found at residues 292 to 297 (Carlson et al. 2001). While there is little information regarding how TBX3 may be post-translationally modified, the TBX3 protein houses 11 Serine-Proline (SP) motifs which are putative phosphorylation sites for many kinases, including the mitogen-activated protein kinases (MAP) (Davis 1993) and cyclin-dependent kinases (Montagnoli et al. 2006). Further characterisation of the structure of the TBX3 protein and its interaction with DNA were shown by Coll et al. (2002) when they solved the crystal structure of the TBX3 DNA-binding domain. While they demonstrate that TBX3 binds the palindromic consensus T-box binding site as two independent monomers, it is predicted that TBX3 will bind its physiological targets as a single monomer.

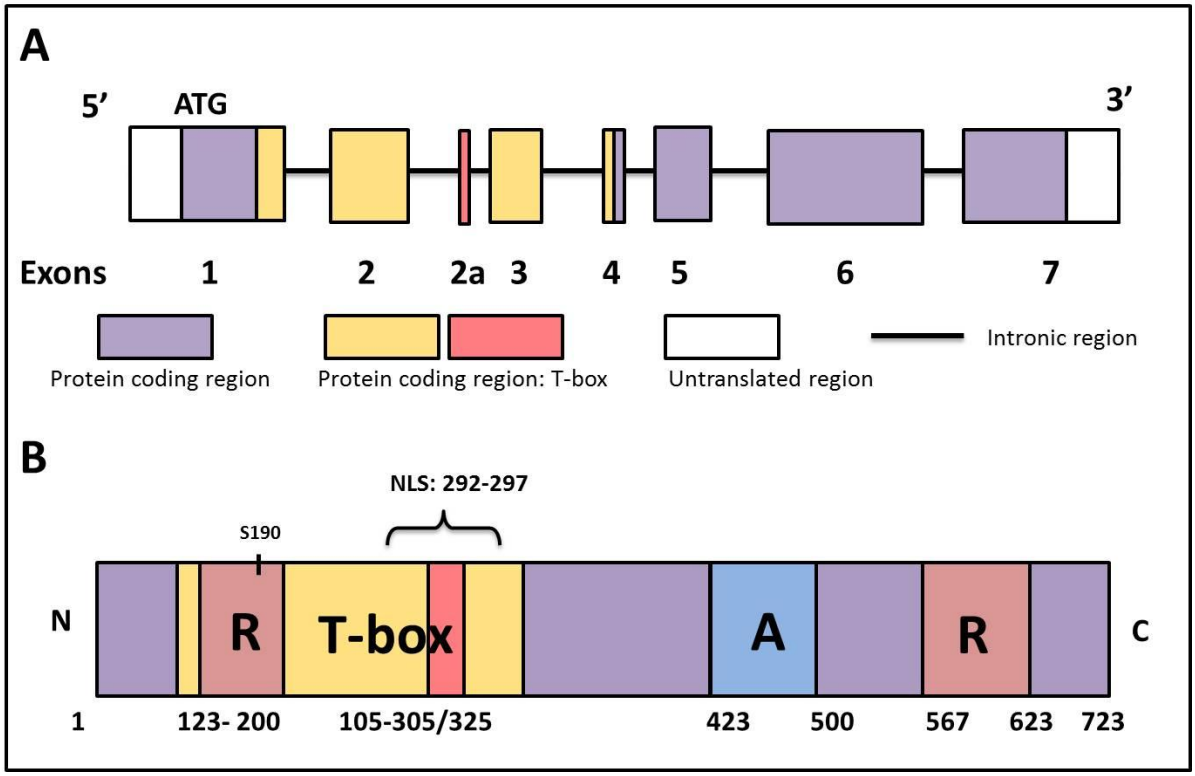

Figure 1.2. **Structure of TBX3 mRNA and protein.**
A. Schematic diagram of human TBX3 mRNA. The TBX3+2a isoform is included in the mRNA through alternative splicing of the second intron. **B.** Schematic diagram of the human TBX3 protein depicting different domains and nuclear localisation signal (NLS) position. The domains include the T-box DNA-binding domain (yellow), which includes an additional 20 amino acids in the TBX3+2a isoform; R, repression domains (pink); A, activation domain (blue). The amino and carboxy termini of the protein are labelled N and C respectively. A serine proline residue (S190) is situated at amino acid position 190.

1.4.2. TBX3 and development

Human TBX3[3] has been found to be expressed in a number of tissues and organs including the limbs, jaw mesenchyme, salivary gland, adult adrenal gland, thyroid, foetal heart, lungs, mammary gland, liver, bladder, uterus, genitals, spleen, and nervous system (Bamshad et al. 1999). Much information on the roles of TBX3 in development has been derived from UMS and mouse models where Tbx3 has been mutated. While most UMS associated mutations occur in the T-box, mutations which lead to truncated versions of the TBX3 protein are also thought to produce non-functional TBX3 (Bamshad et al. 1999). It is worth noting that a study by Klopocki et al. (2006) described a 1.26 Mb deletion encompassing the *TBX3* gene in a single patient with UMS. Furthermore, a recent study reported that UMS abnormalities displayed by mice homozygous for the deletion of the entire Tbx3 T-box results from an aberrantly localised protein (Frank et al. 2013) UMS is characterised by malformations in axillary hair, abnormal dentition, mammary gland aplasia, loss of areola, limb abnormalities and defects in the heart, jaw and genitalia (Packham & Brook 2003). It is of course important to note that TBX3 is expressed in a number of tissues and organs whose development is unaffected in UMS patients. Thus, the behaviour of cells expressing TBX3 appears extremely sensitive to its expression level. In the UMS mouse model Tbx3 homozygous mutant mice die in utero by E11.5 and exhibit aplasia of the mammary glands as well as malformations of the posterior limbs. These abnormalities are synonymous with the UMS phenotype seen in humans (Davenport et al. 2003). Heterozygote female mice display mammary gland aplasia and a minor genital anomaly (Davenport et al. 2003; Jerome-majewska et al. 2005). Together, the phenotypes resulting from mutations in TBX3 have suggested the importance of this gene in the development of, at the very least, the heart, mammary glands and limbs.

1.4.3. TBX3 in cancer

TBX3 is overexpressed in several cancers including melanoma, breast, pancreatic, lung, ovarian, liver and head and neck (Fan et al. 2004; Hoek et al. 2004; Rodriguez et al. 2008; Hansel et al. 2004; Liu et al. 2012; Lomnytska et al. 2006; Renard et al. 2007; Burgucu et al. 2012; Humtsoe et al. 2012) and its expression was found to correlate with rapid cell proliferation, invasiveness and tumour size in uterine and cervical cancer (Lyng et al. 2006). Upregulated levels of TBX3 have been directly linked to cancer development and progression as TBX3 has been shown to bypass senescence, evade apoptosis and to contribute to tumour formation and invasion. There is, however, little information on the mechanisms by which TBX3 contributes to this disease state. Interestingly, there are a few

[3] The accepted convention will be used for human, TBX3, and when referring to both mouse and human, Tbx3/TBX3 will be used.

recent high-throughput studies which also suggest a tumour suppressor role for TBX3 in particular cancer contexts.

1.4.3.1. TBX3 and apoptosis

A number of compelling studies over the past two decades have shown that apoptosis provides a natural barrier to cancer and that tumour cells have developed numerous strategies for resisting this form of cell death (Hanahan & Weinberg 2011). Interestingly, it has been shown that one such strategy may involve the expression of TBX3. This was first demonstrated by Carlson et al. (2002) who ectopically expressed TBX3 in MEFs and observed a suppressed apoptotic response, as well as decreased $p19^{ARF}$ and p53 protein levels. In addition, knock down of TBX3 has been shown to induce apoptosis in a rat bladder cancer cell line (Ito et al. 2005), as well as inhibit beta catenin-mediated cell survival and increase sensitivity to doxyrubicin in human colon carcinoma and osteosarcoma cell lines (Renard et al. 2007). Furthermore, Humtsoe et al. (2012) suggested that TBX3 may play an important role in protecting squamous cell carcinoma against anoikis, a specific form of cell death induced by anchorage-dependent cells detaching from the surrounding extracellular matrix. On the contrary, overexpression or knock down of TBX3 in mammary epithelial cells (MECs) was shown to have no effect on apoptosis (Platonova et al. 2007). This indicates that the ability of TBX3 to evade apoptosis may be cell context specific and therefore illustrates the need for a more in-depth analysis of the role of TBX3 in apoptosis.

1.4.3.2. TBX3 in tumour formation, cell invasion and metastasis

The acquired ability of cancer cells to invade the surrounding tissue and metastasise from the primary site to distant regions of the body has been identified as a hallmark of cancer (Hanahan & Weinberg 2000). Metastatic cancer is the cause of 90% of cancer deaths (Bogenrieder & Herlyn 2003) and is accompanied by a change in the adhesive properties of the cell due to deregulated levels of cadherin cell adhesion molecule family members, namely an increase in N-cadherin and a loss of E-cadherin expression (Leber & Efferth 2009). Interestingly, there is evidence to suggest that TBX3 plays an important role in tumour formation and invasion in breast cancer and melanoma (Peres et al. 2010; Renard et al. 2007; Rodriguez et al. 2008; Mowla et al. 2010). Using in vitro cell proliferation and tumour-forming ability assays as well as an in vivo nude mouse model, Peres et al. (2010) demonstrated that TBX3 can promote anchorage-independent growth, tumour-forming ability and migration of vertical growth phase melanoma cells. Furthermore, overexpressing TBX3 in non-tumourigenic early stage radial growth phase melanoma cells was shown to be sufficient to

promote these cells to form tumours and invade surrounding tissue in nude mice (Peres & Prince 2013). TBX3 knock down in liver cancer and melanoma cells also led to a reduction in anchorage-independent growth and a decrease in invasive potential, respectively (Renard et al. 2007; Rodriguez et al. 2008). Rodriguez et al (2008) further revealed that the decreased invasiveness of TBX3 knock down cells could be attributed to an increase in E-cadherin expression (**Figure 1.3**) and that the E-cadherin promoter can be directly repressed by TBX3. A novel signalling pathway which leads to TBX3 upregulation was identified by Mowla et al. (2010) where a phorbol ester, tetradecanoylphorbol acetate (TPA), was shown to induce TBX3 upregulation in an activator protein 1 (AP-1)-dependent manner. The authors show that TPA-induced migration of MCF-7 cells was mediated, in part, by TBX3 and AP-1 factors which were found to bind directly to a TPA response element in the TBX3 promoter in vitro and in vivo. Lastly, in a microarray analysis study by Humtsoe et al. (2010) TBX3 was shown to be upregulated following induction of EMT in head and neck squamous cell carcinoma. These findings are important as EMT is thought to play a role in the dissemination or movement of cancerous cells from their primary site to other areas of the body (Micalizzi et al. 2010).

1.4.3.3. TBX3 and cancer stem cells

Cancer stem cells (or cancer stem-like cells) (CSCs) can be described as a subset of self-replicating cells found within a tumour which have characteristics associated with normal stem cells. In recent years, the CSC hypothesis has gained momentum as important studies have shown that CSCs make up a significant percentage of the cells within the tumour environment of certain cancers (Quintana et al. 2008). It is also believed that these cells may play a major role in drug resistance and therefore relapse due to their ability to survive following chemotherapeutic treatment (Fillmore & Kuperwasser 2008). A study by Fillmore et al. (2010) is of particular interest to this dissertation as it identified TBX3 as a mediator of CSC expansion (**Figure 1.3**). The authors showed that the addition of estrogen can expand the CSC population in a panel of ERα positive breast cancer cell lines and that fibroblast growth factor 9 (FGF9) expression is necessary for this expansion in a paracrine manner. Importantly, they demonstrate that estrogen and FGF9 expression led to an increase in the levels of TBX3 which causes expansion of breast CSCs. Interestingly, TBX3 and FGF are important mediators in the embryonic development of the mammary gland, where FGF activates TBX3 and TBX3 in turn activates FGF in a positive feedback loop (Eblaghie et al. 2004).

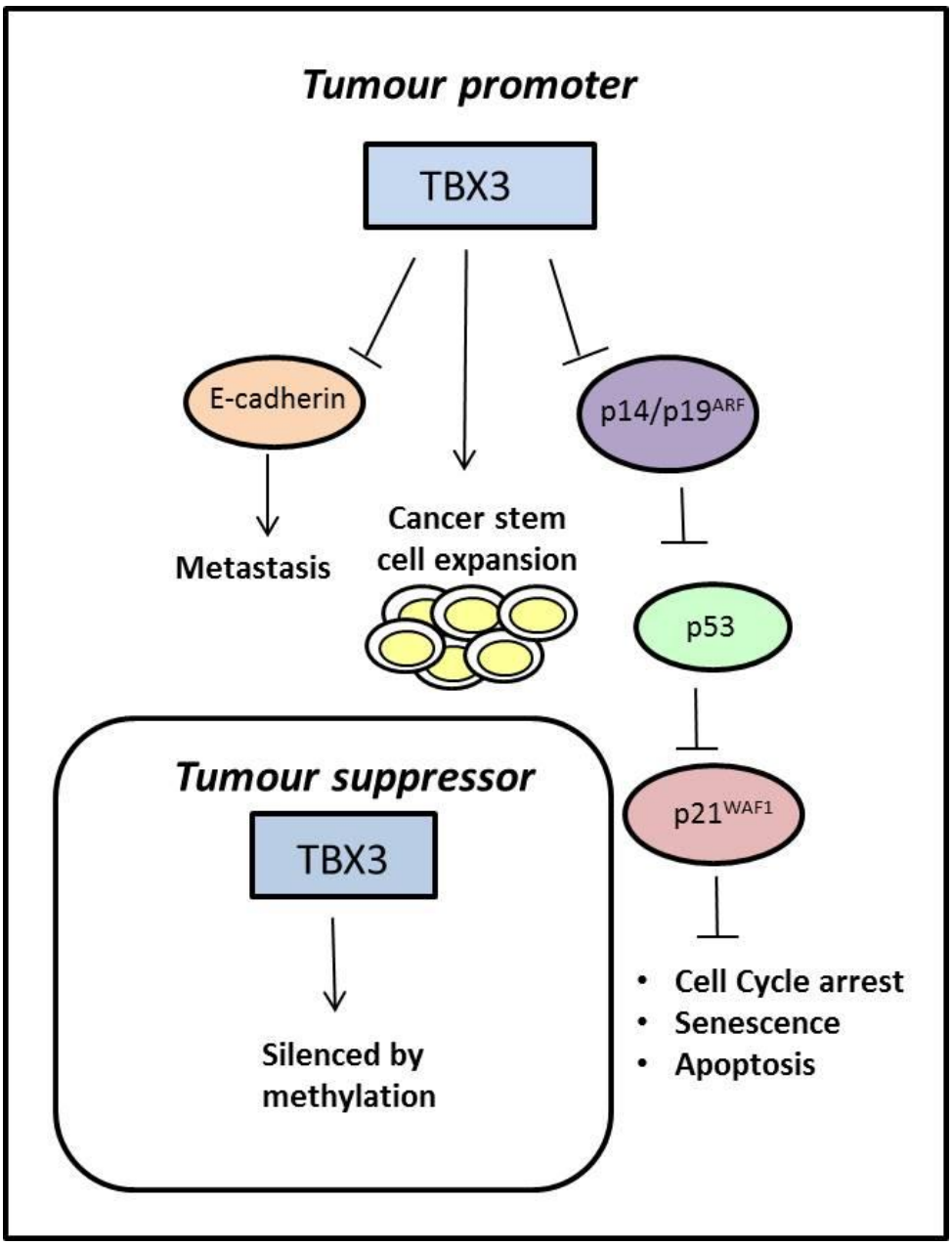

Figure 1.3. **A summary of the tumour promoting and tumour suppressor properties of TBX3.**
TBX3 promotes tumourigenesis by repressing expression of the cell adhesion molecule E-cadherin as well as the p14/p19^{ARF} pathway. In addition TBX3 upregulation leads to cancer stem cell expansion. TBX3 can also be viewed as a tumour suppressor as its expression has been shown to be silenced by methylation in certain cancers.

1.4.3.4. The tumour suppressor properties of TBX3

In contrast to a significant body of research implicating TBX3 as a tumour promoter, there is also some evidence that TBX3 may act as a tumour suppressor in certain cellular contexts. In a microarray study, Lyng et al. (2006) showed that TBX3 levels were down-regulated in uterine and cervical cancer samples positive for lymph node metastases and that TBX3 expression correlated with an increase in progression-free survival. In addition, studies have shown that *TBX3* is epigenetically silenced by methylation in glioblastoma, bladder and gastric cancer (**Figure 1.3**) (Kandimalla et al. 2012; Etcheverry et al. 2010; Yamashita et al. 2006). *TBX3* methylation in bladder cancer was associated with the progression of non-muscle invasive tumours (Pta) to muscle-invasive tumours (MI) and patients in which *TBX3* was not methylated were shown to have a significantly better progression-free survival rate (Kandimalla et al. 2012). In addition, *TBX3* methylation was associated with a significantly lower survival rate in a cohort of glioblastoma patients (Etcheverry et al. 2010) and while genomic screening identified *TBX3* as a methylated gene in at least one gastric cancer cell line (Yamashita et al. 2006), the possibility that this may be related to the development and progression of gastric cancers has not yet been investigated. These studies put forward the exciting notion that TBX3 may have a tumour promoting or a tumour supressing role in cancers of different cellular origins and contexts.

1.4.3.5. TBX3 and the cell cycle

Uncontrolled or deregulated cell proliferation is a hallmark of cancer (Hanahan & Weinberg 2000) and earlier studies pointed to TBX3 contributing to the oncogenic process by directly repressing negative cell cycle regulators. To protect against cancer, the cell cycle is therefore tightly regulated and the mammalian cell cycle is divided into two major phases, interphase and mitosis (M phase) (Schafer 1998). Interphase is comprised of gap 1 (G1) and gap 2 (G2) phase, which include important DNA-damage and size restriction checkpoints, and S phase where the DNA is replicated. G0 phase is the phase denoted to cells which permanently or temporarily leave the cell cycle or stop dividing. Nuclear and cytoplasmic division is observed during M phase, which is further subdivided into prophase, prometaphase, metaphase, anaphase, telophase and cytokinesis. The mammalian cell cycle and its key regulators are summarised in **Figure 1.4**.

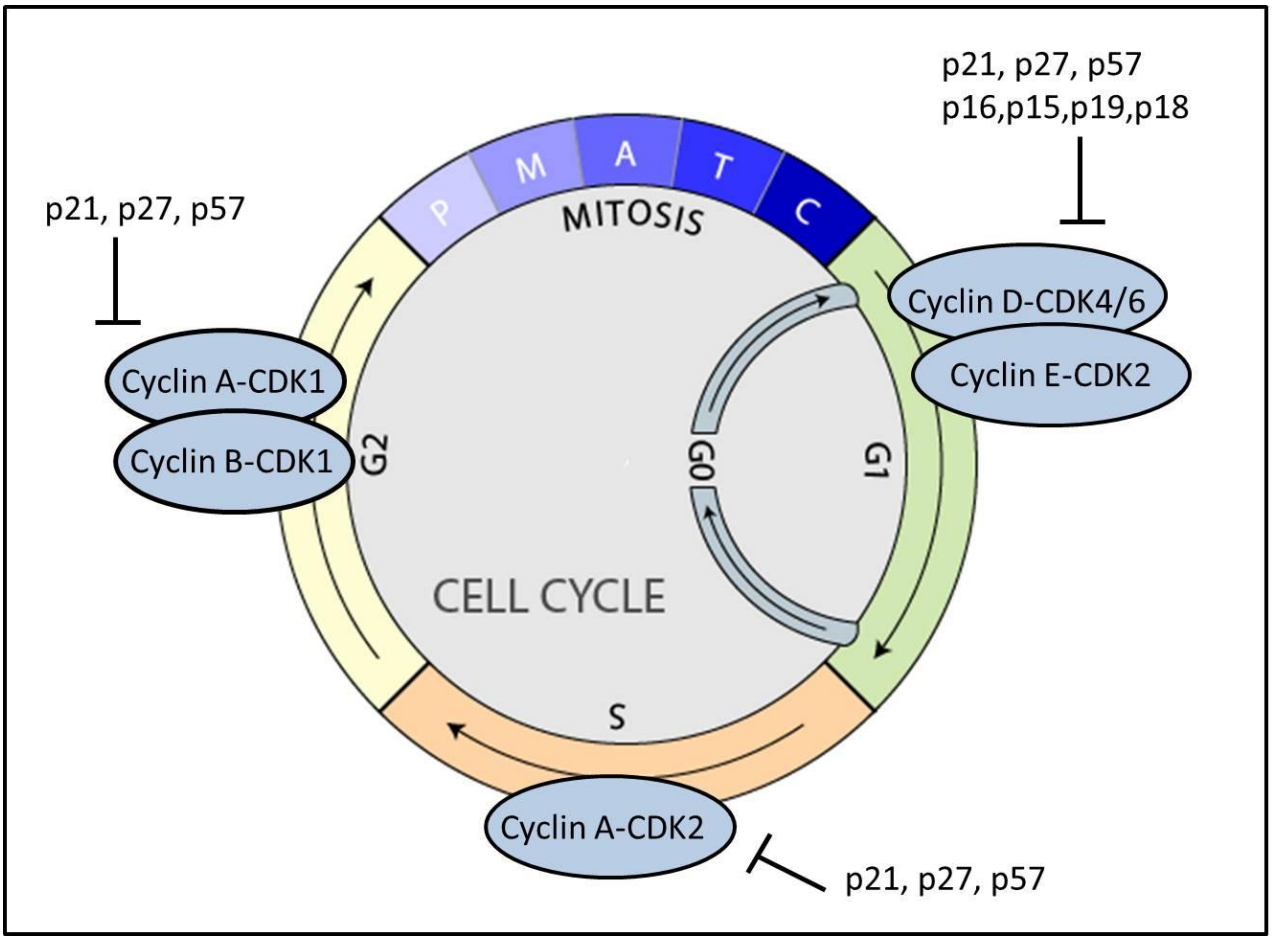

Figure 1.4. **Diagram of the mammalian cell cycle.**
The cell cycle includes phases Gap1 (G1), Gap 0 (G0), DNA replication (S), Gap2 (G2) and Mitosis (M) and is controlled by Cyclin/CDK complexes and CDKIs. P: prophase, M: metaphase, A: anaphase, T: telophase and C: cytokinesis. Image was adapted from the image sourced from http://essayweb.net/biology/celldivision.shtml.

The cell cycle is controlled by 3 important families of proteins which include the cyclins, cyclin-dependent kinases (CDKs) and CDK inhibitors (CDKIs). Cyclins are regulatory proteins that are synthesized and degraded in a cyclical fashion and include cyclins A, B, C, D and E (Glotzer et al. 1991). CDKs phosphorylate regulatory proteins required to drive the cell cycle through its phases and they are only catalytically active when they bind appropriate cyclins which direct them to their substrates (Malumbres & Barbacid 2005). Indeed, it is well established that specific cyclin-CDK complexes are responsible for regulating the different cell cycle phases for example, cyclin A-CDK2 and cyclin A-CDK1/cyclin B-CDK1 are required for transition through S and G2/M respectively (John et al. 2001). Furthermore, cyclin-CDK activity is regulated by CDKIs which, in response to cellular stress, are responsible for arresting the cell at G1/S, S, G2/M and the spindle assembly check-point (Besson et al. 2008). CDKIs are classified into two families: the inhibitors of kinase 4 (INK4) family which include $p16^{INK4a}$, $p15^{INK4b}$, $p18^{INK4c}$ and $p19^{INK4d}$ and the cyclin inhibitor protein/kinase inhibitor protein (Cip/Kip) family which include $p21^{WAF1}$, $p27^{Kip1}$ and $p57^{Kip2}$ (Lodish et al., 2001). These families differ in their inhibitory properties as members of the INK4 family function by preventing interaction between CDKs with their relevant cyclin, whereas Cip/Kip family members form a tertiary structure with the cyclin-CDK complex to inhibit its activity (Hartwell & Kastan 2011).

The ability of TBX3 to control the cell cycle was first observed by Brummelkamp et al. (2002) who demonstrated that TBX3 can mediate repression of the CDKI, $p19^{ARF}$ (the mouse homolog of human $p14^{ARF}$) (**Figure 1.3**). Under conditions of cellular stress, $p19^{ARF}$ plays an important role in stabilising the tumour suppressor p53. This is achieved by $p19^{ARF}$ sequestering the ubiquitin ligase murine double minute 2 (mdm2) which prevents it from associating with and ubiquitinating p53 and thus blocking p53 degradation (Agrawal et al. 2006; Sherr & Weber 2000). Once stable, p53 is post-translationally modified which allows it to activate its downstream target genes, which are mostly involved in processes that provide barriers to cancer, such as cell cycle arrest, senescence, apoptosis and DNA repair. CDKIs are amongst p53 targets and as described below, TBX3 was shown to prevent senescence and apoptosis by repressing CDKIs in a p53-dependent and –independent manner.

Using a temperature sensitive mouse striatal cell line containing a retroviral cDNA expression library, Brummelkamp et al. (2002) were able to isolate the Tbx3 gene from cells which did not senesce. In the same study, ectopic expression of TBX3 in MEFs led to the bypass of senescence resulting in the immortalisation of these cells. This correlated with an inhibition of $p19^{ARF}$ expression and following a UMS associated point mutation in the TBX3 DNA-binding domain (T-box), the repression of $p19^{ARF}$ was alleviated and the cells could no longer bypass senescence. Furthermore, TBX3 was shown to repress $p19^{ARF}$ in a p53-independent manner in MECs resulting in an increase in cell proliferation

(Platonova et al. 2007) and knock down of TBX3 in both a rat bladder cancer cell line and hepatoblasts was shown to inhibit cell proliferation (Ito et al. 2005; Suzuki et al. 2008). TBX3 has also been shown to directly repress $p14^{ARF}$ (Lingbeek et al. 2002) and Yarosh et al. (2008) demonstrated, using a histone decetylase (HDAC) inhibitor, that in MCF-7 breast cancer cells, TBX3 interacts with HDACs to mediate this repression. A recent study by Burgucu et al. (2012) has also shown that TBX3 is able to repress PTEN, a tumour suppressor gene which modulates cell cycle progression (Sun et al. 1999) and can arrest cells in G1 by decreasing cyclin D1 expression and inhibiting its nucleur localisation (Radu et al. 2003). While the biological context in which TBX3-mediated PTEN repression occurs has not yet been elucidated this may represent an additional mechanism through which TBX3 can exert pro-proliferative activity.

The $p19^{ARF}$-Mdm2-p53-$p21^{WAF1}$ pathway plays an important role in regulating cell cycle control and Prince et al. (2004) spectulated that this pathway may be targeted at multiple points by TBX2 and TBX3. Indeed, the authors showed that TBX2 is able to repress the $p21^{WAF1}$ (refered to as p21) promoter and there is preliminary evidence that TBX3 is also able to repress p21. A study by Carlson et al. (2002) first indicated that TBX3 may regulate p21 expression when TBX3 was transfected into immortalised fibroblasts which resulted in a corresponding decrease in p21 protein levels. Interestingly, when a truncated version of the *TBX3* gene, lacking the entire C-terminus housing the reported repression and activation domains, was transfected into the same cells p21 levels were upregulated. This suggests that the C-terminal repression domain may be mediating the repression of p21 by TBX3. Following this, Platonova et al. (2007) showed that TBX3 overexpression in MECs led to a decrease in p21 mRNA levels, and the reverse was found to be true when TBX3 was knocked down in these cells. Suzuki et al. (2008) provided additional support when similar qRT-PCR results were obtained in hepatoblasts. Lastly, a study which challenged what was previously known about the functionality of the TBX3 isoforms, TBX3 and TBX3+2a, showed that these isoforms can both repress p21 in luciferase assays (Hoogaars et al. 2008). Using EMSA experiments in 501 mel melanoma cells, Hoogaars et al. (2008) also showed that an unlabelled p21 probe could compete for binding with Tbx3 and Tbx3+2a to the same extent as an unlabelled consensus T-element probe. Although these studies have given some insight into the regulation of p21 by TBX3, the authors provide neither a physiological context for this regulation nor a full characterisation of the mechanism.

1.5. p21

p21 has been reported to have multiple roles within the cell including cell cycle regulation, senescence, apoptosis, DNA repair and differentiation (Umar et al. 1996; Decesse et al. 2001; Parker et al. 1995; Ciccarelli et al. 2005; Jung et al. 2010). The p21 protein was discovered in the 1990s by several independent studies and it was initially described by a number of different names based on the function it was found to perform. In 1992, p21 was pulled down as an interacting partner of cyclin D1, proliferating cell nuclear antigen (PCNA) and cyclin-dependent kinase 2 (CDK2) in immunoprecipitation experiments (Xiong et al. 1992). The authors of this study described p21 as a 21 kDa protein whose association with CDK2 was dependent on cyclin D1, but whose molecular identity was unknown. The following year, p21 was identified as a downstream target of the tumour suppressor, p53, and was therefore given the name wild-type activated p53 fragment 1 (WAF1) (El-Deiry et al. 1993). In an attempt to identify the genes through which p53 was exerting its biological function, El-Deiry et al. (1993) used a subtractive hybridization approach to detect genes highly induced by p53 in a human brain tumour cell line. WAF1 was identified and further structural and functional analysis showed that it was a 21kDa protein whose gene was mapped to chromosome 6p21.2 and which exhibited tumour cell growth suppressive properties. Using a yeast two-hybrid screen, Harper et al. (1993) identified a protein called CDK-interacting protein 1 (CIP1) that associated with G1 CDKs. CIP1 was shown to prevent entry into S phase by inhibiting the ability of the cyclin E-CDK2 and cyclin D-CDK4 complexes to phosphorylate the retinoblastoma (Rb) protein, a well-established tumour suppressor protein which controls entry into S phase. It was later shown that CIP1 and p21 are the same protein and that overexpression of CIP1/p21 can lead to a G1 arrest due to p21 selectively binding to CDK-cyclin complexes that regulate G1/S (Harper et al. 1995). A year after the discovery of CIP1, Noda et al. (1994) screened a cDNA library from senescent human diploid fibroblasts in order to isolate genes important in inhibiting DNA synthesis during senescence. They identified a factor which they called senescent cell derived inhibitor1 (Sdi1), whose expression increased 10 to 20 fold in senescent cells, as compared with early passage cells. This gene was also mapped to chromosome 6 and later found to be the same gene as *WAF1, CIP1* and *p21*.

1.5.1. Gene and protein

The *p21* gene encodes a 164 amino acid residue protein (El-Deiry et al. 1993) but alternative splicing can also give rise to other variants (**Figure 1.5A**). p21B, for instance, is a smaller protein of 123 amino acids which is ubiquitously expressed in several human tissues (Nozell & Chen 2002). Although p21B is generally less abundant than p21, it is also induced by DNA-damage and p53, and it

also shares a number of common response elements with p21. In addition to p21B, other alternate p21 transcripts have been identified in MCF-7 cells treated to induce p53 expression (Radhakrishnan et al. 2006). These transcripts seem to be fully dependent on p53 expression as their levels are undetectable when p53 is knocked down. This is in contrast to classical p21 which has reduced but detectable levels in p53 knock down cells. It is possible that these alternative transcript promoters may help to open up the chromatin to enhance transcription of the classical p21 promoter or may play a compensatory role when the classical promoter is silenced (Radhakrishnan et al. 2006). The rest of this review will focus on classical p21, also known as p21 variant 1 (see **Figure 1.5A**).

As p21 functions predominantly to repress cyclin-CDK activity, regions of the protein which are responsible for carrying out this function have been extensively studied and mapped (**Figure 1.5B**). The p21 protein houses two cyclin binding sites namely Cy1, found at residues 17 to 24 in the N-terminus and Cy2, a weaker site, at residues 152 to 158 in the C-terminus (Chen et al. 1996). Cy1 is a conserved site necessary for the binding of cyclin E-CDK2, cyclin A-CDK2 and cyclin D-CDK4 and, indeed, when the Cy1 region was mutated this binding was abrogated (Timofeev et al. 2004). In addition to the cyclin binding sites, Cy1 and Cy2, the kinase binding site in the N-terminus (residues 49 to 71) is needed for full inhibition of cyclin-CDK activity (Goubin & Ducommun 1995). In addition, the C-terminus also houses the NLS (Rodríguez-Vilarrupla et al. 2002) as well as a PCNA binding site at residues 142 to 163. PCNA is important in guiding DNA polymerase along the DNA during replication and also functions in DNA repair as well as chromatin assembly (Kelman 1997). Levels of PCNA rise in S phase when the cell is synthesizing DNA for the next round of replication and therefore the presence of a PCNA binding site in the p21 protein can induce suppression of DNA replication when PCNA binds to p21 (Flores-Rozas et al. 1994).

The p21 protein can be post-translationally regulated through phosphorylation events which in turn affect the stability, rate of degradation, localisation and activity of the protein (Timofeev et al. 2004). p21 is an unstable protein with a half-life of approximately 30 minutes (Sheaff et al. 2000) and while free p21 lacks a stable secondary or tertiary structure, when it binds to its biological targets it undergoes a shift to a more ordered conformation (Kriwacki et al. 1996). p21 is also transcriptionally regulated and some key cis-elements in the p21 promoter are shown in **Figure 1.5C**. Sites which have been identified in the p21 promoter include two functional p53 binding sites at position -2892 and -3442 (Saramäki et al. 2006; Chin et al. 1997), a number of E-boxes which enhance its transcription and six Sp-1/Sp-3 binding sites through which a number of transcription factors can bind and regulate p21 (Nakano et al. 1997). In addition, a T-element identified close to the initiator

of the p21 promoter (Prince et al. 2004) indicates that T-box factors could also potentially regulate the *p21* gene (**Figure 1.5C**).

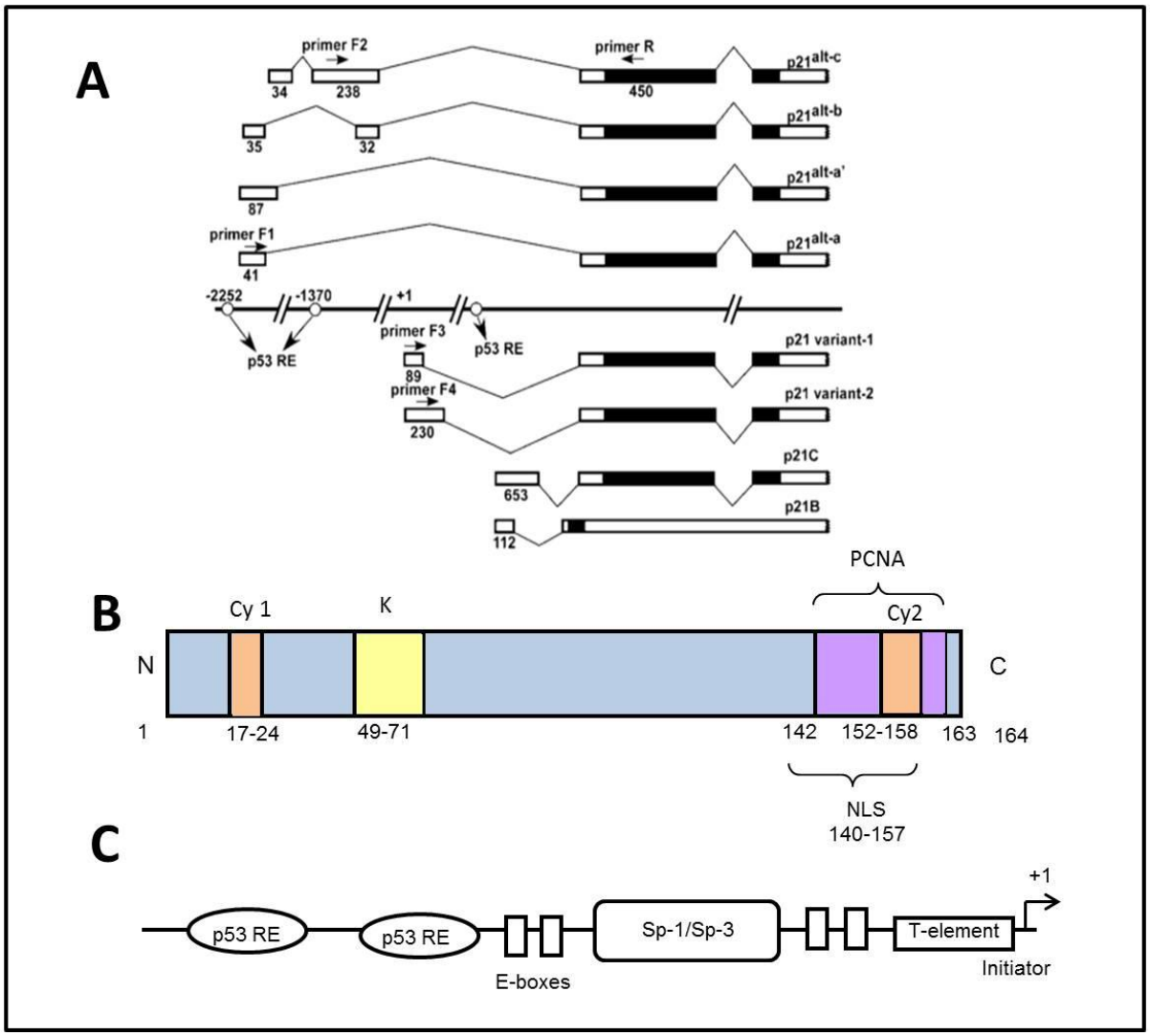

Figure 1.5. **The splice variants, protein and promoter structure of p21.**
A. The multiple splice variants of p21 (image sourced from Radhakrishanan et al. 2006). **B.** p21 protein structure including cyclin binding domains (Cy1 and Cy2), a CDK binding domain (K), a PCNA binding domain and nuclear localisation signal (NLS). **C.** Human p21 promoter including p53 response elements (RE), E-boxes, Sp-1/Sp-3 binding sites and a previously described T-element by Prince et al. (2004).

1.5.2. The biological functions of p21

As mentioned earlier, p21 has multiple biological roles but only the literature pertaining to its function in the cell cycle, senescence and apoptosis will be described as they are the most relevant to this dissertation.

1.5.2.1. Cell cycle regulation

p21 was originally identified because of its ability to arrest human fibroblasts in G1 phase (Harper et al. 1993; El-Deiry et al. 1994) and this was confirmed by Deng et al. (1995) who observed that MEFs lacking p21 were significantly deficient in their G1 checkpoint. p21-null colon cancer cells were also shown to display an impaired p53-dependent G1 arrest following DNA-damage, compared to their parental counterparts. At a molecular level, p21 induces a G1 arrest by preventing phosphorylation of Rb by cyclin D-CDK4/6 and cyclin E-CDK2. This prevents the release of E2F from Rb and hence the ability of E2F to transcriptionally activate genes needed for transition into S phase (Sherr & Roberts 1999).

In addition to its well-known role as a negative regulator of the G1/S transition, p21 has also been shown to assist in progression into S phase (LaBaer et al. 1997). p21 binds cyclin D and this was shown to be necessary for the assembly of cyclin D with its appropriate CDK to promote progression into S phase (Sherr & Roberts 1995; LaBaer et al. 1997). This was supported by observations that the assembly of the cyclin D-CDK complex was compromised in p21-deficient mice (Cheng et al. 1999). Furthermore, in p21 and p27 (a closely related CIP family protein) double knockout mice, cyclin D was inefficiently transported to the nucleus and these defects could be rescued by reintroducing both p21 and p27. It is thought that the switch between p21 exerting a cell cycle arrest or promoting S-phase progression is dependent on the levels of p21. While low p21 levels are thought to promote complex assembly of cyclin D and a relevant CDK, high levels of p21 appears to result in it performing its canonical cell cycle inhibitory activity (LaBaer et al. 1997).

There is also some evidence to suggest that p21 regulates entry into mitosis. p21 mRNA levels were found to peak in G1, decrease in S and to increase again in G2/M (Li et al. 1994). Consistent with these observations, immunofluorescence microscopy performed in non-transformed fibroblasts revealed that while p21 is absent from the nucleus at S phase, it re-appears in the nucleus at late G2 (Dulić et al. 1998). In addition, MEFs derived from p21-null mice showed a significant reduction in

pre-mitotic cells suggesting that p21 is required for entry into mitosis. Lastly, Bunz et al. (1998) showed that following γ irradiation of colon cancer cells, the DNA-damage induced G2 arrest only occurred if p53 and p21 were activated.

1.5.2.2. Senescence

Senescence is a biological process by which cells irreversibly exit the cell cycle at the end of their lifespan or in response to cellular stress and it has been well-established that senescence provides a natural barrier to cancer (Acosta & Gil 2012). As mentioned earlier, an initial study found p21 to be upregulated in senescent cells (Noda et al. 1994). Following this study, the disruption of the *p21* gene in normal human diploid fibroblasts was shown to lead to the bypass of senescence (Brown et al. 1997) and ectopic expression of p21 induced a senescence-like phenotype in the same cells (McConnell et al. 1998). In addition, an in vivo double knockout mouse model revealed that p16 and p21 co-operate to maintain cellular senescence (Takeuchi et al. 2010). There is, however, some controversy as to the role of p21 in senescence and some studies report contradictory data. For example, p21-null murine fibroblast are able to enter senescence and have a lifespan comparable to their wild-type counterparts (Pantoja & Serrano 1999). In addition, Bond et al. (1995) showed that while mutation of the p53 protein can cause human diploid fibroblasts to bypass senescence, this is not coupled with an inhibition of p21 expression. The exact role of p21 in senescence in normal human fibroblasts therefore remains unclear. In addition to the role that p21 may be playing in normal cells, it has also been shown to induce senescence when overexpressed in human bladder and lung cancer cells (Fang et al. 1999; Wang et al. 1999).

1.5.2.3. Apoptosis

Apoptosis is a genetically programmed mechanism of cell death which occurs normally during development and ageing to maintain cellular homeostasis (Elmore 2007). It also acts as a defence mechanism when cells are damaged and provides an important barrier to cancer. p21 has been implicated as both a positive and negative regulator of apoptosis and this is thought to be dependent on the type of stress signal which is initiated, the subcellular localisation of p21 and the cell type. As p21 is a direct target of p53, it becomes activated in response to a variety of stress signals including DNA-damage, oncogene activation, hypoxia, nutrient deprivation, nucleotide imbalances, reactive oxygen species (ROS) levels and heat shock (Millau et al. 2009). The p53 response may cause cells to undergo cell cycle arrest and/or apoptosis and interestingly, E2F-

associated phospho-protein (EAPP) has been identified as a key regulator in the reciprocal switch between p21-mediated cell cycle arrest and apoptosis in the context of osteosarcoma cells (Andorfer & Rotheneder 2011). EAPP binds to the p21 promoter to regulate its expression and when EAPP was present at high levels this was shown to cause resistance to apoptosis and a higher percentage of G1 arrested cells. When EAPP was knocked down, however, this brought about sensitivity to apoptosis.

A few studies have indicated p21 as a pro-apoptotic factor, including a study by Wu et al. (2002) who showed that ectopic p21 expression can induce p53-independent apoptosis in a human ovarian cancer cell line. In addition, when p21 was expressed alongside the HPV protein E7 in human osteosarcoma cells, p21 was also able to induce apoptosis in a caspase-independent manner (Kaznelson et al. 2004). Additional studies that focused on the ability of certain chemotherapeutics to induce apoptosis in cancer cells, have identified p21 as a key player in this process. p21 can increase the susceptibility of glioblastoma and ovarian cancer cells to initiate apoptosis in response to cisplatin (Kondo et al. 1996; Lincet et al. 2000). The suggestion that p21 may have an anti-apoptotic role is supported by evidence which showed that the localisation of p21 to the cytoplasm is key to its ability to effectively block apoptosis (Li et al. 2002). For example, when p21 is present in the cytoplasm of human leukemia monocyte cells it has been shown to inhibit apoptosis by binding and inhibiting apoptosis-regulating kinase 1 (ASK1), thereby preventing activation of the MAP-kinase pathway and apoptosis (Asada et al. 1999). In addition, phosphorylation of p21 by AKT causes p21 to move to the cytoplasm (Zhou et al. 2001) and increases its protein stability while promoting cell survival (Li et al. 2002). Furthermore, Zhang et al. (1999) showed that growth arrested lung cancer cells undergo apoptosis due to caspase 3-mediated cleavage and degradation of p21 following DNA-damage. The above evidence clearly demonstrates that more research is needed to elucidate the exact role of p21 in apoptosis.

1.5.3. p21 and cancer

Although mutations in *p21* are infrequent in human cancers (Shiohara et al. 1994), a number of studies have shown that p21 may act to either promote or suppress certain cancer types. Evidence supporting the role of p21 as a tumour suppressor include a study which showed that the loss of p21 can lead to an acceleration in *Ras* oncogenesis in a knockout mammary cancer mouse model (Adnane et al. 2000). Reduced expression of p21 was also observed in melanoma metastatic lesions (Maelandsmo et al. 1996) and p21 has also been shown to act as a tumour suppressor in a chemically-induced mouse skin carcinogenesis model (Philipp et al. 1999) as well as in studies using

p21-deficient mice to investigate their susceptibility to colon cancer (Poole et al. 2004). p21 expression has also been linked to a favourable prognosis in squamous cell lung carcinoma, colorectal cancer, adenocarcinoma of the uterine cervix and head and neck cancer (Komiya et al. 1997; Zirbes et al. 2000; Lu et al. 1998; Kapranos et al. 2001). MicroRNAs and promoter methylation have recently emerged as influential factors in repression of p21 gene expression and this has been shown to correlate with an increase in oncogenic potential and poor prognosis in certain cancer settings. For instance, the miRNA cluster 106b~93~25, has been found to be enriched in gastric cancer and can repress both p53 and p21 gene expression in MCF-7 and Hela cells, therefore facilitating cell cycle progression (Kim et al. 2009). In addition, a study by Yi et al. (2012) showed using microarray analysis that MiR-663 is upregulated in nasopharyngeal carcinoma and that it can target and repress *p21* to promote proliferation and tumourigenesis. In terms of epigenetic silencing, *p21* has been shown to be methylated in rhabdomyosarcoma (Chen et al. 2000), lung cancer (Zhu et al. 2003) and acute lymphoblastic leukaemia (Roman-Gomez 2002). In the latter study 41% of the patient samples were found to have a hypermethylated p21 promoter which was associated with poor prognosis (Roman-Gomez 2002). Interestingly, transcriptional activation of p21 expression using small activating RNAs (saRNA) has been shown to have therapeutic potential in hepatocellular cancer cell lines, where the induction of p21 was shown to markedly increase apoptosis and decrease the viability of these cells (Wu et al. 2011). Similar effects were also seen in a lung carcinoma cell line (Wei et al. 2010) and human bladder cancer cells (Chen et al. 2008).

In contrast to data suggesting that p21 acts as a tumour suppressor, it has been shown to have a tumour promoting role in cervical, breast and oesophageal squamous cell carcinoma (Cheung et al. 2001; Ceccarelli et al. 2001; Sarbia & Gabbert 2000). Using immunohistochemistry, p21 expression was found to be correlated with advanced disease stage in cervical cancer patients and a retrospective study, using multivariate survival analysis, showed that p21 expression was correlated to poor survival in oesophageal squamous cell carcinoma patients. p21 performs its tumour promoting function in breast cancer cells, in part, by repressing an inhibitor of angiogenesis, thiroredoxin-binding protein 2 (TBP2) (Kuljaca et al. 2009). Sustained angiogenesis is a hallmark of cancer and allows the tumour cells access to more nutrients and oxygen for sustained growth (Hanahan et al. 2000). It has also been suggested that p21 can act as a tumour promoter when present in the cytoplasm (Besson et al. 2008) and, indeed, cytoplasmic p21 expression has been shown to be a predictor of poor prognosis in breast cancer (Xia et al. 2004; Winters et al. 2003) as well as an indicator of chemo-resistance in breast and testicular cancer (Xia et al. 2011; Pérez-

Tenorio et al. 2006; Vincent et al. 2012; Koster et al. 2010). Although not confirmed, it may be that cytoplasmic p21 promotes cancer through its anti-apoptotic role.

A recent study by Qian et al. (2013) has implicated p21 in the metastasis of cancer cells where it was shown to be responsible for the switch between proliferation and invasion. p21 protein levels were shown to be increased in a transcriptional manner in MCF-7 cells overexpressing N-cadherin and interestingly these cells were also found to be highly metastatic and to exhibit a dramatic suppression in cell proliferation as compared to their MCF-7 parental counterparts. This suggested that increased p21 expression may be important in halting cell proliferation and allowing for the metastasis of cells. Indeed, when p21 was knocked down in these cells and in invasive breast and metastatic lung cancer, the cells had increased proliferative ability and decreased invasiveness through a matrigel. Furthermore this was confirmed in an in vivo athymic mouse model.

1.6. Project aims

As described in this review, p21 plays a pivotal, albeit confusing, role in many biological processes. Preliminary evidence suggests that p21 can be repressed by the T-box factor TBX3 but a detailed mechanism of this repression has not been fully characterised and whether this repression is physiologically relevant has not been shown. This study investigates this by addressing the following specific aims:

1. To confirm the repression of the p21 promoter by TBX3 and to map the TBX3 domains involved
2. To identify the site(s) in the p21 promoter responsible for mediating repression by TBX3
3. To establish whether TBX3 binds the p21 promoter in vitro and in vivo
4. To determine whether phosphorylation of TBX3 at a putative serine-proline site (S190) regulate its ability to repress p21.
5. To investigate the physiological relevance of p21 regulation by TBX3

2. Materials and Methods

2.1. Plasmid Constructs

2.1.1. p21 promoter luciferase reporter constructs

The wild-type p21 luciferase reporter construct (WTp21-luc; see **Figure 2.1.A**) contains a 2.4kb fragment of the human p21 promoter inserted upstream of a 2.6kb luciferase (luc) reporter gene (El-Deiry et al., 1993). The p21 promoter fragment was cloned into a HindIII site within the pBluescript II KS (+) vector which also contains a chloramphenicol resistance gene (see Appendix 6.1. for vector map). This construct was kindly provided by Professor Chris Marshall of the Institute of Cancer Research, UK. The mutant p21 luciferase reporter construct (Mutp21-luc; see **Figure 2.1.B**) contains a disrupted T-element close to the initiator of the p21 promoter at -121bp. This was generated previously in the laboratory by site-directed mutagenesis where the above mentioned T-element GTGTGA was mutated to CTCTGA (Prince et al., 2004).

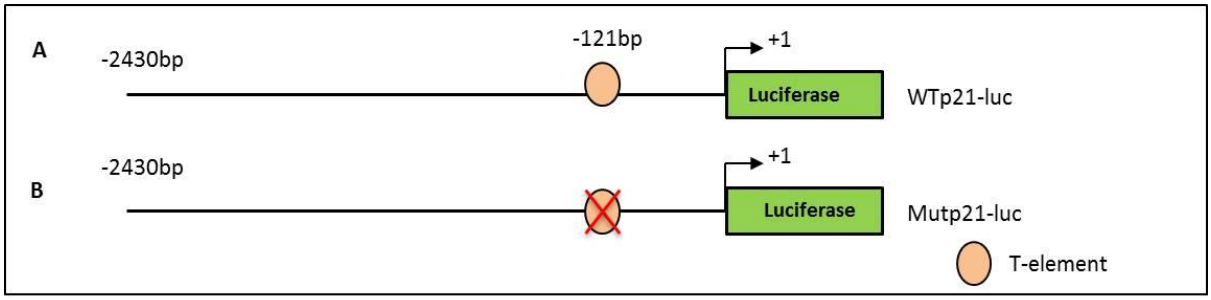

Figure 2.1. **Schematic diagram showing p21 promoter luciferase reporter constructs.**
(A) WTp21-luc **(B)** Mutp21-luc.

2.1.2. Human and mouse TBX3 expression constructs

The wild-type human pCMV-TBX3 expression construct (WT hTBX3), harbouring a 5'-HA tag and ampicillin resistance gene, was kindly provided by Dr Christine Campbell of the Cleveland Clinic Foundation, USA (see Appendix 6.1 for vector map). A schematic of the human TBX3 protein, showing two identified repression domains (R1 and R2), the T-box and a putative activation domain (A) is shown in **Figure 2.2.A**. Also available in our laboratory was a human TBX3 N-terminal expression construct (N-term hTBX3; **Figure 2.2.C**), which lacks the reported activation domain and one of the two known repression domains, as well as a human TBX3 DNA-binding domain mutant

(DBM) expression construct (hTBX3 DBM; **Figure 2.2.B**) which contains a disrupted DNA-binding domain due to a conversion of an arginine to a glycine at position 133 (R133G). The hTBX3 DBM and N-term hTBX3 constructs were generated previously in the laboratory by site-directed mutagenesis and restriction enzyme digest respectively. Furthermore a mouse Tbx3 DBM expression construct (mTBX3 DBM; **Figure 2.2.F**) as well as mouse expression constructs for the two isoforms: Tbx3 and Tbx3+2a (**Figure 2.2. D & E**) were kindly provided by Prof. Colin Goding (Ludwig Institute, University of Oxford, UK). All mouse pCMV Tbx3 expression vectors harbour a 5'-flag tag.

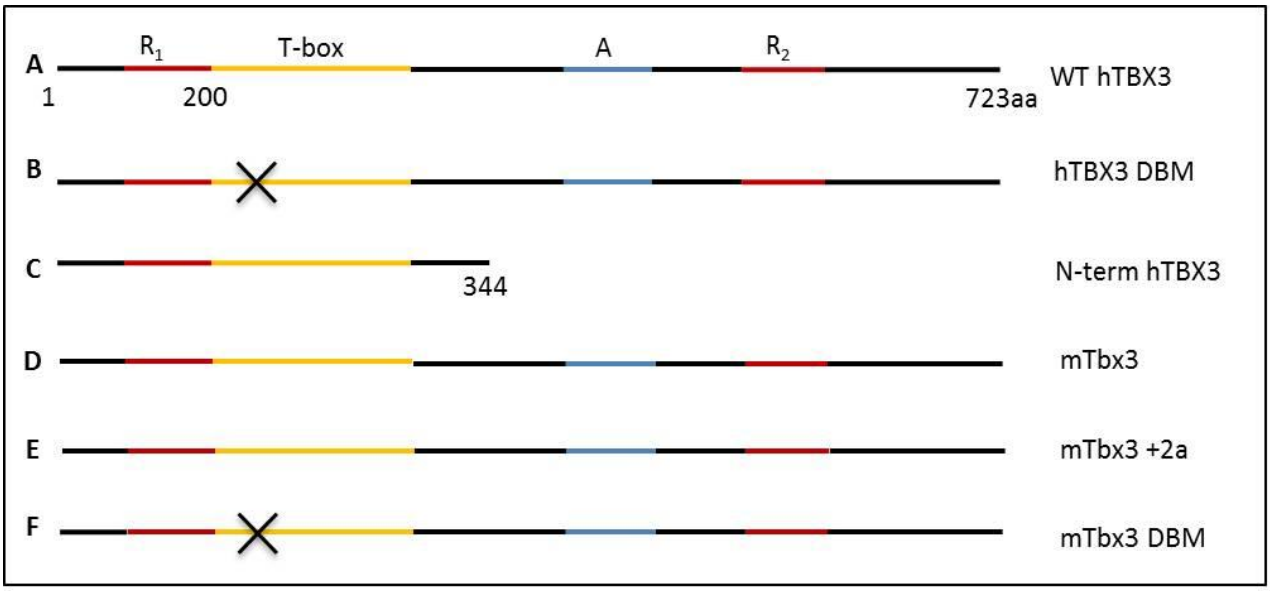

Figure 2.2. **Schematic diagram showing the relative positions of regions important for TBX3 transcriptional activity and human and mouse TBX3/Tbx3 expression constructs.**
(A) Human wild-type TBX3, (B) human DNA-binding mutant (DBM) TBX3, (C) human N-terminal TBX3, (D) mouse Tbx3, (E) mouse Tbx3+2a and (F) mouse Tbx3 DBM.

2.1.3. Generation of pCMV TBX3 S190 A and E mutant constructs

2.1.3.1. Polymerase chain reaction (PCR) and Dpn1 digestion

The TBX3 sequence contains a Serine-proline (SP) site of interest in the N-terminal portion of the protein at residue position 190 (958-963bp). Point mutations were introduced into the human pCMV TBX3 DNA by site-directed mutagenesis using appropriate primer pairs which contained the desired mutation (see **Table 2.1**). These mutations replaced the proline residue with either an alanine (A), which renders the phosphorylation site inactive, or a glutamic acid (E), which mimics phosphorylation. Standard PCR mix contained: 2 X KAPA HiFi hotstart Ready Mix which contains DNA polymerase (Kapa Biosystems, South Africa), 50ng DNA template, 10µM forward primer, 10µM

reverse primer and 1.25µl dimethyl sulfoxide (DMSO) (Sigma, St. Louis, MO, USA) made up in a total volume of 25µl. The parameters for PCR amplification were 2 minutes (min) at 95^{o}C for 1 cycle, 20 seconds (sec) at 98^{o}C, 15 sec at 65^{o}C, 3.2 min at 72^{o}C and 5 min at 72^{o}C for 16 cycles. PCR was performed on an Applied Biosystems 2720 Thermal cycler. Following amplification the PCR products were purified using the QIAquick PCR Purification Kit (Qiagen, USA) according to the manufacturer's instructions. The PCR product was then assessed by agarose gel electrophoresis (see Appendix 6.2) to confirm successful amplification. Following this 1µl Dpn1 endonuclease (10U/µl) was added to the sample. This allowed for the selection of the DNA containing the mutation by digesting the methylated non-mutated parental DNA template. The reaction was allowed to take place for 1 hour (hr) at 37^{o}C followed by heat inactivation of the enzyme at 80^{o}C for 20 min.

Table 2.1. **Sequence of primers used for site-directed mutagenesis.**

Name	dsDNA template	Forward primer
TBX3 S190A MUT	WT pCMV TBX3 FL DNA	5'-CATTCACCCGGAC**gcg**CCCGCTACTGGGGAACAGTGGATG-3'
TBX3 S190E MUT	WT pCMV TBX3 FL DNA	5'-CATTCACCCGGAC**gag**CCGGCTACTGGGGAACAGTGGATG-3'

Primer sequences corresponding to the wild-type DNA are represented in uppercase. Mutations are depicted in lower case.

2.1.3.2. Making competent bacterial cells

5ml of Luria Broth (LB) (See Appendix 6.2) was inoculated with the DH5α strain of *E. coli* and the culture grown overnight with shaking at 37^{o}C. 1ml of the overnight culture was then grown in 100ml of LB for 2-3 hr until early mid-log phase was reached with an OD_{600} reading of 0.5-0.8. Following centrifugation at 3000rpm for 10 min the supernatant of the culture was discarded and the pellet was resuspended in 1ml of ice-cold, freshly made, 100mM calcium chloride ($CaCl_2$). The resuspended cells were then kept on ice for 1 hr. The addition of $CaCl_2$ under cold conditions is thought to change the charge of the membrane and make it more permeable to DNA when the cells are heat shocked. It does however, also make the cells more delicate and therefore cells were handled gently. After incubation on ice, the cells were centrifuged as before at 4^{o}C, the supernatant discarded and the pellet was resuspended in a final volume of 1ml 100mM $CaCl_2$. Competent cells were kept overnight at 4^{o}C and either used immediately or added to 50% glycerol (final volume 15%), snap-frozen in liquid nitrogen and kept at -80^{o}C until later use.

2.1.3.3. Transformation

10µl of the Dpn1 digested DNA was added to 100µl of *E.coli* DH5α competent cells and incubated on ice for 30 min. Following this, the cells were heat-shocked at 42^{o}C for 2 min which allowed for the passage of the DNA through the cell membrane and into the bacterial cells. The cells were then once again placed on ice for 5 min. 300µl of antibiotic-free LB was then added to the cells and the culture was incubated with shaking at 225-250rpm for 2 hr at 37^{o}C. This incubation time allowed the antibiotic-resistance gene, encoded by the transformed DNA plasmid, to be expressed. 100µl of this culture was then added to an LB-agar plate containing the relevant antibiotic (100ug/ml) (see Appendix 6.2) and the plate was inverted and placed at 37^{o}C overnight. The addition of antibiotic to the agar plate allows for antibiotic selection, whereby only the bacterial cells which have taken up the plasmid DNA and express antibiotic resistance will survive and form colonies on the plate. A negative control plate containing untransformed competent cells was also included. These plates contained no colonies. Sterile techniques were practiced throughout the transformation process.

2.1.3.4. Preparation of plasmid DNA (mini-preparation) and confirmation of mutation by sequencing

Following the transformation process, a single colony from the agar plate was picked with a sterile plastic pipette tip and placed in 3ml of LB, containing 1% of the appropriate antibiotic. Large isolated colonies were selected as they were more likely to contain the transformed plasmid DNA and less likely to be satellite colonies. This culture was grown overnight at 37^{o}C with shaking. The QIAprep® Mini-prep kit (Qiagen, USA) was then used to purify the DNA according to the manufacturer's instructions. The purified DNA was then sent for sequencing at Inqaba Biotechnical Industries (Pty) Ltd (South Africa) to confirm the mutation.

2.1.3.5. Large scale maxi-preparation of DNA constructs

Selected mutant constructs were amplified by maxi-prep using the PureYield™ Plasmid Maxiprep system (Promega, USA) according to the manufacturer's instructions. Briefly, a single colony from the agar plate was picked with a sterile plastic pipette tip and placed in 3ml of LB, containing 1% of the appropriate antibiotic. This culture was grown overnight at 37^{o}C with shaking, and the following day 1ml was used to inoculate 400ml of LB, containing 1% of the appropriate antibiotic. The 400ml culture was grown overnight with shaking at 37^{o}C and then underwent centrifugation at 5000xg for

10 min at room temperature (RT) in a Beckman coulter Avanti J-E centrifuge with a JA-10 rotor. Following this, the supernatant was discarded and the pellet resuspended in 12ml Cell Resuspension Solution. 12ml of Cell Lysis Solution, which has an alkaline pH, was then added to lyse the cells and denature the chromosomal DNA. The tube was inverted and allowed to incubate for 3 min at RT. The addition of 12ml Neutralising Solution followed to neutralise the cell lysate and cause the chromosomal DNA to re-nature and aggregate with the cellular proteins. The tube was inverted 10-15 times to ensure complete precipitation of cellular debris. Centrifugation at 14000xg for 20 min at RT followed which separated the chromosomal DNA, protein and cell debris from the rest of the solution containing plasmid DNA. The DNA was then purified by adding the sample to a PureYield™ Maxi Binding Column assembled onto a PureYield™ Clearing Column placed on a vacuum manifold. Maximum vacuum was applied to allow the lysate to pass through the membrane and the DNA to remain on the membrane. 5ml Endotoxin Removal Wash and 20ml Column Wash was then added to and passed through the column one after another. The membrane was then dried by applying the vacuum for 5 min and then the DNA eluted by adding 1.5ml nuclease-free water to the column and centrifuging at 2000xg for 5 min.

2.2. Cell culture

2.2.1. Cell lines and culture conditions

COS7 SV-40 (Simian virus 40) transformed monkey kidney cells, HEK293 human kidney cells and CT-1 immortalised human lung fibroblasts were cultured in Dulbecco's modified Eagle's medium (DMEM) (Highveld Biological) (see Appendix 6.3.) whereas radial growth phase melanoma WM1650 cells were grown in Roswell Park Memorial Institute (RPMI) medium (Sigma-Aldrich, USA). Both DMEM and RPMI were supplemented with 10% fetal bovine serum (FBS), 100U/ml penicillin and 100µg/ml streptomycin. FBS provides growth factors and nourishment for the cells to grow and penicillin and streptomycin are antibiotics which are used to prevent infection. In addition, the RPMI medium was supplemented with 200pM cholera toxin and 200nM TPA to increase cell growth. All cells were maintained in a 37°C incubator (5% CO_2 and 65% humidity), sterile technique was practiced when culturing the cells and regular tests for mycoplasma infection were performed. Media was also replaced every 2-3 days.

2.2.2. Mycoplasma test

Cells were grown on a coverslip for approximately 60 hr in antibiotic-free medium followed by fixation in a 1:3 mixture of glacial acetic acid and methanol for 5 sec. The cells were then washed briefly with water to remove the fixing solution and then air-dried at RT for 5 min. Following this the cell nuclei were stained with Hoechst 33258 (0.5 µg/ml) for 30 sec, washed briefly with water to remove excess stain and then mounted on a slide with mounting fluid (see Appendix 6.3.). The cells were viewed immediately by fluorescence microscopy using an Axiovert fluorescent microscope (Zeiss, Germany).

2.2.3. Generation of TBX3 knock down and overexpression cell lines

2.2.3.1. CT-1 TBX3 knock down cell line

TBX3 knock down in the CT-1 cell line was achieved with the following shRNA sequence cloned into the pHIV7-TetR-IRES-GFP lentiviral expression vector (pTIG-shTBX3): 5'-GTGCCTATAGAGATATGTTCGCCTGACCCATGAATATATCTCTATAGGCACTTTTTT-3. The control cell line was generated using the same lentiviral expression vector with a scramble control shRNA sequence: 5'-ATATCTCCGAACGTGTCTCGTCCTGACCCAACGAGACACGTTCGGAGATATTTTTT-3' (pTIG-shScr). In order to maintain knock down the cells were treated with 1µg/ml doxycycline (D9891 Sigma-Aldrich, USA) once every 2-3 days. The cells were cultured in DMEM (Highveld Biological) supplemented with 10% FBS, 100U/ml penicillin and 100µg/ml streptomycin. These cell lines were generated by Ms Aretha Cooper, a PhD student in the laboratory.

2.2.3.2. WM1650 TBX3 overexpression cell line

TBX3 overexpression in the WM1650 radial growth phase melanoma cell line was achieved by transfection of the cells with a pEGFP-N3-empty vector (control) or pEGFP-N3-TBX3 expression vector using Transfectin® (Bio-Rad, USA). The pEGFP-N3-TBX3 construct was generated by cloning TBX3 cDNA from the pcDNA-TBX3 template into the pEGFP-N3 expression vector (BD Bioscience Clontech, USA). Fluorescent-activated cell sorting (FACS) analysis was performed 48 hr after transfection to generate a >98% green fluorescent protein (GFP) positive population of cells. The GFP expressing cells were sorted 3 times over a period of 4 weeks. Cell lines generated using pEGFP-

N3-empty and pEGFP-N3-TBX3 were named WM1650 control and WM1650 TBX3 respectively. These cell lines were generated by Dr Jade Peres, a postdoctoral fellow in the laboratory.

2.3. Luciferase Assays

2.3.1. Transfection

COS7 or HEK293 cells were plated at 5 X 10^4 cells per well in a 12 well plate. One day later cells were transiently transfected using XtremeGENE HP DNA transfection reagent (Roche), according to the manufacturer's instructions. This reagent is comprised of a blend of lipids and acts by forming a complex with the transfected DNA and transports it into the cells. Each transfection and luciferase assay was performed in duplicate where 200ng of the relevant p21-luc reporter plasmid and varying amounts of the TBX3 expression construct or empty vector were transfected. 10ng of the RL-CMV vector (Promega, USA), which contains the cytomegalovirus promoter driving the expression of a renilla reporter, was used as an internal control for transfection efficiency.

2.3.2. Luciferase assay

The Dual-Luciferase Reporter Assay System (Promega, USA) was used to determine relative promoter activity. 30 hr following transfection the cells were washed twice with chilled 1 X Phosphate Buffer Saline (PBS) (see Appendix 6.4.) and the cell lysates were harvested on ice with 100µl Passive Lysis Buffer (PLB, Promega, USA). PLB was prepared in a 1:5 dilution and following its addition to the wells, the plates were shaken at 4^{o}C for 20 min to ensure coverage of the cells by the PLB. The cell lysates were then placed at -80^{o}C and underwent one freeze-thaw cycle to effectively lyse the cells. Luciferase lysate reporter activity was assayed one day following harvest and both the activity of firefly (*Photinus pyralis*) luciferase as well as renilla (*Renilla reniformis*) luciferase were measured. Firefly luciferase catalyses the conversion of luciferin to oxyluciferin and this reaction also allows for the emission of light (**Figure 2.3.**). Renilla luciferase is responsible for converting coelenterate-luciferin (coelenterazine) to coelenteramide in the presence of oxygen. The dual reporter system is a well-designed method of using the above mentioned reporter enzymes to simultaneously measure both the reporter gene activity of the experimental transfected DNA as well as the co-transfected renilla DNA. In order to perform the assay, the lysates were centrifuged for 2 min at 13000rpm so as to separate the cell debris from the rest of the sample. 10µl of each sample was then added to a 96-well plate, 50µl of LARII (Promega, USA) was added to each sample/well and

the luminescent signal of the experimental reporter gene recorded and quantified by a luminometer (Thermo LabSystems, Luminoskan Ascent). Following this, 50µl 1 X Stop & Glo buffer (Promega, USA) was added to the sample which simultaneously quenched the firefly luminescent reaction and initiated the renilla luciferase reaction. Values were recorded by the luminometer and analysed using Ascent Software 2.6 (Thermo Labsystems) and Microsoft Excel (Windows Vista). Relative luciferase activity values were firstly normalised against corresponding renilla activity values, so as to exclude variation in transfection efficiency. Duplicates were then averaged and normalised against an empty vector, so as to exclude non-specific effects of the vector.

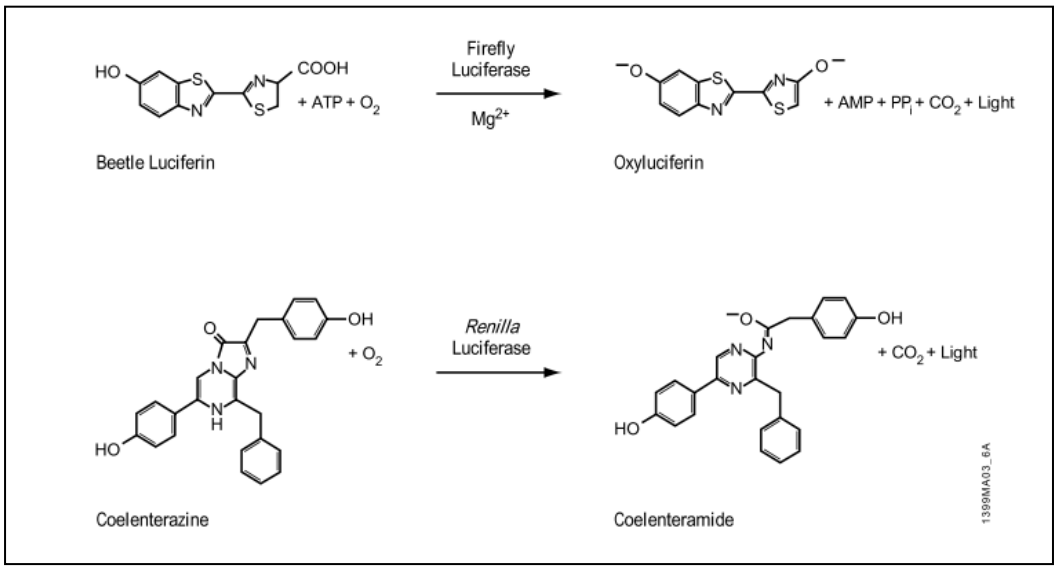

Figure 2.3. **Firefly and Renilla luciferase bioluminescent reactions.**
Image sourced from Dual-Luciferase Reporter Assay System (Promega) Manual.

2.4. Quantitative Real-time Polymerase Chain Reaction (qRT-PCR)

2.4.1. Harvesting RNA

RNA was extracted from cells using the High Pure RNA Isolation Kit (Roche, Germany) according to the manufacturer's instructions. Briefly, a 90% confluent 6cm dish of cells was washed twice in 1 X PBS to remove residual medium. 200µl 1 X PBS and 400µl of lysis buffer were then added to the dish and scraped down using a sterile scraper. The sample was then added to a microfuge tube and vortexed for 15 sec. At this point the lysate was either used directly or stored at -80^{o}C. Following this step the sample was pipetted into a high filter tube, placed in a collection tube and centrifuged at 10000rpm for 15 sec at RT. The flow-through was then discarded and a mixture of 10µl DNase1 and

90µl DNase incubation buffer (final volume 100µl) were added to the column and incubated at RT for 15 min. 500µl of Wash buffer 1 was then added to the column, the sample centrifuged as before and the flow-through discarded. The same step was repeated with 500µl Wash buffer 2. An additional 200µl Wash buffer 2 was added to the column and centrifuged at 13000rpm for 2 min. After discarding the flow-through the filter was moved to a new eppendorf tube and 50µl of elution buffer was added to the column. The column was then centrifuged at 10000rpm for 10 min to elute the RNA. The RNA was either used directly or stored at -80^{o}C.

2.4.2. Reverse transcription

Reverse transcription of RNA was performed using the ImProm-II™ reverse transcription system (Promega, USA) according to the manufacturer's instructions. This allowed the RNA to be converted into complementary DNA (cDNA). Briefly, 1µg of RNA was combined with 1µl of Oligo (dT) primer, made up to a volume of 5µl with sterile water and denatured at 70^{o}C for 5 min. Following this the solution was chilled on ice and then combined with reverse transcription reaction mix (1X ImProm-II™ Reaction buffer, 3mM $MgCl_2$, 0.5mM dNTP mix, 20 units RNasin® ribonuclease inhibitor and 1µl of ImProm-II™ reverse transcriptase) to a final volume of 20µl. After annealing at 25^{o}C for 5 min, the reactions were incubated at 42^{o}C for 1 hr, followed by 15 min incubation at 70^{o}C to inactivate the reverse transcriptase. All tubes and tips used were double autoclaved before use to prevent RNA degradation by RNAses.

2.4.3. qRT-PCR

2.4.3.1. Applied Biosystems StepOnePlus PCR System

qRT-PCR reactions were carried out using 2µl of diluted cDNA, 5µl Power SYBR® Green PCR Master Mix (Applied Biosystems, UK), 0.3µl of forward and reverse primers and 2.4µl sterile water to make a final volume of 10µl. Primers to amplify the human TBX3 and p21 gene were used as well as primers to glucuronidase-beta (GUSB). GUSB is a housekeeping gene which is constitutively and ubiquitously expressed at low levels. It is often used as an internal control for genes which have low expression levels such as transcription factors. Each qRT-PCR was performed in triplicate and a non-template control (NTC), containing water in the place of cDNA template, was also included with every assay to check for contamination. Reactions were set up in a 96-well plate, centrifuged at 1500rpm for 15 min and placed in the StepOnePlus™ PCR system (Applied Biosystems, USA). PCR cycle parameters were: denaturation for 15 min at 95^{o}C, combined annealing and extension for 35 cycles at 60^{o}C for 1 min. The $2^{-\Delta\Delta Ct}$ method was employed to analyse results. Relative mRNA expression levels of TBX3

and p21 were normalised to mRNA levels of GUSB and PCR efficiency correction was calculated using the formula Ratio = (Etarget)CPtarget(control – sample)/(Eref)CPref(control – sample); E: real-time PCR efficiency, CP: crossing-point.

2.4.3.2. Lightcycler Version 3

qRT-PCR was performed using the Sensimix lite kit (Quantace, USA) according to the manufacturer's instructions. For the PCR reaction, 10µl of a master mix containing 1X Sensimix Lite, 1X SYBR Green, Enzyme mix, dH_20 and forward and reverse primers (Qiagen) was made for each reaction and 1µl of cDNA was used per reaction. Primers for TBX3 and p21 were used as well as GUSB primers for internal normalisation. Each qRT-PCR was performed in duplicate and a non-template control (NTC), containing water in the place of cDNA template, was also included with every assay. The capillaries were sealed, centrifuged at 2500rpm for 30 sec and placed in the LightCycler Version 3 (Roche). PCR cycle parameters were: denaturation (15 min at 95^{o}C), annealing and amplification at 35 cycles (5 sec at 95^{o}C; 3 sec at 55^{o}C; 5 sec at 72^{o}C), and a melting (15 sec at 65^{o}C) and a cooling step (30 sec at 40^{o}C). Melting curve analyses was carried out and data was analysed using the $2^{-\Delta\Delta Ct}$ method as described in section 2.4.3.1.

2.5. Western Blot Analysis

2.5.1. Luciferase lysate preparation and protein harvest

Western blot analyses were performed to investigate the levels of transfected protein within cell lysates used for luciferase assays as well as harvested protein samples. To prepare luciferase lysate samples for separation on a SDS-PAGE, 9µl of 5 X protein loading dye (see Appendix 6.4.) was added to 35µl of luciferase lysate and the sample was boiled for 5 min at 100^{o}C. Protein was harvested on ice from 80-90% confluent cells, whereby the medium was removed from the cells, they were washed twice with 1 X chilled PBS and a protein harvesting buffer known as 2 X boiling blue (see Appendix 6.4.) was added to the wells. The cells were lysed by scraping with a sterile plastic scraper, collected in a microfuge tube and then boiled at 100°C for 10 min to denture the protein.

2.5.2. Sodium-dodecyl-sulphate polyacrylamide gel electrophoresis (SDS-PAGE)

Protein samples were electrophoresed on 1.5mm (thick) 8-15% resolving gels with a 5% stacking gel (see Appendix 6.4.). An 8% resolving gel was typically used to detect TBX3, which is a 79.389 kDa protein (UNIPROTKB accession: **O15119)** and 15% resolving gels were used to detect p21, a 21kDa

protein. Gels were cast in Biorad Mini PROTEAN© 3 casting apparatus, placed in the Biorad running tank and the tank was filled with 1 x running buffer (see Appendix 6.4.). In the case of luciferase lysates, the entire lysates volume (44µl) was loaded into the wells, whereas approximately 1/7th of the 2 X boiling blue harvested protein samples was loaded. 6µl of PageRuler Prestained Protein Marker (Fermentas, USA) (See Appendix Figure 6.4.) was also loaded to determine the relative size of the proteins. The running apparatus was connected to the Biorad Powerpack 200 (South Africa) and electrophoresis occurred at 100V for 2 hr to separate the proteins.

2.5.3. Protein transfer onto a nitrocellulose membrane

Electrophoresed proteins were transferred onto Hybond ECL nitrocellulose membrane (Amersham, Biosciences, UK) cut to the size of the gel. Gels were placed in a transfer 'sandwich' cassette consisting of sponges, whatman filter paper, the gel and the nitrocellulose membrane. This cassette was then placed into the transfer unit of the Biorad Mini PROTEAN© 3 transfer tank in the correct orientation. An ice pack was placed in the tank to prevent overheating and the tank was filled with 1 X transfer buffer (see Appendix 6.4.). The transfer apparatus was connected to the Biorad Powerpack 200 and protein transfer took place at 100V for 1.5 hr.

2.5.4. Western blot detection

Following transfer, membranes were rinsed twice briefly with 1 X PBS/0.1% Tween (see Appendix 6.4.) and blocked for 1 hr at RT with blocking buffer (see Appendix 6.4.). Following blocking the membranes were incubated in 1 X PBS/0.1% Tween and 5% milk with appropriate primary antibody dilutions overnight at 4^{o}C with gentle shaking. The membrane was probed with the following primary antibodies: polyclonal rabbit anti-p21 (1:500) (Santa Cruz Biotechnology Inc. C-19), polyclonal rabbit anti-TBX3 (1:500) (Zymed, San Francisco, CA), monoclonal mouse anti-HA (1:1000) (Sigma-Aldrich, H9658), mouse monoclonal anti-flag (1:1000) (Sigma, USA), polyclonal rabbit anti-p38 (1:5000) (Sigma, USA) and monoclonal mouse anti-α tubulin (1:500) (Sigma-Aldrich, sc-8035). The following day membranes were washed in PBS/0.1% Tween (2 X 10 min washes and 2 X 5 min washes) and incubated with horseradish peroxidase-conjugated anti-mouse or anti-rabbit secondary antibody (1:5000) (BioRad, Hercules, CA, USA) for 1 hr. Secondary antibodies were diluted and made up in 5ml of blocking buffer per blot. Membranes were then washed as before in 1 X PBS/0.1% Tween and the signal visualised by enhanced chemiluminescence (ECL) using the SuperSignal West Pico Chemiluminescent Substrate Kit (Pierce, Rockford, IL, USA). 750µl of detection reagent A and detection reagent B was used per blot in a 1: 1 ratio and allowed to incubate on the membrane for 1

min before being enclosed between two acetate sheets. The substrate for horseradish perioxidase (conjugated to the secondary antibody) is found within the detection reagent and therefore oxidation of the substrate is catalysed when the detection reagents comes into contact with the secondary antibody; leading to the emission of light. Membranes were exposed to x-ray film and the resulting chemiluminscent signal captured by developing and fixing the blot. Densitometric analysis was carried out to quantify the bands using Unscan-it gel 6.1. software.

2.6. Non-radioactive Electrophoretic Mobility Shift Assay (EMSA)

2.6.1. Nuclear extraction

Nuclear extract was prepared from confluent CT-1 cells pelleted at 1500rpm for 5 min at 4°C. Following this the cells were resuspended in 1 X PBS and pelleted twice more after which the supernatant was discarded. The cells were then resuspended in cell buffer A (see Appendix 6.5.), incubated on ice for 15 min and then 0.3% triton-X was added followed by a 5 min incubation step on ice. The lysate was then centrifuged for 4 min at 3000rcf at 4°C to separate the cytosolic and nuclear fraction and the nuclear pellet resuspended in cell buffer B (see Appendix 6.5.). DTT and protease inhibitors were also added to prevent degradation of the protein.

2.6.2. Quantification of protein

The nuclear extracts obtained for the non-radioactive EMSA were quantified using the Thermo Scientific Pierce BCA Protein Assay Kit (Rockford, USA). The bicinchoninic acid (BCA) protein assay relies on the colourimetric reaction which takes place when Cu^{+2} is reduced to Cu^{+1} by protein in an alkaline environment. When the BCA molecules present in the solution chelate with one cuprous ion this produces a purple-coloured reaction product which is absorbed at 562nm. This absorbance increases with an increase in protein concentration, and the final colour will continue to develop over time. By using a common protein such as bovine serum albumin (BSA) at known concentrations one is able to plot a standard curve of protein concentration against absorbance. It is this curve from which the concentration of an unknown protein with a particular absorbance can be predicted. A series of BSA standards of known concentrations (A-I) diluted in RIPA buffer (see Appendix 6.5.), as shown in **Table 2.2.**, were prepared and assayed alongside the nuclear lysate protein. BCA working reagent was prepared by mixing 50 parts of BCA reagent A with 1 part BCA reagent B. 25µl of each standard as well as the nuclear extract protein were then added to the wells of a 96-well plate in duplicate. 200µl of the BCA working reagent was then added to each well, the plate was covered in

parafilm to avoid evaporation and incubated at 37°C for 30 min. Following this, absorbance at 562nm was measured in a Rayto RT-21000 96-well Microplate reader (China). The measurement from the blank reading was then subtracted from the readings for the standards and the nuclear extract protein. A standard curve was plotted using the absorbance readings for standards A to I versus their known concentration. From the curve the concentration of the nuclear extract protein was determined.

Table 2. 2. **Preparation of diluted albumin (BSA) standards.**
Table sourced from Pierce BCA Protein Assay Kit Instruction manual.

Dilution Scheme for Standard Test Tube Protocol and Microplate Procedure (Working Range = 20–2,000 µg/ml)			
Vial	**Volume of Diluent**	**Volume and Source of BSA**	**Final BSA Concentration**
A	0	300 µl of Stock	2,000 µg/ml
B	125 µl	375 µl of Stock	1,500 µg/ml
C	325 µl	325 µl of Stock	1,000 µg/ml
D	175 µl	175 µl of vial B dilution	750 µg/ml
E	325 µl	325 µl of vial C dilution	500 µg/ml
F	325 µl	325 µl of vial E dilution	250 µg/ml
G	325 µl	325 µl of vial F dilution	125 µg/ml
H	400 µl	100 µl of vial G dilution	25 µg/ml
I	400 µl	0	0 µg/ml = Blank

2.6.3 Biotinylation of oligonucleotide probes

Single stranded oligonucleotides were resuspended in TE buffer (10mM Tris pH 7.6, 1mM EDTA). A final concentration of 100nM p21WT oligonucleotide probe (5'–CTCGAGGCCAGCTGAGGTGTGAGCAGCTGCCG-3') was labelled using the Biotin 3' End DNA Labelling Kit (Thermo Scientific) according to the manufacturer's instructions. Briefly, 25µl ultrapure water, 10µl 5 X TdT reaction buffer, 5µl 1uM unlabelled oligonucleotide, 5µl biotin and 5µl 2U/µl diluted TdT were incubated at 37°C for 30 min. 2.5µl 0.2M EDTA (pH 8.0) was then added to stop the reaction, followed by the addition of 50µl chloroform: isoamyl alcohol (24:1) to extract the TdT. The solution was vortexed briefly and then centrifuged at 13000rpm for 2 min to separate out the phases. The top aqueous phase was then transferred to a fresh microfuge tube, the oligonucleotide and its reverse complement added to the same tube and then heated to 95°C for 2 min to anneal the strands after which it was slowly cooled to RT. The labelled p21WT probe was kept at -20°C before use. The cold p21WT, p21Mut (5'-CTCGAGGCCAGCTGAGGCTCGAGCAGCTGCCG-3') and consensus T-element (5'-CTTAGGGAATTTCACACCTAGGTGTGAAATTCCCT-3') oligonucleotides were made up to a molar excess of 5X and 10X the amount of labelled probe. Their complementary strands were then annealed as for the labelled probe.

2.6.4. EMSA

An 8% non-denaturing polyacrylamide gel (see Appendix 6.5.) was pre-electrophoresed in 0.5% TBE (22.5mM Tris/borate and 0.5mM EDTA) for 1 hr at 100V. The above mentioned oligonucleotides were used in binding reactions with CT-1 nuclear extract and samples for the gel were prepared as follows: 20µg of nuclear extract protein, 1µl polydI/dC (1µg/ml), 4µl 5 X incubation buffer (see Appendix 6.5.), 1µl DTT (10µM), 2µl labelled p21WT probe, 10 X loading dye (see Appendix 6.5.) brought to a final volume of 20µl. Competition was performed using 5 and 10 X molar excess of unlabelled probe and 1µg of TBX3 antibody (sc-17871, Santa Cruz Biotechnology Inc.) was used for supershift analysis. Following the loading of the samples, the gel was run for 2 hr at 200V on ice. The gel was then transferred to a nylon membrane in fresh 0.5% TBE at 0.38A for 30 min. The membrane was then dried and the DNA cross-linked to the membrane using the UV Stratlinker 1800 apparatus (Stratgene). Following this the membrane was incubated in 1 X blocking buffer (see Appendix 6.5.) for 15 min, HRP-Streptavidin-agarose conjugate (1:300) (Pierce) in blocking buffer for 15 min, wash buffer (see Appendix 6.5.) for 5 X 5 min and in equilibration buffer (see Appendix 6.5.) for 5 min. Chemiluminescence detection reagent (LightShift Chemiluminescent EMSA Kit (Pierce)) was added to the membrane and the signal visualised using a UVP biospectrum imagining system (Visionworks LS software).

2.7. Chromatin Immunoprecipitation Assay (ChIP)

2.7.1. Cross-linking, lysis and sonication of cells

CT-1 cells were plated in 15cm tissue culture dishes and harvested at 90% confluence in 40ml RT 1 X PBS. One 15 cm dish was used per antibody. Cell proteins and DNA were cross-linked for 5 min with the addition of 1096ml 36.5% formaldehyde [final concentration 1%] (Sigma, St. Louis, MO, USA) and the reaction quenched thereafter by the addition of 4ml 1.25M glycine for 5 min at RT. The cells were then centrifuged at 1600 rpm for 5 min at 4^{o}C, washed in 15ml chilled 1 X PBS and spun as before. The pellet was resuspended in 1.5ml 1 X PBS and pelleted once more at 1500xg at 4^{o}C for 5 min. This was followed by resuspension of the cell pellet in NCP buffer 1 (see Appendix 6.6.), centrifugation as before, resuspension in NCP buffer 2 (see Appendix 6.6.) and a final centrifugation step as before. The pellet was then resuspended in 500µl of lysis buffer (see Appendix 6.6.) and protease inhibitors for 10 min on ice. The cell lysate DNA was then sheared to fragments between 300-500bp using a Sonicator (MSE Soniprep 150). 16 bursts at 18 amplitude microns for 10 sec with

a period of 30 sec between sonications was used for most experiments. The lysate was kept on ice throughout the sonication step to prevent the sample from overheating. A portion of the sonicated lysate was then run on a 1% agarose gel alongside a GeneRuler™ 100bp DNA ladder (Thermo Scientific) for 40 min at 80V to visualise the size of the sheared DNA. Following this the sample was centrifuged at 13000rpm at 4^{o}C for 10 min and stored at -80^{o}C.

2.7.2. Pre-clearing, immunoprecipitation and extraction

The sonicated lysate was thawed and added to 1ml of RIPA-IP buffer (see Appendix 6.6.) with protease inhibitors. The sample was then added to 90µl of Protein A/G PLUS-agarose beads (Santa Cruz Biotechnology Inc.) which had been washed in RIPA buffer beforehand and the sample rotated for 1.5 hr at 4^{o}C. Following the first pre-clearing step, the sample was pulsed for 15 sec on a bench top centrifuge to collect the beads at the bottom of the tube and the pre-cleared supernatant was transferred to a fresh tube containing 50µl of washed Protein A/G PLUS-agarose beads. This was repeated in a third pre-clear step. 5% of the pre-cleared supernatant was set aside as the input sample and the rest of the supernatant divided in two. 8µg of TBX3 primary antibody (sc-17871, Santa Cruz Biotechnology Inc.) was added to one half of the sample and 8µg normal rabbit IgG (negative control, Santa Cruz Biotechnology) added to the other half. The samples were rotated at 4^{o}C overnight along with the input sample. Following overnight rotation the beads were added to 50µl of washed protein A/G beads and rotated for 3 hr at 4^{o}C. The beads were then once again spun down in a bench top centrifuge to collect the beads, and the beads then washed twice for 10 min in 750µl of the following wash buffers: Wash buffer 1, Wash buffer 2, Wash buffer 3 and Wash buffer 4 (see Appendix 6.6.). The beads were collected and incubated in 100µl of extraction buffer (see Appendix 6.6.) for 15 min at RT with gently tapping of the tube to resuspend the pellet. The beads were then pelleted at 2000xg for 1 min and the supernatant collected. The extraction was repeated with another 100µl of extraction buffer to yield 200µl of supernatant. The input sample was made up to 200µl with extraction buffer. Samples were then incubated at 65^{o}C overnight to reverse the cross-links between DNA and protein.

2.7.3. Purification

100µl phenol and 100µl chloroform were added to the sample, mixed and centrifuged at 14000 rpm for 2 min. The top aqueous layer was then collected and the amount measured. 1/10 of the volume of the sample of 3M NaAc as well as 2.5% of the volume 100% cold ethanol was added, the solution

mixed and centrifuged at 10000rpm for 10 min. 1ml of cold 70% ethanol was then added and the DNA pelleted at 13000rpm for 5 min. The pellet was then air dried and resuspended in 31µl sabax water overnight. The concentration of the DNA was then measured using a ND-1000 Nandrop Spetrophotometer (ThermoScientific, USA).

2.7.4. qRT-PCR

qRT-PCR analysis was performed as explained in section 2.4 using 3µl of DNA and primers spanning the T-element close to the initiator of the p21 promoter (Forward-5'-GGGGCGGTTGTATATCAGGG-3', Reverse-5'-TCTCACCTCCTCTGAGTGCC-3'). GAPDH was used as an internal control. Crossing values (Ct) of TBX3 and IgG DNA were adjusted by normalising against the Ct value of 1% of input DNA and the ΔΔCt method was used to determine fold enrichment. The equation was used as follows: $2^{-(\Delta Ct1-\Delta Ct2)}$ (ΔCt1= TBX3 , ΔCt2 = IgG). An overview of the entire ChIP method is illustrated in **Figure 2.4**.

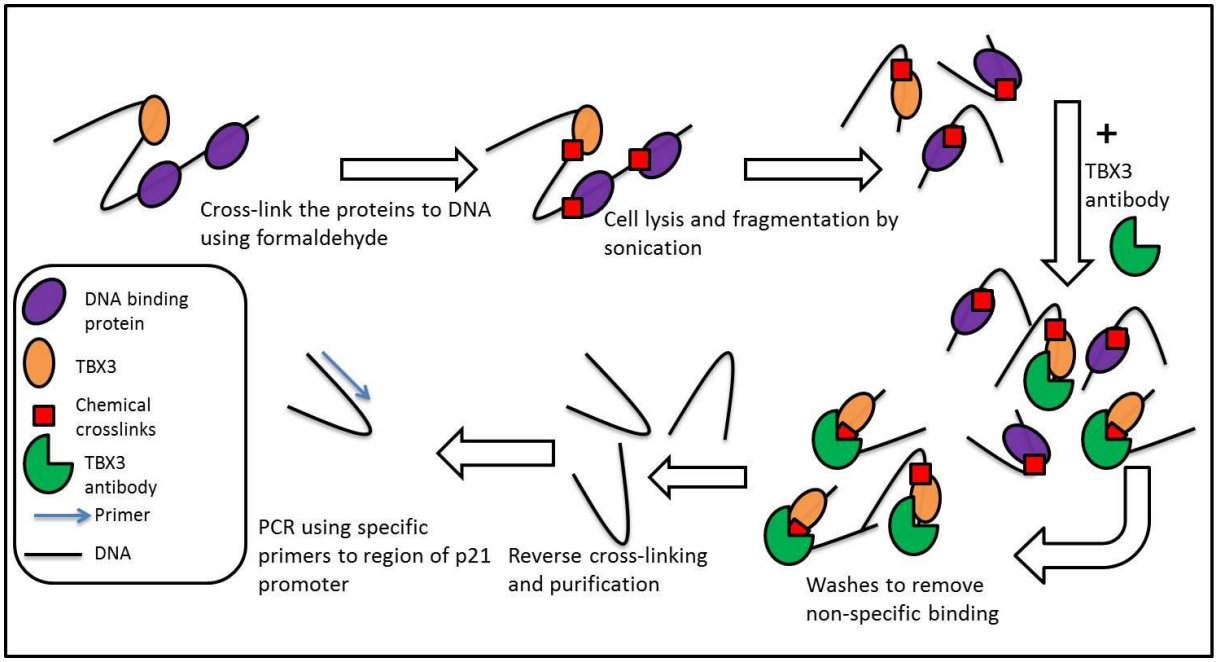

Figure 2.4. **Overview of Chromatin immunoprecipitation (ChIP).**

2.8. DNA Affinity Immunoblot (DAI) Assay

2.8.1. Transfection, whole lysate extraction and quantification and western blot analysis

COS7 cells were plated at 25 X 10^4 in a 6cm dishes. One day later cells were transiently transfected using XtremeGENE HP DNA transfection reagent (Roche), according to the manufacturer's

instructions. 200ng of empty pCMV vector, 100ng of WT TBX3, 100ng of TBX3 SP190A and 200ng of TBX3 S190E was transfected into the cells. All samples were made up to 200ng with empty pCMV vector. Whole cell lysate was harvested 30 hr following transfection. The same protocol was followed as for nuclear extraction in section 2.6.1, however the cytosolic fraction was not separated from the nuclear fraction by centrifugation. Protein concentration was quantified as described in section 2.6.2. 20µg of protein was analysed by western blot analysis as described in section 2.5. An anti-TBX3 antibody was chosen to confirm that the WT TBX3, TBX3 S190A and TBX3 S190E constructs were expressed at equal levels in the cell lysate because COS7 cells have undetectable levels of endogenous TBX3.

2.8.2. Bead preparation

30µl of Dynabeads® M-280 Streptavidin beads (Life Technologies) were placed on a magnet for 1-2 min. The supernatant was then removed and 30µl of 1 X bead binding and washing buffer (see Appendix 6.7) was added to the beads. This was repeated 3 times followed by resuspension of the beads in 60µl of 2 X bead binding and washing buffer. Following this 60µl of washed beads were added to three separate reaction tubes containing 1µg of biotinylated p21 probe (as described in section 2.6.3) and incubated for 15 min at RT with gentle rotation. The biotinylated probe coated beads were then separated with a magnet for 2-3 min and washed 3 times in 1 X bead binding and washing buffer.

2.8.3. DAI

Each reaction of beads/biotinylated probe was resuspended in EMSA binding buffer (see Appendix 6.7), which is a low salt concentration buffer, to a final volume of 200µl. 40µg of WT TBX3, TBX3 S190A and TBX3 S190E protein extract was added to each reaction and incubated for 30 min at 4^{o}C. Following this the protein and probe bound beads were pulled down with a magnet for 2-3 min and then washed 3 time in EMSA binding buffer. 25µl of boiling blue was then added to the samples, followed by boiling for 10 min and detection of the bound protein by western blot analysis as described in section 2.5.

2.9. Statistical analysis

Statistical significance was determined using the student T-test (Excel, Windows Vista). Significance was accepted at $p<0.05$.

3. Results

3.1. TBX3 is a potent transcriptional repressor of the p21 promoter

TBX3 is well known to act as a transcriptional repressor and the protein houses two repression domains R1 and R2 in the C- and N-terminus respectively (Carlson et al. 2001). There is evidence to suggest that the cyclin-dependent kinase inhibitor, p21, is repressed by TBX3 (Carlson et al. 2002; Platonova et al. 2007; Suzuki et al. 2008; Hoogaars et al. 2008) but the details of this regulation have not been elucidated. This was of interest to the current project because p21 is important in controlling cellular processes that protect against malignancy and this repression may represent an additional mechanism by which TBX3 contributes to oncogenesis. To address this the approach was initially to co-transfect COS7 cells with a p21 promoter luciferase reporter construct (depicted in **Figure 3.1A**) together with increasing amounts (100ng-500ng) of a human TBX3 (hTBX3) expression construct and to measure the luciferase activity of the reporter gene. In addition, a pCMV-renilla vector was also transfected into the cells and used as an internal control for transfection efficiency and basal promoter activity was determined using the empty control vector (pCMV). Relative luciferase activity values were normalised to renilla activity and these values were compared to that obtained for the empty pCMV vector. These values were represented as fold repression and the pooled results of three independent experiments each performed in duplicate are shown in **Figure 3.1B**. A clear dosage effect was observed, with as little as 100ng hTBX3 resulting in a 10 fold repression and 500ng hTBX3 leading to an approximately 37 fold repression. To confirm these results, the experiment was repeated in HEK293 human embryonic kidney cells and a similar dose-dependent response, albeit lower, was observed (**Figure 3.1C**). As hTBX3 is expressed as a HA-tagged protein, the levels of transfected TBX3 could be detected by subjecting the luciferase lysates to western blot analysis with an anti-HA antibody. The lower panels of **Figure 3.1B** and **C** confirm successful expression of increasing amounts of transfected TBX3 protein.

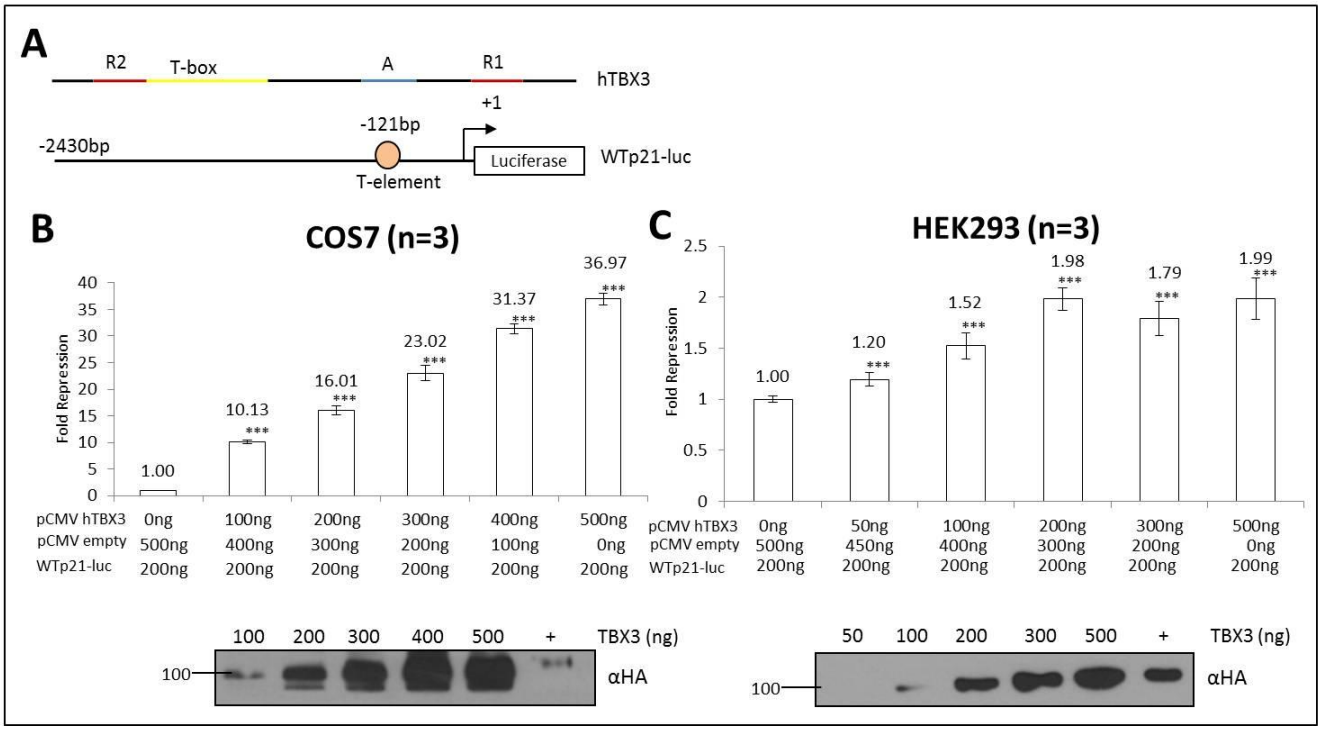

Figure 3.1. **Dose-dependent repression of p21 promoter activity by TBX3.**
A. Schematic diagram of the human TBX3 (hTBX3) expression construct and the p21 promoter luciferase reporter construct used in this study. A=activation domain, R1 and R2=repression domains, T-box=DNA-binding domain. **B.** COS7 and **C.** HEK293 cells were co-transfected with 200ng of the p21 promoter luciferase reporter construct and varying amounts of the hTBX3 expression construct. Thirty hours following transfection cells were lysed and relative luciferase activity measured. Data were normalised against renilla values and fold repression was obtained by comparing the results to that of the empty pCMV vector transfection. This is a pooled result of three independent luciferase experiments each performed in duplicate. A Microsoft Excel student t-test was performed to calculate statistical significance (***$p<0.001$). Error bars indicate the standard error of the mean. **Lower panels**: Western blotting shows expression of HA-tagged hTBX3 protein. HA antibody (1:1000) and goat anti-rabbit secondary antibody (1:5000) were used and the results visualised by chemiluminescence.

3.2. The TBX3 DNA-binding domain is required for repression of p21

The T-box represents the DNA-binding domain which is required for direct binding of T-box factors to their target genes and therefore a mutation in the T-box would be expected to abrogate this ability. Indeed, this approach was previously used to identify E-cadherin and $p19^{ARF}$/$p14^{ARF}$ as genes directly repressed by TBX3 (Rodriguez et al. 2008; Brummelkamp et al. 2002; Lingbeek et al. 2002). Therefore to investigate whether p21 is also a direct target of TBX3, COS7 cells were co-transfected with the p21 promoter luciferase reporter construct together with an empty pCMV vector or vectors expressing a HA-tagged WT hTBX3 or HA-tagged hTBX3 DNA-binding mutant (DBM) (depicted in **Figure 3.2A**). Luciferase activity was measured and fold repression calculated as described for **Figure 3.1**. The results obtained show that while co-transfection with the WT hTBX3 expression construct resulted in an approximately 19 fold repression of the p21 promoter, mutation of the DNA-binding domain significantly abrogated this repression (**Figure 3.2B**). Western blotting of the luciferase lysates with an antibody to HA confirmed that the loss in p21 repression by the hTBX3 DBM was not due to lower levels of expression of this construct (lower panel of **Figure 3.2B**). Furthermore, these results were reproduced in HEK293 cells (**Figure 3.2C**) and in experiments in which the hTBX3 constructs were replaced with the equivalent flag-tagged mouse Tbx3 (mTbx3) expression constructs (**Figure 3.3B & C**). The mouse constructs used allow for the expression of the mTbx3 protein with a flag tag and hence the levels of transfected mTbx3 could be detected by subjecting the luciferase lysates to western blot analysis with an anti-flag antibody (lower panels of **Figure 3.3**). It is important to note that the mTbx3 DBM was expressed as a double band in HEK293 cells but not COS7 cells for reasons that are currently unknown. Together these results show that the DNA-binding domain of TBX3 is important for its repression of p21 and that this repression is likely due to direct binding of p21 by TBX3.

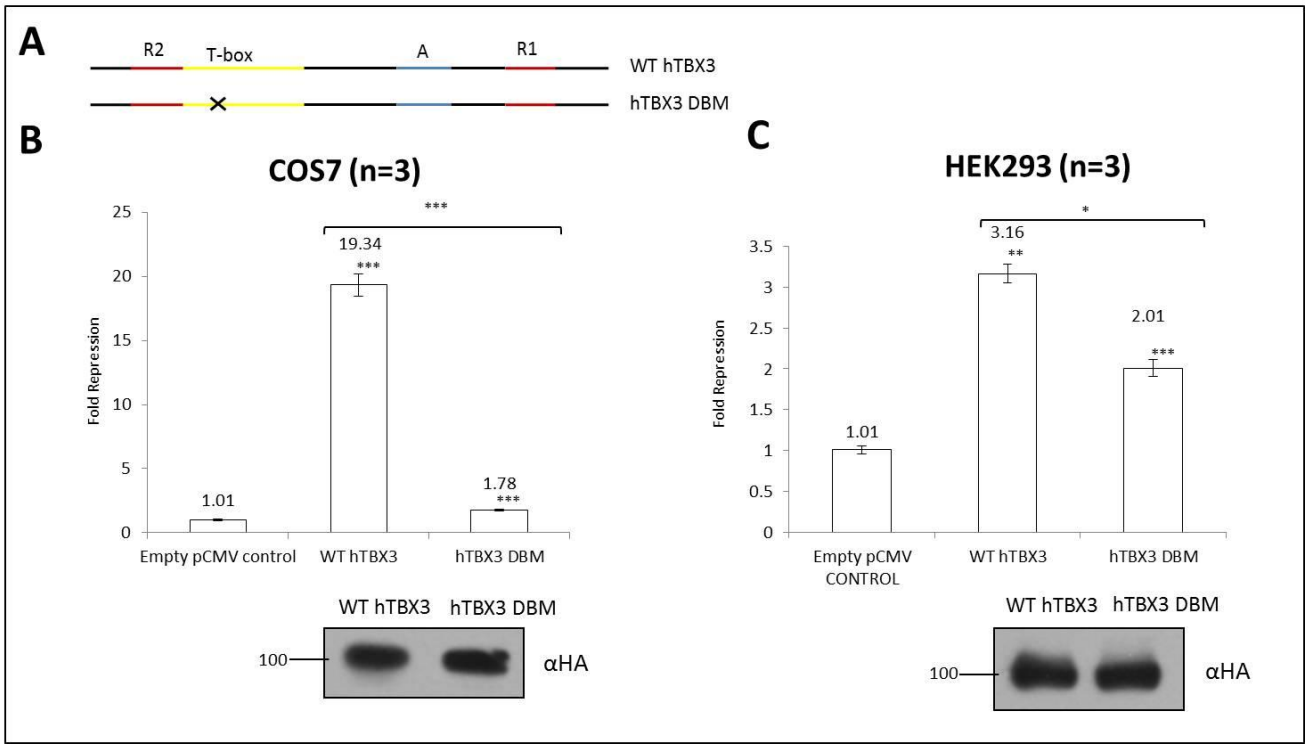

Figure 3.2. **The hTBX3 DNA-binding domain is required for repression of the p21 promoter.**
A. Schematic diagram of the WT hTBX3 and hTBX3 DBM expression constructs. **B.** COS7 and **C.** HEK293 cells were co-transfected with 200ng of p21 promoter luciferase reporter construct together with pCMV empty, WT hTBX3 or hTBX3 DBM expression constructs. Thirty hours following transfection cells were lysed and relative luciferase activity measured. Data were normalised against renilla values and fold repression was obtained by comparing the results to that of the empty pCMV vector transfection. This is a pooled result of three independent luciferase experiments each performed in duplicate. A Microsoft Excel student t-test was performed to calculate statistical significance (*p<0.05; **p<0.01, ***p<0.001). Error bars indicate the standard error of the mean. **Lower panels:** Western blotting shows expression of HA-tagged WT hTBX3 and hTBX3 DBM proteins. HA antibody (1:1000) and goat anti-rabbit secondary antibody (1:5000) were used and the results visualised by chemiluminescence.

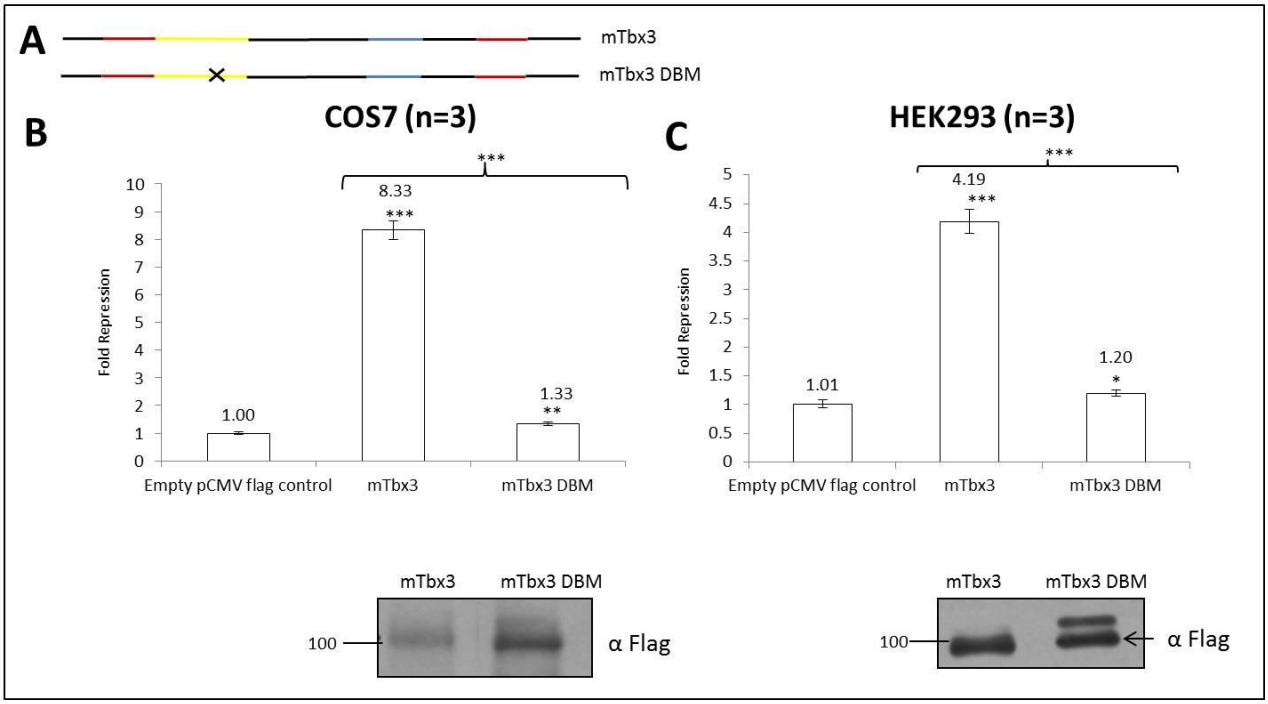

Figure 3.3. **The mouse (m) Tbx3 DNA-binding domain is required for repression of the p21 promoter.**
A. Schematic diagram of the WT mTbx3 and mTbx3 DBM expression constructs. **B.** COS7 and **C.** HEK293 cells were co-transfected with 200ng of p21 promoter luciferase reporter construct together with 400ng of pCMV empty, WT mTbx3 or mTbx3 DBM expression constructs. Thirty hours following transfection cells were lysed and relative luciferase activity measured. Data were normalised against renilla values and fold repression was obtained by comparing the results to that of the empty pCMV vector transfection. This is a pooled result of three independent luciferase experiments each performed in duplicate. A Microsoft Excel student t-test was performed to calculate statistical significance (*p<0.05; **p<0.01, ***p<0.001). Error bars indicate the standard error of the mean. **Lower panels**: Western blots of transfected flag-tagged mTbx3 and mTbx3 DBM proteins. Flag primary antibody (1:1000) and goat anti-mouse secondary antibody (1:5000) were used and the results visualised by chemiluminescence.

3.3. The TBX3 N-terminal domain plays an important role in transcriptional repression of p21

TBX3 has two dominant repression domains, R1, which resides in the C-terminus at amino acids 567-623 and a second repression domain, R2, in the N-terminus (position 123-200). R1 was previously reported to be the dominant repression domain and to determine if this is indeed the case for the repression of p21 promoter activity, a hTBX3 expression construct lacking this domain (referred to as N-term hTBX3; see **Figure 3.4A**) was used in luciferase assays as described earlier. Briefly, COS7 cells were co-transfected with the p21 promoter luciferase reporter construct and the empty pCMV vector, a WT hTBX3 or the N-term hTBX3 expression construct. Whereas expression of the WT hTBX3 led to a 23.05 fold repression of the p21 promoter, expression of the N-term hTBX3 construct resulted in only an 11.43 fold repression (**Figure 3.4B**). The loss of the R1 repression domain thus led to an approximately 50% decrease in the ability of TBX3 to repress p21. This experiment was repeated in HEK293 cells and quite unexpectedly, the N-term hTBX3 protein exhibited a comparable ability to repress the p21 promoter as the WT TBX3 protein (**Figure 3.4C**). Western blots shown in the lower panels of **Figure 3.4B** and **C** confirm similar levels of expression of transfected hTBX3 proteins. Together these results suggest that in contrast to what was previously reported by Carlson et al (2001), other domains in the N-terminal portion of the protein, including the R2 domain, may also be playing a significant role in the repression of p21 by TBX3.

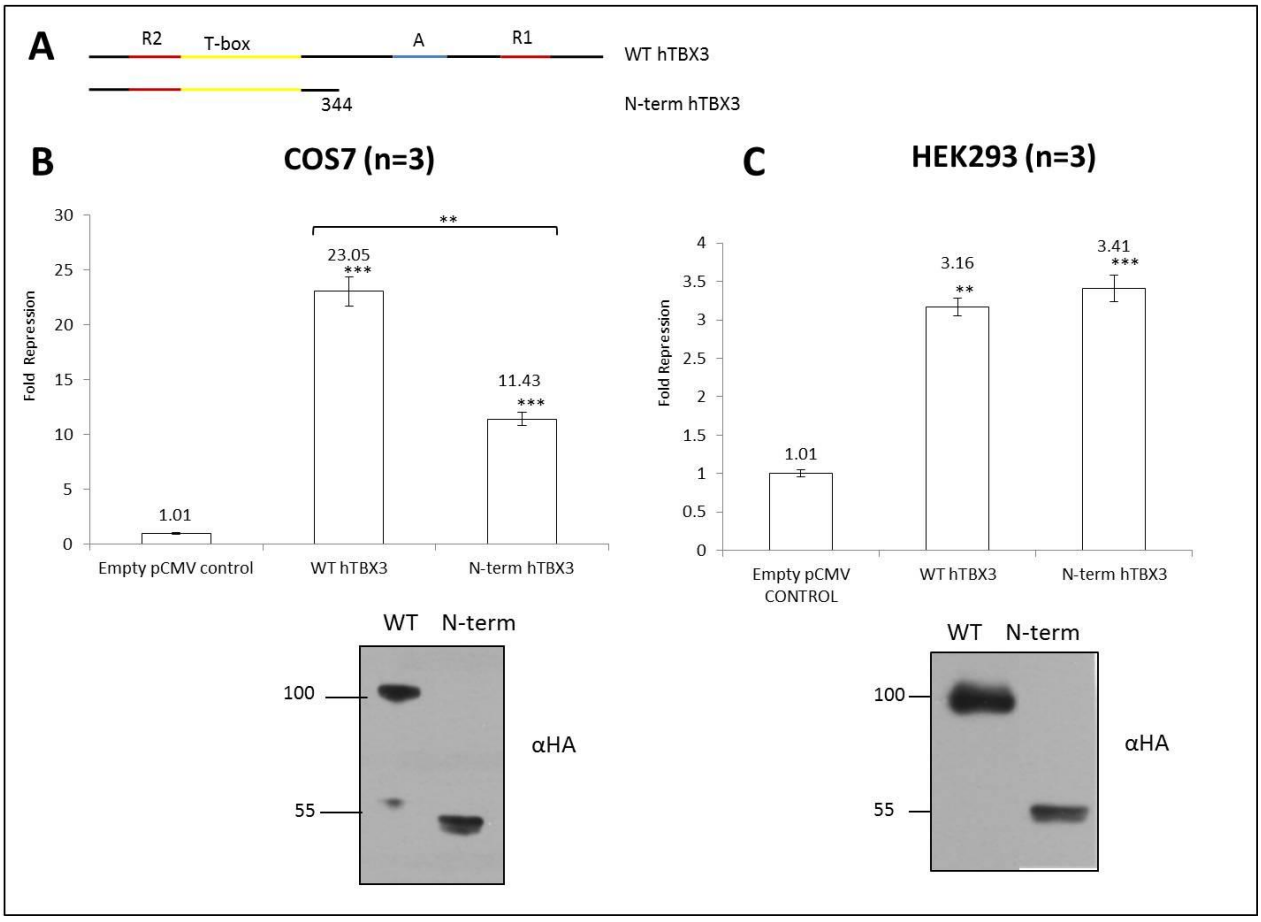

Figure 3.4. **The TBX3 N-terminal domain plays an important role in transcriptional repression of p21.**
A. Schematic diagram of the WT hTBX3 and N-term hTBX3 expression constructs. **B.** COS7 and **C.** HEK293 cells were co-transfected with 200ng of p21 promoter luciferase reporter construct together with pCMV empty, hTBX3 or N-term hTBX3 expression constructs. Thirty hours following transfection cells were lysed and relative luciferase activity measured. Data were normalised against renilla values and fold repression was obtained by comparing the results to that of the empty pCMV vector transfection. This is a pooled result of three independent luciferase experiments each performed in duplicate. A Microsoft Excel student t-test was performed to calculate statistical significance (**p<0.01, ***p<0.001). Error bars indicate the standard error of the mean. **Lower panels**: Western blotting shows expression of HA-tagged WT hTBX3 and N-term hTBX3 proteins. HA primary antibody (1:1000) and goat anti-rabbit secondary antibody (1:5000) were used and the results visualised by chemiluminescence.

3.4. The TBX3 and TBX3+2a isoforms have comparable ability to repress the p21 promoter

TBX3 has been shown to exist as several isoforms (Bamshad et al. 1999), with TBX3 and TBX3+2a being the most studied. TBX3+2a contains an insertion of exon 2a within the T-box DNA-binding domain and there is conflicting evidence in the literature regarding whether these isoforms perform distinct or similar functions (Hoogaars et al. 2008; Fan et al. 2004). This study therefore compared the capacity of these two TBX3 isoforms to repress p21 promoter activity in luciferase reporter assays, using the mouse mTbx3 and mTbx3+2a expression constructs because they were available in our laboratory (**Figure 3.5A**). It is important to note that human and mouse TBX3 are highly homologous and previous experiments showed that they are both able to repress the p21 promoter directly via the DNA-binding domain (see **Figure 3.3B & C**). COS7 cells were co-transfected with a p21 promoter luciferase reporter construct and an empty pCMV vector or the mTbx3 or mTbx3+2a expression constructs, and luciferase activity was measured. **Figure 3.5B** shows that the mTbx3 and mTbx3+2a isoforms repress the p21 promoter approximately 8.3 and 7.5 fold respectively. This difference is not statistically significant which suggests that they are functionally similar in their ability to repress the p21 promoter in COS7 cells. Furthermore, when the same experiment was performed in HEK293 cells, mTbx3 was shown to be only 1.14 fold more efficient than mTbx3+2a in repressing the p21 promoter (**Figure 3.5C**). When the lysates used for this luciferase assay were subjected to western blotting, mTbx3 and mTbx3+2a were shown to be expressed at comparable levels suggesting that the observed ability of the two isoforms to repress the p21 promoter is not skewed by unequal expression (lower panel of **Figure 3.5B&C**). Similar to the expression of the mTbx3 DBM, an additional band was observed for the mTbx3+2a in HEK293 cells and again the reason for this is unclear. These results support data that suggest that the TBX3 and TBX3+2a isoforms are functionally similar in their ability to repress target genes.

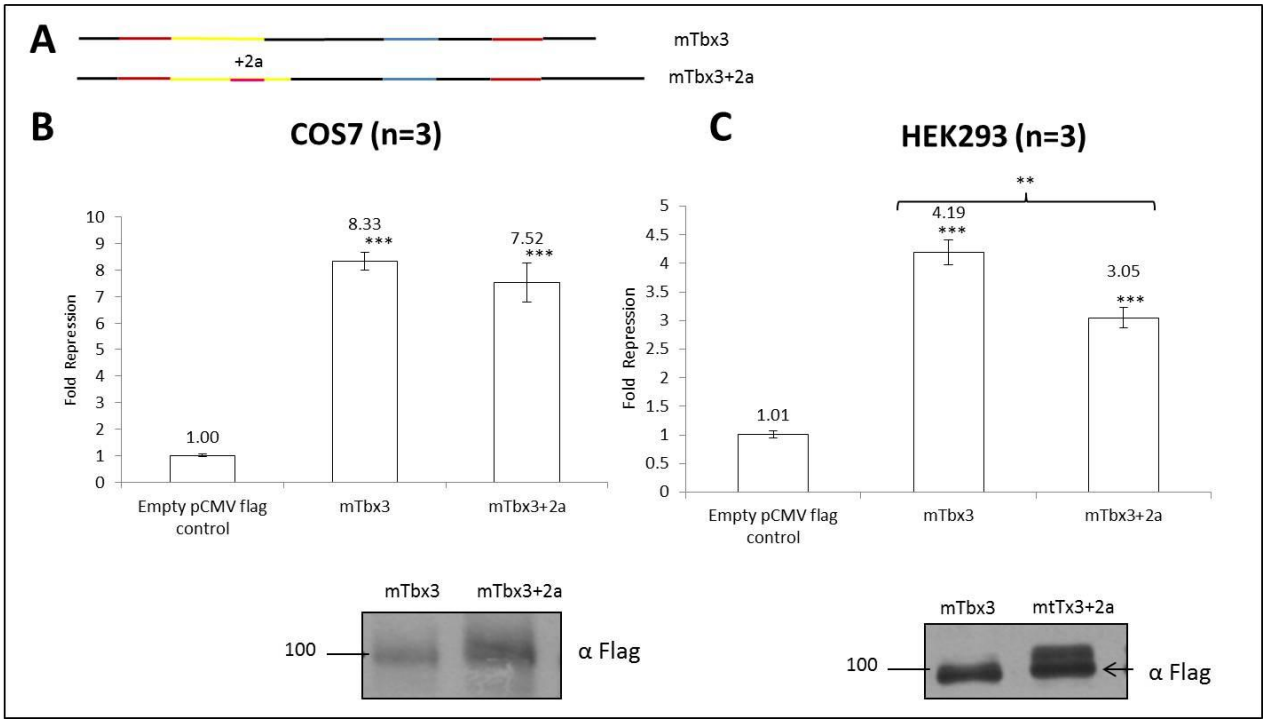

Figure 3.5. **The mTbx3 and mTbx3+2a isoforms have comparable ability to repress the p21 promoter.**
A. Schematic diagram of the mTbx3 and mTbx3+2a expression constructs. **B.** COS7 and **C.** HEK293 cells were co-transfected with 200ng of p21 promoter luciferase reporter construct together with 400ng of pCMV empty, mTbx3 or mTbx3+2a expression constructs. Thirty hours following transfection cells were lysed and relative luciferase activity measured. Data were normalised against renilla values and fold repression was obtained by comparing the results to that of the empty pCMV vector transfection. This is a pooled result of three independent luciferase experiments each performed in duplicate. A Microsoft Excel student t-test was performed to calculate statistical significance (**p<0.01, ***p<0.001). Error bars indicate the standard error of the mean. **Lower panels**: Western blot of transfected flag-tagged mTbx3 and mTbx3+2a proteins. Flag primary antibody (1:1000) and goat anti-mouse secondary antibody (1:5000) were used and the results visualised by chemiluminescence.

3.5. The T-element at -121bp of the p21 promoter mediates repression by TBX3

All T-box proteins tested have been shown to regulate their target genes by binding to the 24bp palindromic sequence AATTT(G/C)ACACCTAGGTGTGAAATT (Kispert and Herrmann, 1993; Müller and Herrmann, 1997) or to a variety of differently spaced and orientated half sites, such as AGGTGTGAAATT, within this palindrome (Kispert et al., 1995; Conlon et al., 2001; Papaioannou, 2001). These T-box consensus sites are known as T-elements and while examination of the p21 promoter identified 19 putative T-elements (**Figure 3.6**), a perfect match AGGTGTGA was found close to the initiator (position -121bp) that was conserved between the human, mouse, and rat p21 promoters (**Figure 3.7A**). Furthermore, TBX2, which is highly homologous to TBX3, was previously shown to repress the p21 promoter via this site and a p21 promoter luciferase reporter construct in which this site was mutated (Mutp21) (GTGTGA→ CTCTGA) was available in our laboratory (depicted in **Figure 3.7B**; Prince et al., 2004). To test whether the T-element at -121bp was also involved in mediating the repression of p21 by TBX3, COS7 and HEK293 cells were co-transfected with the hTBX3 expression construct and either the WTp21 or the Mutp21 promoter luciferase reporter construct and luciferase activity was measured as previously described. The results obtained demonstrate that mutation of the T-element at -121bp completely abrogated the ability of TBX3 to repress the p21 promoter in COS7 cells and led to a 54% loss in repression in the HEK293 cells (**Figure 3.7C & D**). Together these results indicate that the T-element at -121bp, which is close to the p21 initiator, plays a key role in mediating p21 repression by TBX3 and that in some cells other sites may also be important.

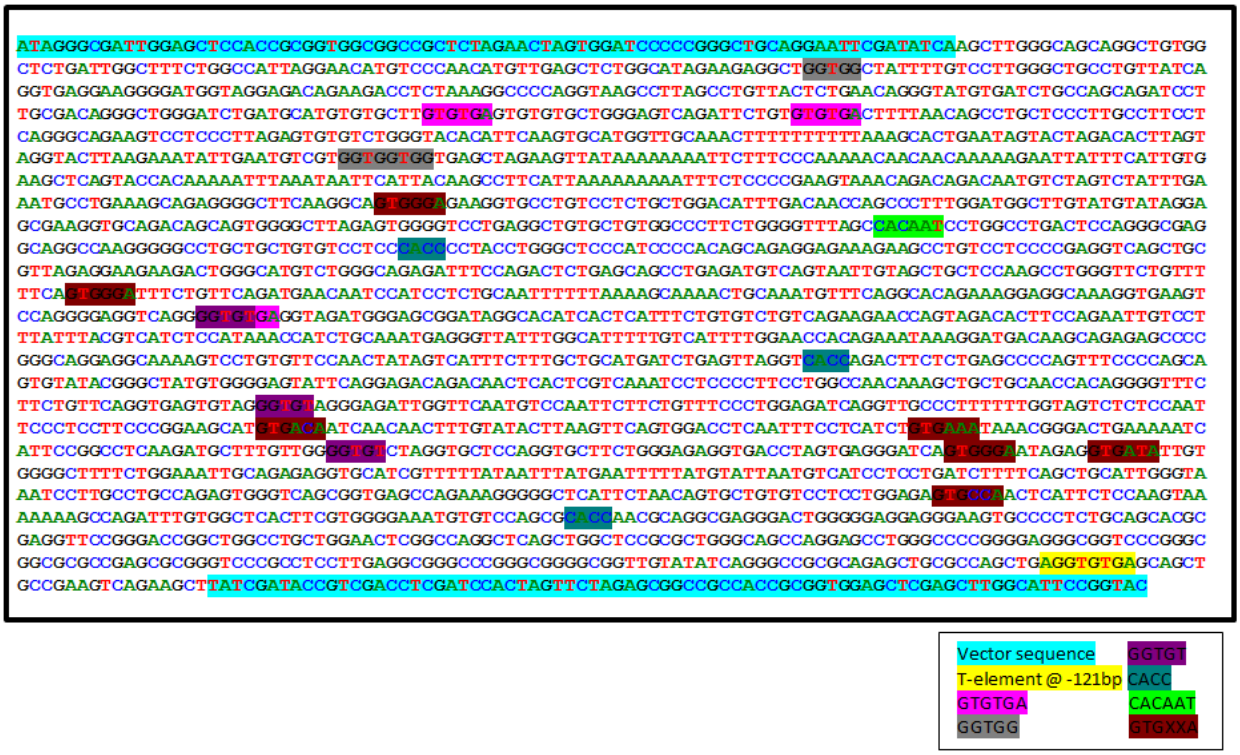

Figure 3.6. **The p21 promoter sequence containing putative T-elements.**
The p21 promoter construct was sequenced and analysed manually for potential T-elements. The T-element at position -121bp is highlighted in yellow.

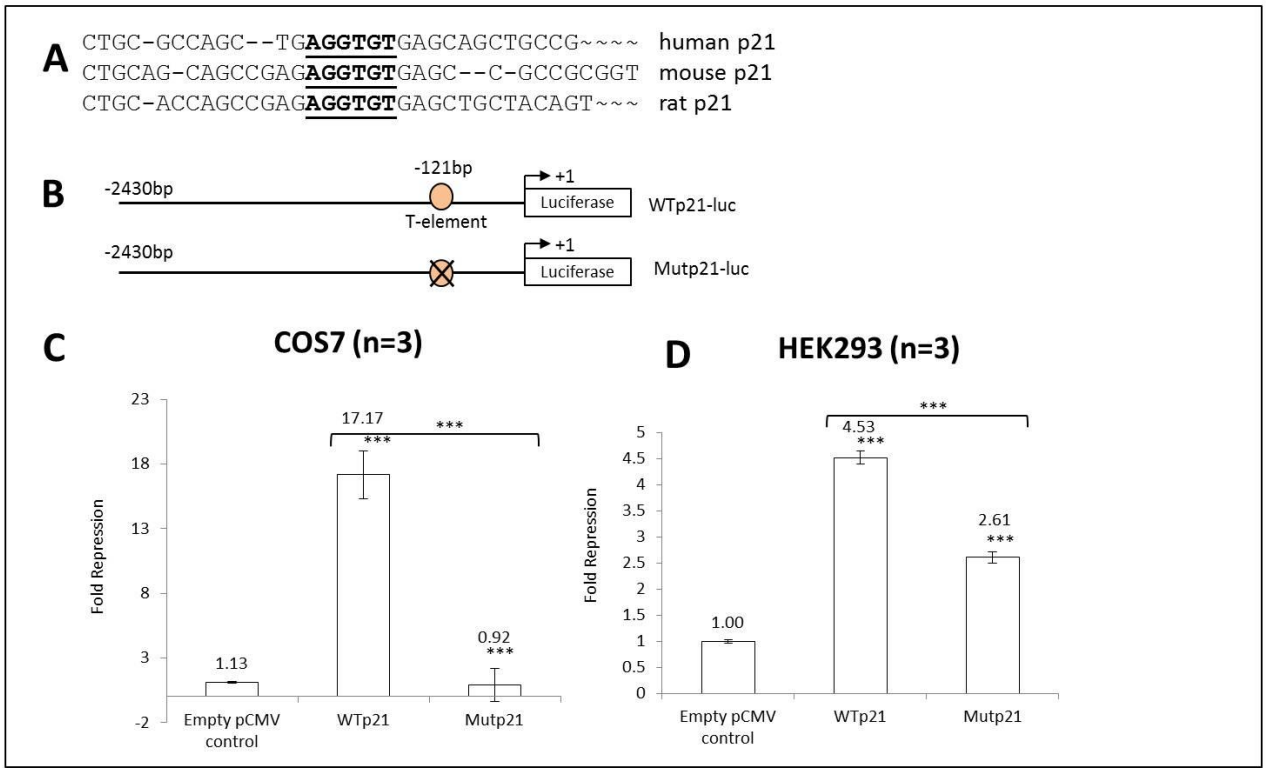

Figure 3.7. **The T-element at -121bp of the p21 promoter mediates repression by TBX3.**
A. Alignment showing conservation of the T-element at position -121bp across the human, mouse and rat p21 promoters. **B.** Schematic diagram of the WTp21 and mutant p21 (Mutp21) promoter constructs. **C.** COS7 and **D.** HEK293 cells were co-transfected with either 400ng pCMV empty vector or hTBX3 expression construct together with 200ng of WTp21 or Mutp21 luciferase reporter constructs. Thirty hours following transfection cells were lysed and relative luciferase activity measured. Data were normalised against renilla values and fold repression was obtained by comparing the results to that of the empty pCMV vector transfection. This is a pooled result of three independent luciferase experiments each performed in duplicate. A Microsoft Excel student t-test was performed to calculate statistical significance (***$p<0.001$). Error bars indicate the standard error of the mean.

3.6. TBX3 binds the T-element at -121bp in the p21 promoter in vitro

To verify that TBX3 binds the T-element at -121bp in the p21 promoter, an electromobility shift assay was performed. Briefly, nuclear extract from CT-1 fibroblast cells, which express high levels of TBX3, was incubated with a biotin-labelled probe spanning this T-element and protein-bound biotinylated oligonucleotides were run on an acrylamide gel, transferred to a nylon membrane and analysed by chemiluminescence using streptavidin-HRP conjugate. As controls, unlabelled oligonucleotides containing either the wild-type (WT) or mutated (Mut) T-element were used to compete for binding (**Figure 3.8A**). **Figure 3.8B** shows that nuclear factors are able to bind to the labelled probe to form a detectable complex (**lane 2**) because no complex forms for the probe only control (**lane 1**). In addition, unlabelled consensus T-element (**lanes 3 & 4**) as well as unlabelled WT probe at a 5X and 10X molar excess (**lanes 5 & 6**) were able to compete for binding of p21 more efficiently than the mutant probe (**lanes 7 & 8**). Furthermore, TBX3 binds the p21 promoter T-element in vitro because in the presence of the TBX3 antibody a block shift of the complex is observed (**lane 9**). Please note that a block shift occurs when the antibody added interferes with the binding of the protein of interest to the probe and therefore the intensity of the complex weakens.

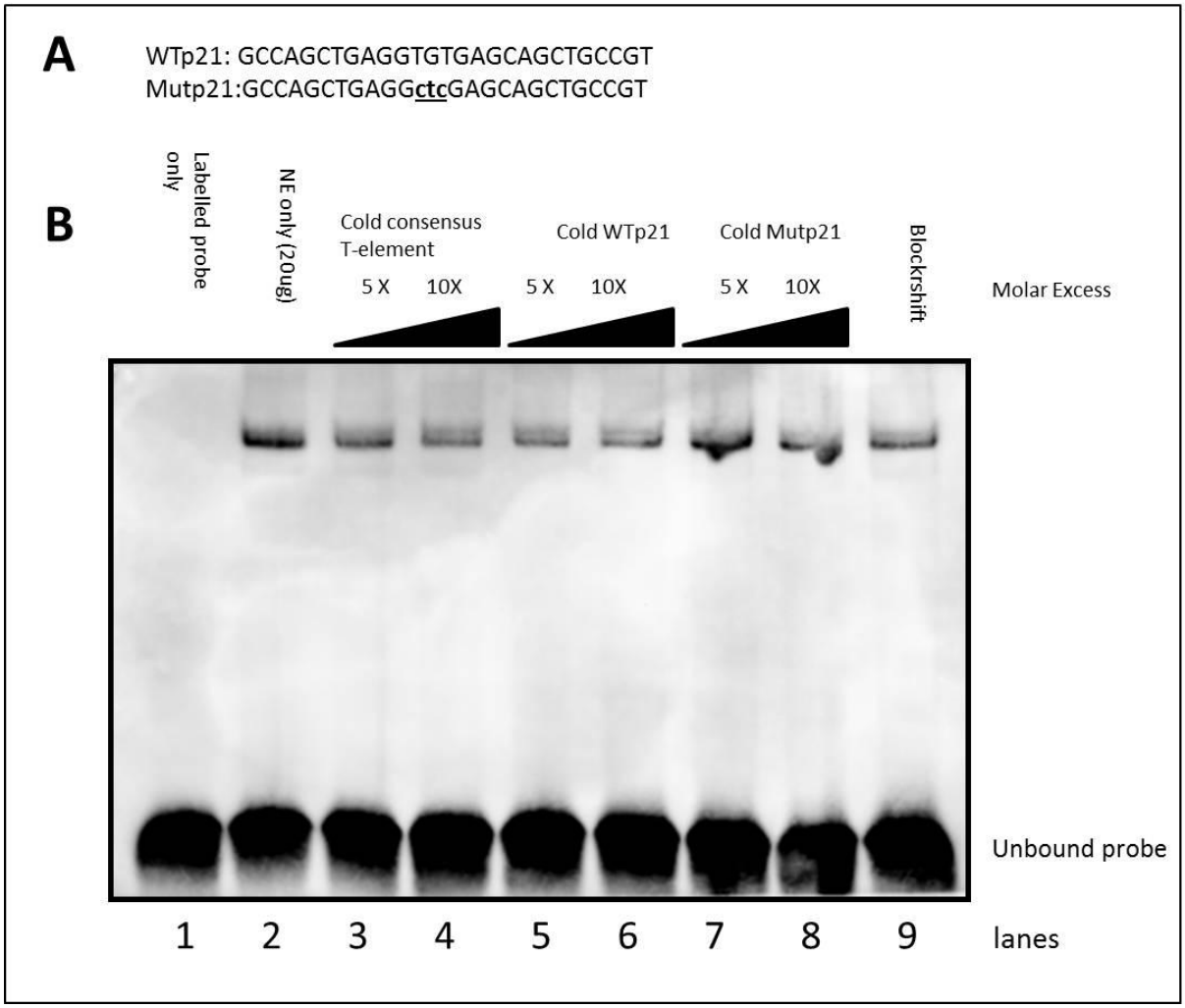

Figure 3.8. **TBX3 binds the T-element at -121bp in the p21 promoter in vitro.**
A. Wild-type (WT) and mutant (Mut) p21 probes. The lowercase letters indicate the mutated base pairs of the T-element. **B.** Electrophoretic mobility shift assay using nuclear extract and biotin-labelled WTp21 oligo as a probe. Lane 1 and 2 represent labelled probe only and labelled probe incubated in nuclear extract respectively. Competition reactions were performed with 5X and 10X molar excess of unlabelled oligo containing WT (lanes 5&6) or Mut (lanes 7&8) p21 T-elements, as well as unlabelled consensus T-element as a positive control (lanes 3&4). Lane 9 shows a blockshift when an antibody to TBX3 (8µg) was included in the reaction.

3.7. TBX3 can bind the p21 promoter in vivo

In order to validate the above results in vivo, Chromatin Immunoprecipitation (ChIP) assays were performed. Briefly, CT-1 fibroblast cells were fixed with paraformaldehyde to cross-link the protein to DNA, the chromatin was then extracted and sheared and the TBX3-bound DNA pulled down using an antibody to TBX3. The cross-links were reversed by heating and the DNA extracted and subjected to qRT-PCR with primers spanning a region of the p21 promoter containing the T-element at -121bp (**Figure 3.9A**). Primers specific to GAPDH were included in these experiments as a negative control. The results show that relative to the non-specific IgG control, there was an approximate 2.84 fold enrichment of TBX3 occupancy on the p21 promoter but not on the GAPDH control (**Figure 3.9B**). In addition, the input, IgG, TBX3 and non-template control qRT-PCR samples were analysed by agarose gel electrophoresis to confirm that an expected 132bp region was indeed amplified by the primer (**Figure 3.9C**). This data suggest that TBX3 binds the p21 promoter in the region of the T-element at -121bp in vivo.

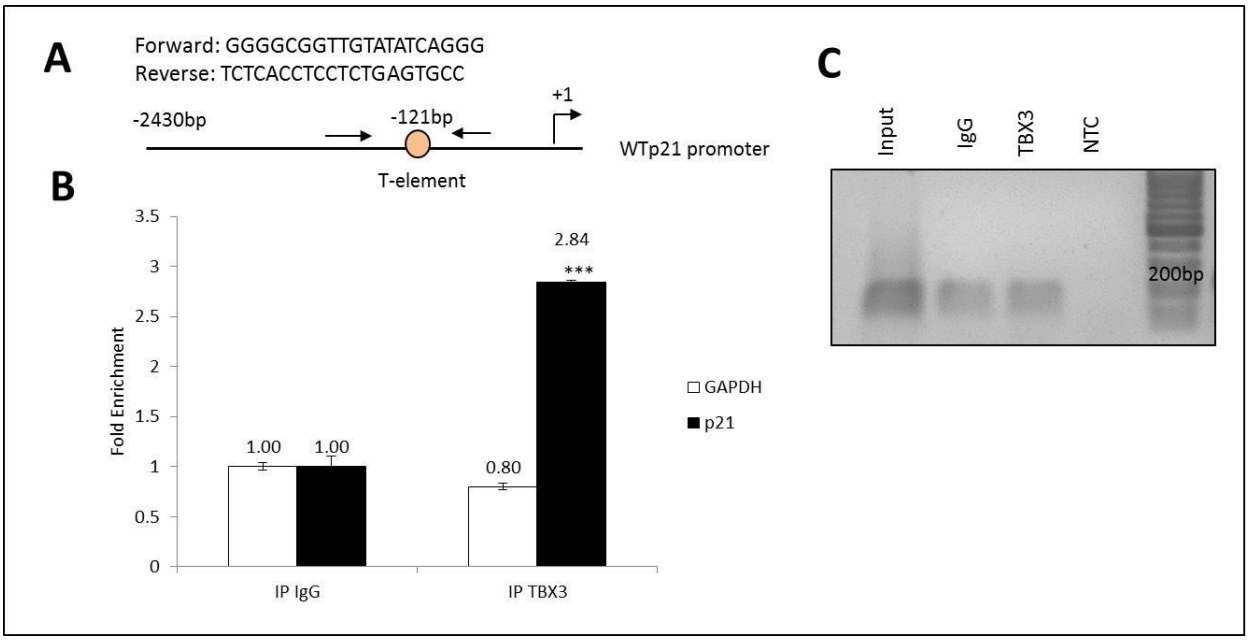

Figure 3.9. **TBX3 binds the p21 promoter in vivo.**
A. Sequence of forward and reverse primers designed to amplify the p21 promoter containing the T-element at -121bp and a schematic of where they bind to the promoter to produce a 132bp product. **B.** CT-1 fibroblast cell lysates were used in a ChIP assay performed with antibodies against TBX3 or IgG (negative control). Immunoprecipitated DNA was assayed by qRT-PCR with primers against the p21 promoter or GAPDH (negative control). The pooled results of two ChIP experiments each performed in triplicate is shown. A Microsoft Excel student t-test was performed to calculate statistical significance (***$p<0.001$). Error bars indicate the standard error of the mean. **C.** The input, IgG, TBX3 and non-template control (NTC) qRT-PCR products were analysed by agarose gel electrophoresis to confirm their size of 132bp.

3.8. Phosphorylation of TBX3 at Serine-Proline 190 can affect its ability to repress p21

To further characterise the mechanism(s) involved in regulating the repression of p21 by TBX3, we focussed on factors that may regulate TBX3 expression. This approach was based on preliminary evidence in our laboratory that suggests that TBX3 protein levels and function may be regulated by phosphorylation. Serine proline (SP) motifs are the minimum potential target sites for phosphorylation by specific kinases and a SP site at residue 190, which resides within the DNA-binding domain of the TBX3 protein, was identified. This site was found to be highly conserved across a number of species (**Figure 3.10A**). To test whether phosphorylation at this site regulates TBX3's ability to regulate p21, site-directed mutagenesis was performed. Briefly, SP190 was mutated to either an alanine (A), to abolish phosphorylation or a glutamic acid (E), to mimic phosphorylation. The effect of these mutations was assessed using luciferase assays where COS7 cells were co-transfected with 200ng of a p21 promoter luciferase reporter construct and the pCMV empty vector, WT TBX3, TBX3 S190A or TBX3 S190E expression constructs (**Figure 3.10A**). **Figure 3.10B** depicts the pooled results of three independent experiments each performed in duplicate, which shows the effect of WT TBX3 and the TBX3 S190A and TBX3 S190E mutants on the p21 promoter. While the WT TBX3 and TBX3 S190A proteins repressed the p21 promoter, pseudophosphorylation of TBX3 (TBX3 S190E) led to a significant loss in the ability of TBX3 to repress the p21 promoter. To exclude the possibility that the results obtained may be due to different levels of TBX3 expression for the different constructs, lysates used for the luciferase assays were also subjected to western blotting. Results show that equal protein expression was observed for each of the constructs (lower panel of **Figure 3.10B**). These results suggest that phosphorylation of S190 does indeed play a role in regulating the transcriptional activity of TBX3 on the p21 promoter.

Since S190 resides within the TBX3 DNA-binding domain, the possibility that phosphorylation at this site may be interfering with the ability of TBX3 to bind to the p21 promoter was further investigated using a DNA affinity immunoblot (DAI) assay. Lysates of COS7 cells transfected with the empty vector, WT TBX3, TBX3 S190A or TBX3 S190E constructs were incubated with biotinylated p21 T-element probes and a pull-down performed with streptaviden magnetic beads. This was followed by western blot analysis of the protein which shows that WT TBX3 binds the T-element at -121bp in the p21 promoter and that the TBX3 S190A mutant has a stronger affinity for this site (**Figure 3.10C**). In contrast, the TBX3 S190E protein was unable to bind this site since no signal was obtained in lysates transfected with this construct. To exclude the possibility that the results obtained may be due to different levels of TBX3 expression for the different constructs, lysates used for the DAI assays were also subjected to western blotting. Results show that equal protein expression was observed

for each of the constructs (lower panel of **Figure 3.10C**). Together the results suggest that phosphorylation of TBX3 at SP190 abolishes its binding and consequently repression of the p21 promoter.

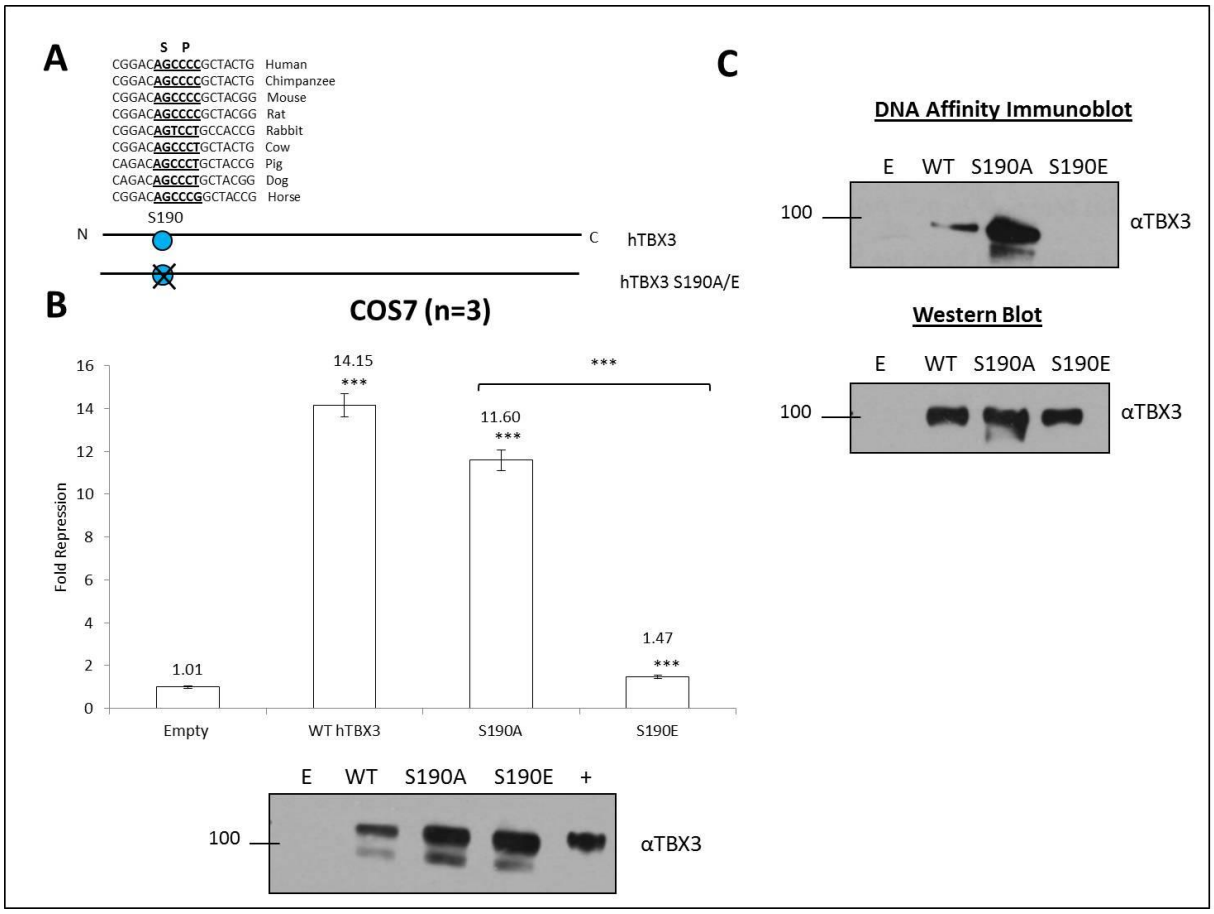

Figure 3.10. **Phosphorylation of TBX3 at Serine-Proline 190 can affect its ability to repress p21.**
A. Alignment showing conservation of the S190 residue of the TBX3 protein across a number of different species as well as a schematic diagram of the WT TBX3 and TBX3 S190A/E mutant expression constructs. **B.** COS7 cells were co-transfected with 200ng of p21 promoter luciferase reporter construct together with pCMV empty, WT TBX3, TBX3 S190A or TBX3 S190E expression constructs. Thirty hours following transfection cells were lysed and relative luciferase activity measured. Data were normalised against renilla values and fold repression was obtained by comparing the results to that of the empty pCMV vector transfection. This is a pooled result of three independent luciferase experiments each performed in duplicate**.** A Microsoft Excel student t-test was performed to calculate statistical significance (***p<0.001). Error bars indicate the standard error of the mean. **Lower panels*:*** Western blots of transfected TBX3 protein. Antibodies to TBX3 (1:500) and goat anti-rabbit secondary antibody (1:5000) were used and the results visualised by chemiluminescence. **C.** DNA-affinity immunoblot assay. Lysates from COS7 cells transfected with empty vector, WT TBX3, TBX3 S190A or TBX3 S190E constructs were incubated with a biotinylated probe matching the T-element at position -121bp of the p21 promoter. A pull-down was performed using streptavidon magnetic beads and the lysates run on an 8% SDS-PAGE gel and analysed by western blotting. An antibody to TBX3 (1:500) and a goat anti-rabbit secondary antibody (1:5000) were used and the results visualised by chemiluminescence. **Lower panel**: Western blotting to check the expression of the WT TBX3, TBX3 S190A and TBX3 S190E constructs. An antibody to TBX3 (1:500) and goat anti-rabbit secondary antibody (1:5000) were used and the results visualised by chemiluminescence.

3.9. The physiological relevance of the repression of the p21 gene by TBX3

The above data begged the question as to whether the repression of p21 by TBX3 is physiologically relevant. To address this, endogenous p21 mRNA and protein levels in control cells (CT-1 and WM1650) and cells in which TBX3 was either stably knocked down (CT-1 shTBX3) or overexpressed (WM1650 TBX3) were compared using qRT-PCR and western blotting respectively. The CT-1 cells are immortalised embryonic lung fibroblasts which express high levels of TBX3 and the WM1650 cells are radial growth phase melanoma cells that express undetectable levels of TBX3 and they were therefore selected for knock down and overexpression of TBX3 respectively. These cell lines were established in our laboratory and therefore available for use in this study.

3.9.1. p21 mRNA and protein levels increase when TBX3 is knocked down in the CT-1 cell line

Total RNA from the CT-1 shScramble and CT-1 shTBX3 cell lines was extracted and reverse transcribed to cDNA. TBX3 and p21 mRNA levels were quantified using qRT-PCR with primers specific to TBX3 and p21 respectively and relative expression levels were normalised against levels of GUSB, a housekeeping gene. It was anticipated that if TBX3 was indeed a potent repressor of the p21 promoter, low TBX3 mRNA levels would lead to a decrease in TBX3 protein levels and thus an upregulation of p21 mRNA levels. Indeed, when TBX3 mRNA levels were knocked down by approximately 30%, there was a corresponding 43% increase in p21 mRNA levels (**Figure 3.11A**). Protein was also harvested from the CT-1 shScramble and CT-1 shTBX3 cell lines and the levels of TBX3 and p21 protein detected by western blot analysis. **Figure 3.11B** and **C** represent the results of two independent experiments which each show that p21 levels are upregulated in the TBX3 knock down cell line and that there is a direct correlation between the degree of TBX3 knock down and upregulation of p21 protein levels. **Figure 3.11B** shows that an 86% knock down of TBX3 corresponded with a 4.75 fold increase in p21 levels, whereas **Figure 3.11C**, shows that a 40% knock down of TBX3 correlated with a substantially less dramatic increase of 2.43 fold in p21 expression. This is indicative that p21 levels are directly affected by TBX3.

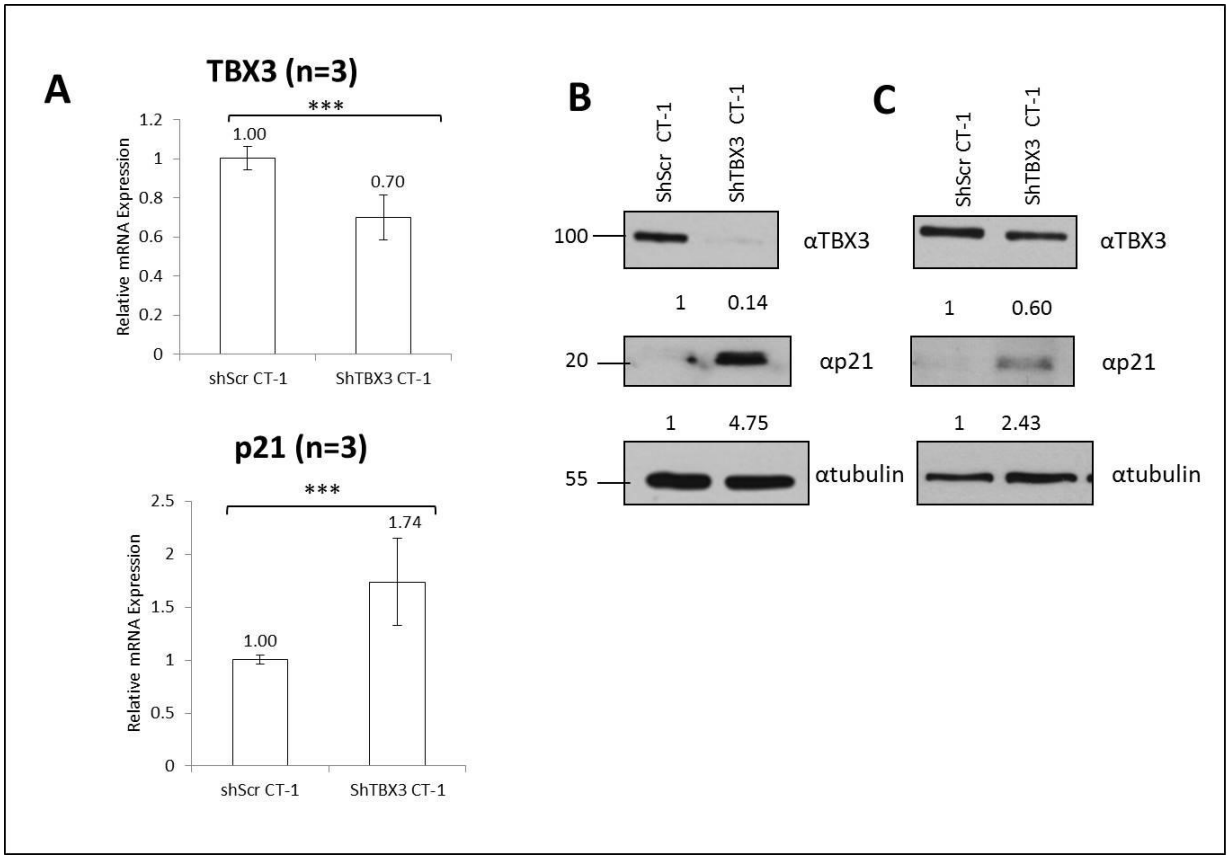

Figure 3.11. **qRT-PCR and western blot analysis of TBX3 and p21 mRNA and protein expression in a control (shScramble) and TBX3 knock down (shTBX3) CT-1 fibroblast cell line.**
A. RNA was harvested and the levels of TBX3 and p21 quantified using qRT-PCR. The reaction was normalised against GUSB levels and a negative water control, containing no cDNA, was also used to determine if there was any contamination (data not shown). This is a pooled result of three independent qRT-PCR experiments each performed in triplicate. A Microsoft Excel student t-test was performed to calculate statistical significance (*** =p<0.001). Error bars indicate standard error of the mean. **B & C.** Western blots of TBX3 and p21 protein levels in shScramble CT-1 and shTBX3 CT-1 cells. Protein was harvested and TBX3 and p21 levels were quantified using antibodies to TBX3 (1:500) and p21 (1:500) and a goat anti-rabbit secondary antibody (1:5000). The data were normalised to a tubulin loading control. These western blots shown are representative of three independent experiments.

3.9.2. p21 mRNA and protein levels decrease in the WM1650 TBX3 overexpressing cell line

Total RNA for the WM1650 control and WM1650 TBX3 overexpressing cells was harvested and reverse transcribed to cDNA and TBX3 and p21 mRNA levels were quantified using qRT-PCR as described above. It was hypothesized that an increase in TBX3 mRNA levels will serve to enhance the ability of TBX3 to repress the p21 promoter and hence to downregulate p21 mRNA levels. Indeed, compared to the control cells, TBX3 mRNA levels in the WM1650 TBX3 overexpressing cells show an approximate 40 fold increase in TBX3 levels (**Figure 3.12A**) which corresponds with a statistically relevant 74% decrease in p21 mRNA levels. Protein was also harvested from control WM1650 cells and WM1650 TBX3 cells and the levels of TBX3 and p21 protein detected by western blot analysis (**Figure 3.12B).** The results show that TBX3 is indeed overexpressed in these cells and that this corresponds to a decrease in p21 protein levels.

Taken together, the results show that the repression of p21 transcription by TBX3 is physiologically relevant since altering the levels of cellular TBX3 impacts on p21 mRNA and protein levels.

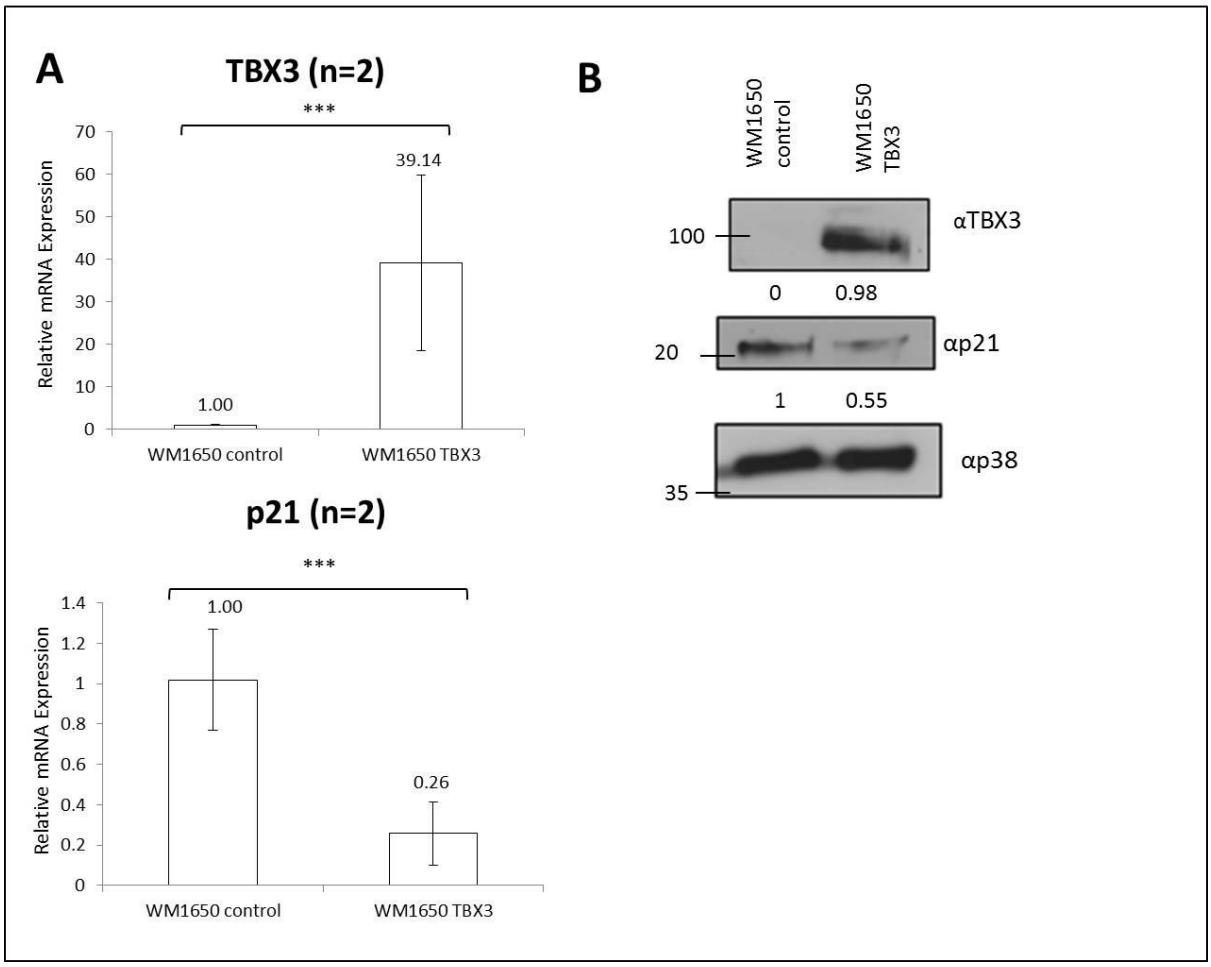

Figure 3.12. **qRT-PCR and western blot analysis of TBX3 and p21 mRNA and protein expression in control and TBX3 overexpressing WM1650 melanoma cell lines.**

A. RNA was harvested and the levels of TBX3 and p21 quantified using qRT-PCR. The reaction was normalised against GUSB levels and a negative water control, containing no cDNA, was also used to determine if there was any contamination (data not shown). This is a pooled result of two independent qRT-PCR experiments each performed in duplicate. A Microsoft Excel student t-test was performed to calculate statistical significance (***$p<0.001$). Error bars indicate standard error of the mean. **B.** Western blot of TBX3 and p21 protein levels in WM1650 control and WM1650 TBX3 cells. Protein was harvested and TBX3 and p21 levels were quantified using antibodies to TBX3 (1:500) and p21 (1:500) and a goat anti-rabbit secondary antibody (1: 5000). The data were normalised to a p38 loading control.

4. Discussion

The overexpression of TBX3 in a range of different cancer types has implicated this particular T-box family member in oncogenesis. However, little is known about the detailed mechanism(s) through which TBX3 may be contributing towards cancer. A potential mechanism is thought to lie in the ability of TBX3 to bypass senescence and/or evade apoptosis by repressing cell cycle regulators, including the cyclin-dependent kinase inhibitors $p14^{ARF}$/$p19^{ARF}$ and p21. However, while the direct repressive effects of TBX3 on $p14^{ARF}$/$p19^{ARF}$ has been well characterised (Brummelkamp et al. 2002; Lingbeek et al. 2002), it has not yet been established whether p21 is a direct TBX3 target gene and the mechanism by which TBX3 regulates p21 has yet to be elucidated. This study has therefore addressed a number of questions regarding how TBX3 may be regulating the *p21* gene and provides compelling in vitro and in vivo data to show that p21 is a direct target of TBX3. Furthermore, it identifies key domains in the TBX3 protein responsible for repressing p21 promoter activity and reveals a site in the p21 promoter that mediates, in part, the repression by TBX3. Evidence is also provided to support the possibility that phosphorylation of TBX3 at a serine-proline (SP) motif in its DNA-binding domain regulates it ability to bind and transcriptionally regulate p21. Lastly, the repression of p21 by TBX3 is shown to be physiologically relevant in knock down and overexpression cell culture models.

An intact $p19^{ARF}$-Mdm2-p53-p21 pathway is important for protecting cells from becoming cancerous because it regulates cellular processes including cell cycle arrest, senescence and apoptosis. There has been speculation that TBX3 may be contributing to oncogenesis by disabling the $p19^{ARF}$-Mdm2-p53-p21 pathway at multiple points. Indeed, TBX3 was previously shown to inhibit senescence by repressing $p19^{ARF}$/$p14^{ARF}$ (Brummelkamp et al. 2002; Lingbeek et al. 2002) and preliminary data suggest that TBX3 may also repress p21. While studies have yielded preliminary and indirect evidence to suggest that this is indeed the case (Hoogaars et al. 2008; Platonova et al. 2007; Suzuki et al. 2008; Carlson et al. 2002), the current study is the first to show that p21 is a direct target of TBX3 and to fully characterise the transcriptional mechanisms involved. Indeed, using luciferase reporter assays, the p21 promoter is shown to be robustly repressed by TBX3 in a dose-dependent manner in the COS7 and HEK293 cell lines (**Figure 3.1B & C**). Interestingly, the fold repression obtained in the two cell lines varied dramatically, with the COS7 cells yielding much higher fold repression than the HEK293 cells. For example, whereas in COS7 cells, 100ng of a hTBX3 expression construct led to a 10 fold repression of the p21 promoter luciferase construct, only a 1.52 fold

repression was observed in HEK293 cells. It is possible that this differential response may be due to the different p53 status of these two cell lines. While COS7 cells were established with the Simian Virus (SV)-40 large T-antigen which immortalises cells by inactivating, in part, the p53 protein (Ali & DeCaprio 2001), HEK293 cells were transformed with sheared adenoviral DNA and express wild type p53 (Graham et al. 1977). The weaker repressive response observed in the HEK293 cells could therefore be explained by the presence of active p53 which through its ability to activate p21 may counteract the repressive effect of TBX3 on p21 expression. The repression of p21 by TBX3 was also shown to be a direct effect because mutation of the TBX3 DNA-binding domain almost completely abrogated, or significantly reduced, repression of the p21 promoter in COS7 and HEK293 cells respectively (**Figures 3.2 & 3.3**). These results provided an initial indication that there was a direct interaction between the TBX3 protein and the p21 promoter.

Two repression domains have previously been identified in the N- and C-termini of the TBX3 protein called R2 and R1 respectively and when the Gal4 binding domain was fused to different regions of TBX3 and tested on a luciferase reporter driven by Gal4 bindings sites, R1 was shown to be the dominant of the two (Carlson et al. 2001). Furthermore, Carlson et al. (2001) have shown that the R1 domain is necessary for the immortalisation of primary embryonic fibroblasts and that most UMS associated mutants lack this domain which results in TBX3 losing its ability to transcriptionally repress its targets. In a later study this group also showed that $p19^{ARF}$ and p21 protein expression decreases when TBX3 is overexpressed in HO-Myc cells and when a truncated version of TBX3, lacking the C-terminus, is expressed instead, this effect is abrogated. In addition, they showed that the C-terminal portion of the protein is required for the anti-apoptotic activity of TBX3 (Carlson et al. 2002). Interestingly, a TBX3 truncated protein lacking the C-terminus harbouring R1 had a significantly reduced ability to repress p21 in COS7 cells but had comparable ability to WT TBX3 to repress p21 in HEK293 cells (**Figure 3.4**). This suggests that the R2 domain may also be involved in the repression of p21 and the possibility that other domains in the N-terminal region of the TBX3 protein may also play a role cannot be excluded. To determine if R2 does indeed plays a role in the repression of p21 was difficult to explore because R2 resides within the DNA-binding domain and therefore mutating it could in turn disrupt DNA binding. Together the results from the current study with that of Carlson et al. (2001; 2002) suggest that the role of different domains in the ability of TBX3 to transcriptionally repress its targets may be cell type and target specific.

There is little information in the literature regarding the mechanisms that regulate TBX3 expression post-translationally and how this may affect its ability to regulate its targets. To the best of my knowledge, there is only one published study which reported that phosphorylation of TBX3 by the p38 mitogen-activated protein (MAP) kinase enhances its ability to transcriptionally repress it's well known target, E-cadherin (Yano et al. 2011). Interestingly, in the current study the TBX3 protein was shown to have 11 serine-proline (SP) motifs which are consensus sites for many kinases including the MAP kinases (Davis 1993) and cyclin-dependent kinases (CDKs) (Montagnoli et al. 2006). Of particular interest was a SP motif at residue 190 because it resides within the TBX3 DNA-binding domain and was found to be highly conserved in a range of species suggesting that it may be important for TBX3 transcriptional activity. Indeed this site was shown to be important for regulation of the *p21* gene because a S190E mutant, which mimics phosphorylation, was unable to bind or transcriptionally repress p21 (**Figure 3.10.B & C**). While the kinase that may phosphorylate TBX3 at this SP site was not identified, the results of the study by Yano et al. (2011) would suggest that it is unlikely to be p38 because their findings indicate that phosphorylation by p38 leads to enhanced TBX3 transcriptional activity. Future experiments should identify the kinase responsible for phosphorylating TBX3 at S190 because it may reveal an important mechanism by which TBX3 transcriptionally regulates its target genes which has implications for our understanding of its oncogenic role.

The TBX3 protein exists as several isoforms with TBX3 and TBX3+2a being the most studied. The TBX3+2a isoform is an alternatively spliced transcript (Bamshad et al. 1999) containing an additional stretch of 20 amino acids inserted within the DNA-binding domain of the protein. There has been some debate as to whether this insertion interferes with TBX3+2a transcriptional activity and hence it being functionally different to TBX3. Indeed, a study by Fan et al. (2004) showed that whereas the overexpression of TBX3 immortalised MEFs, the overexpression of TBX3+2a accelerated senescence of these cells. To determine whether this difference in function is caused by differential target binding, the authors performed an in vitro DNA-binding assay and they show that unlike TBX3, TBX3+2a, was unable to bind a consensus T-element. In contrast, Hoogaars et al. (2008) demonstrated that when ectopically expressed in the embryonic heart of mice both TBX3 and TBX3+2a isoforms suppressed chamber formation and repressed expression of cardiac chamber markers Nppa and Cx40. The results from the current study support that of Hoogaars et al. (2008) which suggest that TBX3 and TBX3+2a are functionally similar. Mouse (m)Tbx3 and mTbx3+2a repressed the p21 promoter to the same degree in COS7 cells and mTbx3 was only 1.14 fold more

efficient than mTbx3+2a in repressing the p21 promoter in HEK293 cells (**Figure 3.5**). Interestingly, there is evidence to suggest that TBX3 interacts with some co-factors via its DNA-binding domain which suggest that the 20 amino acid insertion in the TBX3+2a protein may result in it interacting with different co-factors to TBX3. This would explain why in some studies TBX3 and TBX3+2a regulate the same targets and in others they regulate different targets because it would depend on the availability of co-factors which would be cell context dependent. It is worth noting that two other T-box factors, TBX5 and TBX20, have also been identified to have multiple isoforms resulting from alternative splicing and similar supposed contradictory results have also been reported for the different isoforms (Debenedittis & Jiao 2011). For example, the TBX5a and TBX5b isoforms were shown to have different binding affinities to DNA however, depending on the cellular context and target gene, they were also shown to be functionally similar (Debenedittis & Jiao 2011).

When the p21 promoter was analysed for sites that may be mediating the repression by TBX3, 19 putative T-elements were identified and a T-element close to the initiator of the p21 promoter (-121bp) was found to be important for binding (**Figure 3.8**) and repression by TBX3. Indeed, when it was mutated the repression by TBX3 was completely abrogated in COS7 cells and significantly reduced in HEK293 cells (**Figure 3.7C & D**). This result would suggest that whereas the T-element at -121bp in the p21 promoter is the only site mediating repression by TBX3 in COS7 cells, other sites including TBX3-cofactor binding sites, may also be involved in the regulation of p21 by TBX3 in HEK293 cells. Furthermore, the T-element at -121bp of the p21 promoter is highly conserved amongst several species and was previously shown by Prince et al. (2004) to be required for the repression of p21 by TBX2 (Prince et al. 2004). It would therefore be interesting to determine whether the highly homologous TBX2 and TBX3 have redundant functions in regulating the p21 promoter at this site or whether the availability of co-factors may determine which one of the two regulates p21.

It is worth noting that a study by Hoogaars et al. (2008), which used in vitro DNA-binding assays, also demonstrated that TBX3 is able to bind a probe containing the T-element at -121bp. However, rather than observing a blockshift they observed a supershift with their antibody. The authors used cell extracts of 501 melanoma cells which were transfected with either flag-TBX3 or flag-TBX3+2a and their competition assays employed unlabelled probes containing either a consensus T-element or the T-element at -121bp of the p21 promoter. A possible explanation for their results differing from

the results of the current study may be that they used transfected flag-TBX3 protein and an antibody to flag while the current study used endogenous TBX3 protein with an antibody to TBX3. Their conditions were therefore artificial and may not accurately reflect what happens with endogenous TBX3 protein. Furthermore, Hoogaars et al. (2008) did not test a probe containing a mutation of the T-element at -121bp in their competition assays and therefore did not unequivocally show that this specific site is bound by TBX3, nor did they perform in vivo DNA-binding assays. In this regard, the current study provides for the first time, conclusive data that TBX3 binds the T-element at -121bp and using ChIP assays, that TBX3 binds a region of the p21 promoter containing this site in vivo (**Figure 3.9B**). Importantly, the repression of p21 by TBX3 is shown to be physiologically relevant in cell culture models in which TBX3 was either knocked down or overexpressed (**Figures 3.11 & 3.12**).

Based on previous reports that TBX3 is able to bypass senescence by repressing the CDKI, $p19^{ARF}$, it is tempting to speculate that the findings of the current study provide an additional mechanism by which TBX3 may override senescence. However, TBX3 has never been shown to contribute directly to cancer progression by compromising the senescence checkpoint in vivo. It is therefore possible that TBX3 may be contributing to oncogenesis by inhibiting the pro-apoptotic function of p21, and/ or its role in DNA replication and repair which are important in maintaining genomic integrity (Millau et al. 2009). However, these functions of p21 will only be observed under conditions of cellular stress and the experiments performed in the current study were conducted under unstimulated conditions. It would therefore be important to explore this by performing experiments under conditions of cellular stress.

In conclusion, this study provides compelling in vitro and in vivo data that TBX3 transcriptionally binds and represses p21 and that it involves a T-element close to the p21 initiator. Furthermore, both TBX3 repression domains and phosphorylation at S190 in its DNA-binding domain are demonstrated to be important in the repression of p21. In addition, the Tbx3 and Tbx3+2a isoforms are shown to be functionally similar in their ability to repress the p21 promoter. Finally, the transcriptional repression of p21 by TBX3 is shown to be physiologically relevant in a TBX3 knock down and overexpression model.

5. References

Acosta, J.C. & Gil, J., 2012. Senescence : a new weapon for cancer therapy. *Cell*, 22(4), pp.211–219.

Adnane, J. et al., 2000. Loss of p21WAF1/CIP1 accelerates Ras oncogenesis in a transgenic/knockout mammary cancer model. *Oncogene*, 19(47), pp.5338–47.

Agrawal, A. et al., 2006. Regulation of the p14ARF-Mdm2-p53 pathway: an overview in breast cancer. *Experimental and molecular pathology*, 81(2), pp.115–22.

Agulnik, S.I. et al., 1996. Evolution of mouse T-box genes by tandem duplication and cluster dispersion. *Genetics*, 144(1), pp.249–254.

Ali, S.H. & DeCaprio, J., 2001. Cellular transformation by SV40 large T antigen: interaction with host proteins. *Seminars in cancer biology*, 11(1), pp.15–23.

Andorfer, P. & Rotheneder, H., 2011. EAPP: Gatekeeper at the crossroad of apoptosis and p21-mediated cell-cycle arrest. *Oncogene*, 30(23), pp.2679–90.

Andreou, A.M. et al., 2007. TBX22 Missense Mutations Found in Patients with X-Linked Cleft Palate Affect DNA Binding , Sumoylation and Transcriptional Repression. *The American Journal of Human Genetics*, 81, pp.700–712.

Arora, R., Metzger, R.J. & Papaioannou, V.E., 2012. Multiple roles and interactions of Tbx4 and Tbx5 in development of the respiratory system. *PLoS genetics*, 8(8), p.e1002866.

Asada, M. et al., 1999. Apoptosis inhibitory activity of cytoplasmic p21 Cip1 / WAF1 in monocytic differentiation. *EMBO J*, 18(5), pp.1223–1234.

Ataliotis, P. et al., 2005. XTbx1 is a Transcriptional Activator Involved in Head and Pharyngeal Arch Development in Xenopus laevis. *Developmental dynamics*, 232, pp.979–991.

Atreya, I. et al., 2007. The T-box transcription factor eomesodermin controls CD8 T cell activity and lymph node metastasis in human colorectal cancer. *Gut*, 56(11), pp.1572–8.

Bamshad, M. et al., 1999. The spectrum of mutations in TBX3: Genotype/Phenotype relationship in ulnar-mammary syndrome. *American journal of human genetics*, 64(6), pp.1550–62.

Basson, C.T. et al., 1997. Mutations in human TBX5 cause limb and cardiac malformation in Holt-Oram syndrome. *Nature Genetics*, 15(1), pp.30–35.

Besson, A., Dowdy, S.F. & Roberts, J.M., 2008. CDK inhibitors: cell cycle regulators and beyond. *Developmental Cell*, 14(2), pp.159–169.

Bogenrieder, T. & Herlyn, M., 2003. Axis of evil: molecular mechanisms of cancer metastasis. *Oncogene*, 22(42), pp.6524–36.

Bond, J.A. et al., 1995. Mutant p53 Rescues Human Diploid Cells from Senescence without Inhibiting the Induction of SDI1 / WAF1. *Cancer research*, 55, pp.2404–2409.

Boogaard, M. Van Den et al., 2012. Genetic variation in T-box binding element functionally affects SCN5A / SCN10A enhancer. *The Journal of Clinical Investigation*, 122(7), pp.23–28.

Boogerd, C.J.J. et al., 2011. Sox4 mediates Tbx3 transcriptional regulation of the gap junction protein Cx43. *Cellular and molecular life sciences*.

Braybrook, C. et al., 2001. The T-box transcription factor gene TBX22 is mutated in X-linked cleft palate and ankyloglossia. *Nature genetics*, 29(2), pp.179–83.

Brown, J.P., Wei, W. & Sedivy, J.M., 1997. Bypass of senescence after disruption of p21CIP1/WAF1 gene in normal diploid human fibroblasts. *Science (New York, N.Y.)*, 277(5327), pp.831–4.

Brummelkamp, T.R. et al., 2002. TBX-3, the gene mutated in Ulnar-Mammary Syndrome, is a negative regulator of p19ARF and inhibits senescence. *The Journal of biological chemistry*, 277(8), pp.6567–72.

Bruneau, B.G. et al., 2001. A murine model of Holt-Oram syndrome defines roles of the T-box transcription factor Tbx5 in cardiogenesis and disease. *Cell*, 106(6), pp.709–721.

Bunz, F. et al., 1998. Requirement for p53 and p21 to sustain G2 arrest after DNA damage. *Science*, 282(5393), pp.1497–1501.

Burgucu, D. et al., 2012. Tbx3 represses PTEN and is over-expressed in head and neck squamous cell carcinoma. *BMC cancer*, 12(481).

Carlson, H. et al., 2001. A dominant repression domain in Tbx3 mediates transcriptional repression and cell immortalization: relevance to mutations in Tbx3 that cause ulnar-mammary syndrome. *Human molecular genetics*, 10(21), pp.2403–13.

Carlson, H. et al., 2002. Tbx3 impinges on the p53 pathway to suppress apoptosis, facilitate cell transformation and block myogenic differentiation. , pp.3827–3835.

Carreira, S. et al., 1998. Brachyury-related transcription factor Tbx2 and repression of the melanocyte-specific TRP-1 promoter. *Molecular and cellular biology*, 18(9), pp.5099–108.

Casey, E.S. et al., 1998. The T-box transcription factor Brachyury regulates expression of eFGF through binding to a non-palindromic response element. *Development*, 125, pp.3887–3894.

Cavard, C. et al., 2009. Gene expression profiling provides insights into the pathways involved in solid pseudopapillary neoplasm of the pancreas. *Journal of Pathology*, 218, pp.201–209.

Ceccarelli, C. et al., 2001. Quantitative p21(waf-1)/p53 immunohistochemical analysis defines groups of primary invasive breast carcinomas with different prognostic indicators. *International journal of cancer. Journal international du cancer*, 95(2), pp.128–34.

Chapman, D.L. et al., 1996. Expression of the T-box family genes, Tbx1-Tbx5, during early mouse development. *Developmental dynamics an official publication of the American Association of Anatomists*, 206(4), pp.379–390.

Chen, B. et al., 2000. Inhibition of the Interferon- γ / Signal Transducers and Activators of Transcription (STAT) Pathway by Hypermethylation at a STAT-binding Site in the p21 WAF1 Promoter Region. *Cancer research*, 60, pp.3290–3298.

Chen, J. et al., 1996. Cyclin-Binding Motifs Are Essential for the Function of p21 CIP1. *Molecular and Cellul*, 16(9), pp.4673–4682.

Chen, P., Tian, D. & Liu, M., 2008. The role of Tbx2 in pancreatic cancers and its regulation by Wnt/β-catenin signaling. *The Chinese-German Journal of Clinical Oncology*, 7(7), pp.404–409.

Chen, Z. et al., 2008. Antitumor effect of dsRNA-induced p21(WAF1/CIP1) gene activation in human bladder cancer cells. *Molecular Cancer Therapeutics*, 7(3), pp.698–703.

Cheng, M. et al., 1999. The p21(Cip1) and p27(Kip1) CDK "inhibitors" are essential activators of cyclin D-dependent kinases in murine fibroblasts. *the The European Molecular Biology Organization Journal*, 18(6), pp.1571–1583.

Cheung, T.H. et al., 2001. Aberrant expression of p21(WAF1/CIP1) and p27(KIP1) in cervical carcinoma. *Cancer letters*, 172(1), pp.93–8.

Chin, P.L., Momand, J. & Pfeifer, G.P., 1997. In vivo evidence for binding of p53 to consensus binding sites in the p21 and GADD45 genes in response to ionizing radiation. *Oncogene*, 15(1), pp.87–99.

Ciccarelli, C. et al., 2005. p21WAF1 expression induced by MEK/ERK pathway activation or inhibition correlates with growth arrest, myogenic differentiation and onco-phenotype reversal in rhabdomyosarcoma cells. *Molecular cancer*, 4(41).

Coll, M., Seidman, J.G. & Müller, C.W., 2002. Structure of the DNA-bound T-box domain of human TBX3, a transcription factor responsible for ulnar-mammary syndrome. *Structure*, 10(3), pp.343–56.

Dalerba, P. et al., 2003. Immunology and immunotherapy of colorectal cancer. *Critical reviews in oncologyhematology*, 46(1), pp.33–57.

Darnell, J.E., 2002. Transcription factors as targets for cancer therapy. *Nature Reviews Cancer*, 2(10), pp.740–749.

Davenport, T.G., Jerome-Majewska, L.A. & Papaioannou, V.E., 2003. Mammary gland, limb and yolk sac defects in mice lacking Tbx3, the gene mutated in human ulnar mammary syndrome. *Development Cambridge England*, 130(10), pp.2263–2273.

Davis, E. et al., 2008. Ectopic Tbx2 expression results in polyploidy and cisplatin resistance. *Oncogene*, 27(7), pp.976–84.

Davis, R.J., 1993. The Mitogen-activated Protein Kinase Signal Transduction Pathway*. *The Journal of biological chemistry*, 268(2), pp.14553–14556.

Debenedittis, P. & Jiao, K., 2011. Alternative splicing of T-box transcription factor genes. *Biochemical and Biophysical Research Communications*, 412(4), pp.513–517.

Decesse, J.T. et al., 2001. RB regulates transcription of the p21/WAF1/CIP1 gene. *Oncogene*, 20(8), pp.962–71.

Deng, C. et al., 1995. Mice Lacking p21 CIP1/WAF1 Undergo Normal Development ,But Are Defective in Gl Checkpoint Control. *Cell*, 82, pp.875–884.

Dimova, I. et al., 2009. Genomic markers for ovarian cancer at chromosomes 1 , 8 and 17 revealed by array CGH analysis. *Tumorigenesis*, 95, pp.357–366.

Dobrovolskaia-Zadvadskaia, N., 1927. Sur la mortification spontanee de la queue chez la souris nouveau-nee et sur l'existence d'un caractere herditaire "non-viable." *Current Research in Social Biology*, 97, pp.114–116.

Dulić, V. et al., 1998. Nuclear accumulation of p21Cip1 at the onset of mitosis: a role at the G2/M-phase transition. *Molecular and Cellular Biology*, 18(1), pp.546–557.

Duo, S. et al., 2009. Expression and clinical significance of tbx2 in pancreatic cancer. *Asian Pacific journal of cancer prevention : APJCP*, 10(1), pp.118–22.

Eblaghie, M.C. et al., 2004. Interactions between FGF and Wnt signals and Tbx3 gene expression in mammary gland initiation in mouse embryos. *Journal of anatomy*, 205(1), pp.1–13.

El-Deiry, W.S. et al., 1993. WAF1, a potential mediator of p53 tumor suppression. *Cell*, 75(4), pp.817–825.

El-Deiry, W.S. et al., 1994. WAF1/CIP1 is induced in p53-mediated G1 arrest and apoptosis. *Cancer research*, 54(5), pp.1169–74.

Elmore, S., 2007. Apoptosis: a review of programmed cell death. *Toxicologic pathology*, 35(4), pp.495–516.

Etcheverry, A. et al., 2010. DNA methylation in glioblastoma: impact on gene expression and clinical outcome. *BMC genomics*, 11(701).

Fan, W. et al., 2004. TBX3 and its isoform TBX3+2a are functionally distinctive in inhibition of senescence and are overexpressed in a subset of breast cancer cell lines. *Cancer research*, 64(15), pp.5132–9.

Fang, L. et al., 1999. p21Waf1/Cip1/Sdi1 induces permanent growth arrest with markers of replicative senescence in human tumor cells lacking functional p53. *Oncogene*, 18(18), pp.2789–2797.

Farin, H.F. et al., 2013. Transcriptional Repression by the T-box Proteins Tbx18 and Tbx15 Depends on Groucho Corepressors. *The Journal of biological chemistry*, 282, pp.25748–25759.

Fernando, R.I. et al., 2010. The T-box transcription factor Brachyury promotes epithelial-mesenchymal transition in human tumor cells. *In Vitro*, 120(2), pp.533–545.

Fillmore, C.M. et al., 2010. Estrogen expands breast cancer stem-like cells through paracrine FGF/Tbx3 signaling. *Proceedings of the National Academy of Sciences of the United States of America*, 107(50), pp.21737–42.

Fillmore, C.M. & Kuperwasser, C., 2008. Human breast cancer cell lines contain stem-like cells that self-renew, give rise to phenotypically diverse progeny and survive chemotherapy. *Breast cancer research : BCR*, 10(2), p.R25.

Flores-Rozas, H. et al., 1994. Cdk-interacting protein 1 directly binds with proliferating cell nuclear antigen and inhibits DNA replication catalyzed by the DNA polymerase delta holoenzyme. *Proceedings of the National Academy of Sciences of the United States of America*, 91(18), pp.8655–9.

Frank, D.U. et al., 2013. Mouse Tbx3 Mutants Suggest Novel Molecular Mechanisms for Ulnar-Mammary Syndrome R. Dettman, ed. *PLoS ONE*, 8(7), p.e67841.

Garg, V. et al., 2003. GATA4 mutations cause human congenital heart defects and reveal an interaction with TBX5. *Letters to Nature*, 21, pp.443–447.

Glotzer, M., Murray, A.W. & Kirschner, M.W., 1991. Cyclin is degraded by the ubiquitin pathway. *Nature*, 349(6305), pp.132–138.

Gonzalez, A. et al., 2013. Control of Hes7 Expression by Tbx6 , the Wnt Pathway and the Chemical Gsk3 Inhibitor LiCl in the Mouse Segmentation Clock. *PloS one*, 8(1), p.e53323.

Goubin, F. & Ducommun, B., 1995. Identification of binding domains on the p21Cip1 cyclin-dependent kinase inhibitor. *Oncogene*, 10(12), pp.2281–2287.

Graham, F.L. et al., 1977. Characteristics of a human cell line transformed by DNA from human adenovirus type 5. *The Journal of general virology*, 36(1), pp.59–74.

Grigorieva, I. V & Thakker, R. V, 2011. Transcription factors in parathyroid development: lessons from hypoparathyroid disorders. *Annals of the New York Academy of Sciences*, 1237, pp.24–38.

Habets, P.E.M.H. et al., 2002. Cooperative action of Tbx2 and Nkx2.5 inhibits ANF expression in the atrioventricular canal: implications for cardiac chamber formation. *Genes & Development*, 16(10), pp.1234–1246.

Hanahan, D. & Weinberg, R.A., 2011. Hallmarks of cancer: the next generation. *Cell*, 144(5), pp.646–674.

Hanahan, D. & Weinberg, R.A., 2000. The hallmarks of cancer. *Cell*, 100(1), pp.57–70.

Hanahan, D., Weinberg, R.A. & Francisco, S., 2000. The Hallmarks of Cancer Review University of California at San Francisco. *Hormone Research*, 100, pp.57–70.

Hansel, D.E. et al., 2004. Met proto-oncogene and insulin-like growth factor binding protein 3 overexpression correlates with metastatic ability in well-differentiated pancreatic endocrine neoplasms. *Clinical cancer research: an official journal of the American Association for Cancer Research*, 10(18 Pt 1), pp.6152–8.

Harper, J.W. et al., 1995. Inhibition of cyclin-dependent kinases by p21. *Molecular Biology of the Cell*, 6, pp.387–400.

Harper, J.W. et al., 1993. The p21 Cdk-interacting protein Cip1 is a potent inhibitor of G1 cyclin-dependent kinases. *Cell*, 75(4), pp.805–16.

Hartwell, L.H. & Kastan, M.B., 2011. Cycle Control and Cancer. *Advancement Of Science*, 266(5192), pp.1821–1828.

Harvey Lodish, Arnold Berk, S. Lawrence Zipursky, Paul Matsudaira, D.B. and J.D., 2001. *Molecular Cell Biology (4th edition)*, Freeman & Co.

He, M.-L. et al., 2002. Induction of apoptosis and inhibition of cell growth by developmental regulator hTBX5. *Biochemical and Biophysical Research Communications*, 297(2), pp.185–192.

Herrmann, B.G. et al., 1990. Cloning of the T gene required in mesoderm formation in the mouse. *Nature*, 343(6259), pp.617–622.

Hiroi, Y. et al., 2001. Tbx5 associates with Nkx2-5 and synergistically promotes cardiomyocyte differentiation. *Nature Genetics*, 28(3), pp.276–280.

Hoek, K. et al., 2004. Expression profiling reveals novel pathways in the transformation of melanocytes to melanomas. *Cancer research*, 64(15), pp.5270–82.

Hoogaars, W.M.H. et al., 2008. TBX3 and its splice variant TBX3 + exon 2a are functionally similar. *Pigment cell & melanoma research*, 21(3), pp.379–87.

Humtsoe, J.O. et al., 2012. Transcriptional profiling identifies upregulated genes following induction of epithelial-mesenchymal transition in squamous carcinoma cells. *Experimental cell research*, 318(4), pp.379–90.

Hurlin, P.J. et al., 1999. Mga, a dual-specificity transcription factor that interacts with Max and contains a T-domain DNA-binding motif. *The EMBO journal*, 18(24), pp.7019–28.

Imajyo, I. et al., 2012. T-box transcription factor Brachyury expression is correlated with epithelial-mesenchymal transition and lymph node metastasis in oral squamous cell carcinoma. *International journal of oncology*, 41(6), pp.1985–95.

Ismail, A. & Bateman, A., 2009. Expression of TBX2 promotes anchorage-independent growth and survival in the p53-negative SW13 adrenocortical carcinoma. *Cancer letters*, 278(2), pp.230–40.

Ito, A. et al., 2005. Tbx3 expression is related to apoptosis and cell proliferation in rat bladder both hyperplastic epithelial cells and carcinoma cells. *Cancer letters*, 219(1), pp.105–12.

Jacobs, J.J. et al., 2000. Senescence bypass screen identifies TBX2, which represses Cdkn2a (p19(ARF)) and is amplified in a subset of human breast cancers. *Nature genetics*, 26(3), pp.291–9.

Jerome, L.A. & Papaioannou, V.E., 2001. DiGeorge syndrome phenotype in mice mutant for the T-box gene, Tbx1. *Nature genetics*, 27(3), pp.286–291.

Jerome-majewska, L.A. et al., 2005. Tbx3 , the Ulnar-Mammary Syndrome Gene , and Tbx2 Interact in Mammary Gland Development Through a p19 Arf / p53- Independent Pathway. *Developmental dynamics*, 234, pp.922–933.

John, P.C., Mews, M. & Moore, R., 2001. Cyclin/Cdk complexes: their involvement in cell cycle progression and mitotic division. *Protoplasma*, 216(3-4), pp.119–142.

Jung, Y.-S., Qian, Y. & Chen, X., 2010. Examination of the expanding pathways for the regulation of p21 expression and activity. *Cellular signalling*, 22(7), pp.1003–12.

Kandimalla, R. et al., 2012. Genome-wide Analysis of CpG Island Methylation in Bladder Cancer Identified TBX2 , TBX3 , GATA2 , and ZIC4 as pTa-Specific Prognostic Markers. *European Urology*, 61, pp.1245–1256.

Kapranos, N. et al., 2001. p53, p21 and p27 protein expression in head and neck cancer and their prognostic value. *Anticancer Research*, 21(1B), pp.521–528.

Kartikasari, A.E.R. et al., 2013. The histone demethylase Jmjd3 sequentially associates with the transcription factors Tbx3 and Eomes to drive endoderm differentiation. *The EMBO journal*, 32(10), pp.1393–408.

Kawamura, A., Koshida, S. & Takada, S., 2008. Activator-to-repressor conversion of T-box transcription factors by the Ripply family of Groucho/TLE-associated mediators. *Molecular and cellular biology*, 28(10), pp.3236–44.

Kaznelson, D.W. et al., 2004. Simultaneous human papilloma virus type 16 E7 and cdk inhibitor p21 expression induces apoptosis and cathepsin B activation. *Virology*, 320(2), pp.301–12.

Kelman, Z., 1997. PCNA: structure, functions and interactions. *Oncogene*, 14(6), pp.629–640.

Kim, Y. et al., 2009. Functional links between clustered microRNAs : suppression of cell-cycle inhibitors by microRNA clusters in gastric cancer. *Nucleic acids research*, 37(5), pp.1672–1681.

Kispert, A. & Herrmann, Bernhard G, 1993. The Brachyury gene encodes a novel DNA binding protein. *The EMBO*, 12(8), pp.3211–3220.

Kispert, A. & Herrmann, Bernhard G., 1993. The Brachyury gene encodes a novel DNA binding protein. *The EMBO Journal*, 12(8), pp.3211–3220.

Kispert, A., Koschorz, B. & Herrmann, B.G., 1995. The T protein encoded by Brachury is a tissue-specific transcription factor. *The EMBO Journal*, 14(19), pp.4763–4772.

Klopocki, E. et al., 2006. Ulnar-mammary syndrome with dysmorphic facies and mental retardation caused by a novel 1.28 Mb deletion encompassing the TBX3 gene. *European journal of human genetics : EJHG*, 14(12), pp.1274–9.

Komiya, T. et al., 1997. P21 Expression As a Predictor for Favorable Prognosis in Squamous Cell Carcinoma of the Lung. *Clinical cancer research : an official journal of the American Association for Cancer Research*, 3(10), pp.1831–5.

Kondo, S. et al., 1996. WAF1/CIP1 increases the susceptibility of p53 non-functional malignant glioma cells to cisplatin-induced apoptosis. *Oncogene*, 13(6), pp.1279–1285.

Korzh, V. & Grunwald, D., 2001. Èa-Zavadskaõ Èa Nadine Dobrovolskaõ and the dawn of developmental genetics. *BioEssays : news and reviews in molecular, cellular and developmental biology*, 23, pp.365–371.

Koster, R. et al., 2010. Cytoplasmic p21 expression levels determine cisplatin resistance in human testicular cancer. *Journal of Clinical Investigation*, 120(10), pp.3594–3605.

Kriwacki, R.W. et al., 1996. Structural studies of p21Waf1/Cip1/Sdi1 in the free and Cdk2-bound state: conformational disorder mediates binding diversity. *Proceedings of the National Academy of Sciences of the United States of America*, 93(21), pp.11504–11509.

Kuljaca, S. et al., 2009. The cyclin-dependent kinase inhibitor, p21(WAF1), promotes angiogenesis by repressing gene transcription of thioredoxin-binding protein 2 in cancer cells. *Carcinogenesis*, 30(11), pp.1865–71.

LaBaer, J. et al., 1997. New functional activities for the p21 family of CDK inhibitors. *Genes & Development*, 11(7), pp.847–862.

Lamolet, B. et al., 2001. A pituitary cell-restricted T box factor, Tpit, activates POMC transcription in cooperation with Pitx homeoproteins. *Cell*, 104(6), pp.849–59.

Leber, M.F. & Efferth, T., 2009. Molecular principles of cancer invasion and metastasis (review). *International journal of oncology*, 34(4), pp.881–895.

Lee, A.J.X. et al., 2011. Chromosomal instability confers intrinsic multidrug resistance. *Cancer research*, 71(5), pp.1858–70.

Li, Y. et al., 1994. Cell cycle expression and p53 regulation of the cyclin-dependent kinase inhibitor p21. *Oncogene*, 9(8), pp.2261–2268.

Li, Y., Dowbenko, D. & Lasky, L. a, 2002. AKT/PKB phosphorylation of p21Cip/WAF1 enhances protein stability of p21Cip/WAF1 and promotes cell survival. *The Journal of biological chemistry*, 277(13), pp.11352–61.

Libermann, T.A. & Zerbini, L.F., 2006. Targeting Transcription Factors for Cancer Gene Therapy. *Current Gene Therapy*, 6(1), pp.17–33.

Lincet, H. et al., 2000. The p21(cip1/waf1) cyclin-dependent kinase inhibitor enhances the cytotoxic effect of cisplatin in human ovarian carcinoma cells. *Cancer Letters*, 161(1), pp.17–26.

Lingbeek, M.E., Jacobs, J.J.L. & Lohuizen, M. Van, 2002. The T-box Repressors TBX2 and TBX3 Specifically Regulate the Tumor Suppressor Gene p14 ARF via a Variant T-site in the Initiator. *Biochemistry*, 277(29), pp.26120 –26127.

Liu, N., Dong, Q. & Wang, E., 2012. Expression of TBX3 is Correlated with Tumor Proliferation and Invasion in Non-small Cell Lung Cancer. *Journal of China Medical University*, 41(4), pp.360–363.

Liu, W.-K., Jiang, X.-Y. & Zhang, Z.-X., 2010a. Expression of PSCA, PIWIL1 and TBX2 and its correlation with HPV16 infection in formalin-fixed, paraffin-embedded cervical squamous cell carcinoma specimens. *Archives of Virology*, 155(5), pp.657–663.

Liu, W.-K., Jiang, X.-Y. & Zhang, Z.-X., 2010b. Expression of PSCA, PIWIL1, and TBX2 in endometrial adenocarcinoma. *Onkologie*, 33(5), pp.241–5.

Lomnytska, M. et al., 2006. Increased expression of cSHMT, Tbx3 and utrophin in plasma of ovarian and breast cancer patients. *International journal of cancer. Journal international du cancer*, 118(2), pp.412–21.

Lu, R., Yang, A. & Jin, Y., 2011. Dual Functions of T-Box 3 (Tbx3) in the Control of Self-renewal and Extraembryonic Endoderm Differentiation in Mouse Embryonic Stem Cells. *Journal of Biological Chemistry*, 286(10), pp.8425–8436.

Lu, X. et al., 1998. Expression of p21 WAF1 / CIP1 in Adenocarcinoma of the Uterine Cervix A Possible Immunohistochemical Marker of a Favorable Prognosis. *Cancer*, 82(12), pp.2409–2417.

Lyng, H. et al., 2006. Gene expressions and copy numbers associated with metastatic phenotypes of uterine cervical cancer. *BMC genomics*, 7, p.268.

Macmurray, A. & Shin, H., 1988. The Antimorphic Nature of the Tc Allele at the Mouse T Locus. *Genetics*, 120, pp.545–550.

Maelandsmo, G. et al., 1996. Cyclin kinase inhibitor p21 in malignant melanoma: Reduced expression in metastatic lesions. *American Journal of Pathology*, 149(6), pp.1813–22.

Mahlamäki, E.H. et al., 2002. Frequent amplification of 8q24, 11q, 17q, and 20q-specific genes in pancreatic cancer. *Genes, chromosomes & cancer*, 35(4), pp.353–8.

Maira, M. et al., 2003. The T-box Factor Tpit Recruits SRC / p160 Co-activators and Mediates Hormone Action The T-box Factor Tpit Recruits SRC / p160 Co-activators and Mediates Hormone Action. *The Journal of biological chemistry*, 278, pp.46523–46532.

Malumbres, M. & Barbacid, M., 2005. Mammalian cyclin-dependent kinases. *Trends in Biochemical Sciences* , 30(11), pp.630–641.

Martin, N. et al., 2012. Physical and functional interaction between PML and TBX2 in the establishment of cellular senescence. *The EMBO Journal*, 31, pp.95–109.

Matheu, A., Collado, M. & Wise, C., 2012. Oncogenicity of the Developmental Transcription Factor Sox9. *Cancer research*, 72(5), pp.1301–1315.

McConnell, B.B. et al., 1998. Inhibitors of cyclin-dependent kinases induce features of replicative senescence in early passage human diploid fibroblasts. *Current biology : CB*, 8(6), pp.351–4.

McCune, K. et al., 2010. Prognosis of hormone-dependent breast cancers: implications of the presence of dysfunctional transcriptional networks activated by insulin via the immune transcription factor T-bet. *Cancer research*, 70(2), pp.685–696.

Merscher, S. et al., 2001. TBX1 is responsible for cardiovascular defects in velo-cardio-facial/DiGeorge syndrome. *Cell*, 104(4), pp.619–629.

Messenger, N.J. et al., 2005. Functional specificity of the Xenopus T-domain protein Brachyury is conferred by its ability to interact with Smad1. *Developmental cell*, 8(4), pp.599–610.

Micalizzi, D.S., Farabaugh, S.M. & Ford, H.L., 2010. Epithelial-mesenchymal transition in cancer: parallels between normal development and tumor progression. *Journal of mammary gland biology and neoplasia*, 15(2), pp.117–34.

Millau, J.-F., Bastien, N. & Drouin, R., 2009. P53 transcriptional activities: a general overview and some thoughts. *Mutation research*, 681(2-3), pp.118–33.

Miller, R.R. & Okkema, P.G., 2011. The Caenorhabditis elegans T-box factor MLS-1 requires Groucho co-repressor interaction for uterine muscle specification. *PLoS genetics*, 7(8), p.e1002210.

Minguillon, C. & Logan, M., 2003. The comparative genomics of T-box genes. *Briefings in functional genomics & proteomics*, 2(3), pp.224–33.

Montagnoli, A. et al., 2006. Identification of Mcm2 Phosphorylation Sites by S-phase-regulating kinases. *The Journal of biological chemistry*, 281, pp.10281–10290.

Mowla, S. et al., 2010. PMA-induced up-regulation of TBX3 is mediated by AP-1 and contributes to breast cancer cell migration. *The Biochemical journal*, 433(1), pp.145–53.

Müller, C.W. & Herrmann, B.G., 1997. Crystallographic structure of the T domain-DNA complex of the Brachyury transcription factor. *Nature*, 389(6653), pp.884–888.

Murakami, M. et al., 2005. A WW domain protein TAZ is a critical coactivator for TBX5, a transcription factor implicated in Holt-Oram syndrome. *Proceedings of the National Academy of Sciences of the United States of America*, 102(50), pp.18034–9.

Naiche, L. a et al., 2005. T-box genes in vertebrate development. *Annual review of genetics*, 39, pp.219–39.

Nakano, K. et al., 1997. Butyrate activates the WAF1/Cip1 gene promoter through Sp1 sites in a p53-negative human colon cancer cell line. *The Journal of biological chemistry*, 272(35), pp.22199–206.

Noda, A. et al., 1994. Cloning of senescent cell-derived inhibitors of DNA synthesis using an expression screen. *Experimental Cell Research*, 211(1), pp.90–98.

Nozell, S. & Chen, X., 2002. p21B, a variant of p21(Waf1/Cip1), is induced by the p53 family. *Oncogene*, 21(8), pp.1285–1294.

Packham, E.A. & Brook, J.D., 2003. T-box genes in human disorders. *Human molecular genetics*, 12(1), pp.37–44.

Palena, C. et al., 2007. The human T-box mesodermal transcription factor Brachyury is a candidate target for T-cell-mediated cancer immunotherapy. *Clinical cancer research : an official journal of the American Association for Cancer Research*, 13(8), pp.2471–8.

Pantoja, C. & Serrano, M., 1999. Murine fibroblasts lacking p21 undergo senescence and are resistant to transformation by oncogenic Ras. *Oncogene*, 18(35), pp.4974–82.

Park, J.C. et al., 2008. Epigenetic silencing of human T (brachyury homologue) gene in non-small-cell lung cancer. *Biochemical and biophysical research communications*, 365(2), pp.221–6.

Parker, S.B. et al., 1995. p53-independent expression of p21Cip1 in muscle and other terminally differentiating cells. *Science*, 267(5200), pp.1024–1027.

Pearce, E.L. et al., 2003. Control of effector CD8+ T cell function by the transcription factor Eomesodermin. *Science (New York, N.Y.)*, 302(5647), pp.1041–3.

Pereira, L. a et al., 2011. Brachyury and related Tbx proteins interact with the Mixl1 homeodomain protein and negatively regulate Mixl1 transcriptional activity. *PloS one*, 6(12), p.e28394.

Peres, J. et al., 2010a. The Highly Homologous T-Box Transcription Factors, TBX2 and TBX3, Have Distinct Roles in the Oncogenic Process. *Genes & Cancer*, 1(3), pp.272–282.

Peres, J. et al., 2010b. The Highly Homologous T-Box Transcription Factors, TBX2 and TBX3, Have Distinct Roles in the Oncogenic Process. *Genes & Cancer*, 1(3), pp.272–282.

Peres, J. & Prince, S., 2013. The T-box transcription factor , TBX3 , is sufficient to promote melanoma formation and invasion. *Molecular Cancer*, 12(117), pp.1–5.

Pérez-Tenorio, G. et al., 2006. Cytoplasmic p21WAF1/CIP1 correlates with Akt activation and poor response to tamoxifen in breast cancer. *International Journal of Oncology*, 28(5), pp.1031–1042.

Pflugfelder, G.O., Roth, H. & Poeck, B., 1992. A homology domain shared between Drosophila optomotor-blind and mouse Brachyury is involved in DNA binding. *Biochemical and Biophysical Research Communications*, 186(2), pp.918–925.

Philipp, J. et al., 1999. Tumor suppression by p27Kip1 and p21Cip1 during chemically induced skin carcinogenesis. *Oncogene*, 18(33), pp.4689–98.

Platonova, N. et al., 2007. TBX3, the gene mutated in ulnar-mammary syndrome, promotes growth of mammary epithelial cells via repression of p19ARF, independently of p53. *Cell and tissue research*, 328(2), pp.301–16.

Poole, A.J. et al., 2004. Tumor suppressor functions for the Cdk inhibitor p21 in the mouse colon. *Oncogene*, 23(49), pp.8128–34.

Prince, S., Carreirs, S. & Vance, K., 2004. Tbx2 Directly Represses the Expression of the p21WAF1 Cyclin-Dependent Kinase Inhibitor. *Cancer Research*, 64(5), pp.1669–1674.

Qian, X. et al., 2013. p21CIP1 mediates reciprocal switching between proliferation and invasion during metastasis. *Oncogene*, 32(18), pp.2292–303.

Quintana, E. et al., 2008. Efficient tumor formation by single human melanoma cells. *Nature*, 456(7222), pp.593–598.

Radhakrishnan, S.K., Gierut, J. & Gartel, a L., 2006. Multiple alternate p21 transcripts are regulated by p53 in human cells. *Oncogene*, 25(12), pp.1812–5.

Radu, A. et al., 2003. PTEN induces cell cycle arrest by decreasing the level and nuclear localization of cyclin D1. *Molecular and cellular biology*, 23(17), pp.6139–6149.

Redmond, K.L. et al., 2010. T-box 2 represses NDRG1 through an EGR1-dependent mechanism to drive the proliferation of breast cancer cells. *Oncogene*, 29(22), pp.3252–3262.

Reinert, T., Modin, C. & Castano, F.M., 2011. Comprehensive Genome Methylation Analysis in Bladder Cancer : Identification and Validation of Novel Methylated Genes and Application of These as Urinary Tumor Markers. *Human Cancer Biology*, 17(1), pp.5582–5592.

Renard, C.-A. et al., 2007. Tbx3 is a downstream target of the Wnt/beta-catenin pathway and a critical mediator of beta-catenin survival functions in liver cancer. *Cancer research*, 67(3), pp.901–10.

Rodriguez, M. et al., 2008. Tbx3 represses E-cadherin expression and enhances melanoma invasiveness. *Cancer research*, 68(19), pp.7872–81.

Rodriguez-Esteban, C. et al., 1999. The T-box genes Tbx4 and Tbx5 regulate limb outgrowth and identity. *Nature*, 398(6730), pp.814–8.

Rodríguez-Vilarrupla, A. et al., 2002. Identification of the nuclear localization signal of p21(cip1) and consequences of its mutation on cell proliferation. *FEBS Letters*, 531(2), pp.319–323.

Roman-Gomez, J., 2002. 5' CpG island hypermethylation is associated with transcriptional silencing of the p21CIP1/WAF1/SDI1 gene and confers poor prognosis in acute lymphoblastic leukemia. *Blood*, 99(7), pp.2291–2296.

Rosenbluh, J. et al., 2012. Catenin-driven cancers require a YAP1 transcriptional complex for survival and tumorigenesis. *Cell*, 151(7), pp.1457–73.

Sakabe, M. et al., 2012. Ectopic retinoic acid signaling affects outflow tract cushion development through suppression of the myocardial Tbx2-Tgfβ2 pathway. *Development (Cambridge, England)*, 139(2), pp.385–95.

Saramäki, A. et al., 2006. Regulation of the human p21(waf1/cip1) gene promoter via multiple binding sites for p53 and the vitamin D3 receptor. *Nucleic acids research*, 34(2), pp.543–54.

Sarbia, M. & Gabbert, H.E., 2000. Modern pathology: prognostic parameters in squamous cell carcinoma of the esophagus. *Recent Results In Cancer Research*, 155, pp.15–27.

Scambler, P.J., 2000. The 22q11 deletion syndromes. *Human molecular genetics*, 9(16), pp.2421–6.

Schafer, K. a., 1998. The Cell Cycle: A Review. *Veterinary Pathology*, 35(6), pp.461–478.

Schneider, M. a et al., 2013. The Transcription Factors TBX2 and TBX3 Interact with Human Papillomavirus 16 (HPV16) L2 and Repress the Long Control Region of HPVs. *Journal of virology*, 87(8), pp.4461–74.

Schulte-Merker, S. et al., 1992. The protein product of the zebrafish homologue of the mouse T gene is expressed in nuclei of the germ ring and the notochord of the early embryo. *Development Cambridge England*, 116(4), pp.1021–1032.

Sheaff, R.J. et al., 2000. Proteasomal Turnover of p21 Cip1 Does Not Require p21 Cip1 Ubiquitination. *Molecular Cell*, 5, pp.403–410.

Sherr, C.J. & Roberts, J.M., 1999. CDK inhibitors : positive and negative regulators of G 1 -phase progression. *Genes & Development*, 13, pp.1501–1512.

Sherr, C.J. & Roberts, J.M., 1995. Inhibitors of mammalian G1 cyclin-dependent kinases. *Genes & Development*, 9(10), pp.1149–1163.

Sherr, C.J. & Weber, J.D., 2000. The ARF/p53 pathway. *Current opinion in genetics & development*, 10(1), pp.94–9.

Shimoda, M. et al., 2012. The T-box transcription factor Brachyury regulates epithelial-mesenchymal transition in association with cancer stem-like cells in adenoid cystic carcinoma cells. *BMC cancer*, 12, p.377.

Shiohara, M. et al., 1994. Absence of WAF1 mutations in a variety of human malignancies. *Nature*, 84, pp.3781–3784.

Showell, C., Binder, O. & Conlon, F.L., 2004. T-box genes in early embryogenesis. *Developmental dynamics : an official publication of the American Association of Anatomists*, 229(1), pp.201–18.

Sinclair, C.S. et al., 2002. TBX2 Is Preferentially Amplified in BRCA1- and BRCA2 -related Breast Tumors. *Cancer Research*, 62, pp.3587–3591.

Singh, M.K. et al., 2005. Tbx20 is essential for cardiac chamber differentiation and repression of Tbx2. *Development (Cambridge, England)*, 132(12), pp.2697–707.

Singh, R. et al., 2009. Tbx20 interacts with smads to confine tbx2 expression to the atrioventricular canal. *Circulation research*, 105(5), pp.442–52.

Smith, J., 1999. T-box genes: what they do and how they do it. *Trends in Genetics*, 15(4), pp.154–158.

Smith, J.C. et al., 1991. Expression of a Xenopus homolog of Brachyury (T) is an immediate-early response to mesoderm induction. *Cell*, 67(1), pp.79–87.

Stennard, F.A. et al., 2005. Murine T-box transcription factor Tbx20 acts as a repressor during heart development, and is essential for adult heart integrity, function and adaptation. *Development Cambridge England*, 132(10), pp.2451–2462.

Stoller, J.Z. & Epstein, J.A., 2005. Identification of a novel nuclear localization signal in Tbx1 that is deleted in DiGeorge syndrome patients harboring the 1223delC mutation. *Human molecular genetics*, 14(7), pp.885–892.

Sun, H. et al., 1999. PTEN modulates cell cycle progression and cell survival by regulating phosphatidylinositol 3,4,5,-trisphosphate and Akt/protein kinase B signaling pathway. *Proceedings of the National Academy of Sciences of the United States of America*, 96(11), pp.6199–204.

Suzuki, A. et al., 2008. Tbx3 controls the fate of hepatic progenitor cells in liver development by suppressing p19 ARF expression. *Development*, 135, pp.1589–1595.

Takashima, Y. & Suzuki, A., 2013. Regulation of organogenesis and stem cell properties by T-box transcription factors. *Cellular and molecular life sciences : CMLS*, 70(20), pp.3929–45.

Takeuchi, J.K. et al., 1999. Tbx5 and Tbx4 genes determine the wing/leg identity of limb buds. *Nature*, 398(6730), pp.810–4.

Takeuchi, S., Takahashi, A. & Motoi, N., 2010. Intrinsic Cooperation between p16 INK4a and p21 Waf1 / Cip1 in the Onset of Cellular Senescence and Tumor Suppression In vivo in the Onset of Cellular Senescence and Tumor Suppression In vivo. *Cancer Research*, 70, pp.9381–9390.

Thiery, J.P., 2002. Epithelial-mesenchymal transitions in tumour progression. *Nature reviews. Cancer*, 2(6), pp.442–54.

Timofeev, O. V., Pospelova, T. V. & Pospelov, V. a., 2004. Functions of p21 Waf1 in Norm and in Stress. *Molecular Biology*, 38(3), pp.309–321.

Trempus, C.S. et al., 2011. A novel role for the T-box transcription factor Tbx1 as a negative regulator of tumor cell growth in mice. *Molecular carcinogenesis*, 50(12), pp.981–91.

Umar, a et al., 1996. Requirement for PCNA in DNA mismatch repair at a step preceding DNA resynthesis. *Cell*, 87(1), pp.65–73.

Vance, K.W. et al., 2005. Tbx2 is overexpressed and plays an important role in maintaining proliferation and suppression of senescence in melanomas. *Cancer research*, 65(6), pp.2260–8.

Vincent, A.J. et al., 2012. Cytoplasmic translocation of p21 mediates NUPR1-induced chemoresistance NUPR1 and p21 in chemoresistance. *FEBS LETTERS*, 586(19), pp.3429–3434.

Vitelli, F. et al., 2003. TBX1 is required for inner ear morphogenesis. *Human Molecular Genetics*, 12(16), pp.2041–2048.

Wang, B. et al., 2012. The T Box Transcription Factor TBX2 Promotes Epithelial- Mesenchymal Transition and Invasion of Normal and Malignant Breast Epithelial Cells. *PloS one*, 7(7), p.e41355.

Wang, Y., Blandino, G. & Givol, D., 1999. Induced p21waf expression in H1299 cell line promotes cell senescence and protects against cytotoxic effect of radiation and doxorubicin. *Oncogene*, 18(16), pp.2643–9.

Wei, J. et al., 2010. p21WAF1 / CIP1 gene transcriptional activation exerts cell growth inhibition and enhances chemosensitivity to cisplatin in lung carcinoma cell. *BMC Cancer*, 10(1), p.632.

Wilson, V. & Conlon, F.L., 2002. The T-box family. *Genome biology*, 3(6), p.REVIEWS3008.

Winters, Z.E. et al., 2003. Cytoplasmic p21WAF1/CIP1 expression is correlated with HER-2/ neu in breast cancer and is an independent predictor of prognosis. *Breast cancer research : BCR*, 5(6), pp.R242–9.

Wu, Q. et al., 2002. Transcriptional regulation during p21-induced apoptosis in human ovarian cancer cells. *Journal of Biological Chemistry*, 277(39), pp.36329 –36337.

Wu, Z. et al., 2011. Anti-cancer effects of p21WAF1 / CIP1 transcriptional activation induced by dsRNAs in human hepatocellular carcinoma cell lines. *Nature Publishing Group*, 32(7), pp.939–946.

Xia, W. et al., 2004. Phosphorylation/cytoplasmic localization of p21Cip1/WAF1 is associated with HER2/neu overexpression and provides a novel combination predictor for poor prognosis in breast cancer patients. *Clinical Cancer Research*, 10(11), pp.3815–3824.

Xia, X. et al., 2011. Cytoplasmic p21 is a potential predictor for cisplatin sensitivity in ovarian cancer. *BMC Cancer*, 11(1), p.399.

Xiong, Y., Zhang, H. & Beach, D., 1992. D type cyclins associate with multiple protein kinases and the DNA replication and repair factor PCNA. *Cell*, 71(3), pp.505–14.

Xu, H. et al., 2004. Tbx1 has a dual role in the morphogenesis of the cardiac outflow tract. *Development*, 131(13), pp.3217–3227.

Yagi, H. et al., 2003. Role of TBX1 in human del22q11 . 2 syndrome. *Mechanism of disease*, 362, pp.1366–1373.

Yamashita, S. et al., 2006. Chemical genomic screening for methylation-silenced genes in gastric cancer cell lines using 5-aza-2'-deoxycytidine treatment and oligonucleotide microarray. *Cancer science*, 97(1), pp.64–71.

Yang, X.R. et al., 2009. T (brachyury) gene duplication confers major susceptibility to familial chordoma. *Nature genetics*, 41(11), pp.1176–8.

Yano, T. et al., 2011. Tara up-regulates E-cadherin transcription by binding to the Trio RhoGEF and inhibiting Rac signaling. *The Journal of cell biology*, 193(2), pp.319–32.

Yarosh, W. et al., 2008. TBX3 is overexpressed in breast cancer and represses p14 ARF by interacting with histone deacetylases. *Cancer research*, 68(3), pp.693–9.

Yi, C. et al., 2012. MiR-663, a microRNA targeting p21, promotes the proliferation and tumorigenesis of nasopharyngeal carcinoma. *Oncogene*, 31, pp.4421–4433.

Yu, J. et al., 2010. Epigenetic inactivation of T-box transcription factor 5, a novel tumour suppressor gene, is associated with colon cancer. *Oncogene*, 29, pp.6464–6474.

Zaragoza, M. V et al., 2004. Identification of the TBX5 transactivating domain and the nuclear localization signal. *Gene*, 330, pp.9–18.

Zhang, Y., Fujita, N. & Tsuruo, T., 1999. Caspase-mediated cleavage of p21 Waf1 / Cip1 converts cancer cells from growth arrest to undergoing apoptosis. *Oncogene*, 18, pp.11131–1138.

Zhang, Z., Huynh, T. & Baldini, A., 2006. Mesodermal expression of Tbx1 is necessary and sufficient for pharyngeal arch and cardiac outflow tract development. *Development (Cambridge, England)*, 133(18), pp.3587–3595.

Zhou, B.P. et al., 2001. Cytoplasmic localization of p21Cip1/WAF1 by Akt-induced phosphorylation in HER-2/neu-overexpressing cells. *Nature Cell Biology*, 3(3), pp.245–252.

Zhu, W. et al., 2003. Methylation of Adjacent CpG Sites Affects Sp1 / Sp3 Binding and Activity in the p21 Cip1 Promoter. *Molecular and Cellular Biology*, 23(12), pp.4056–4065.

Zirbes, T.K. et al., 2000. Prognostic impact of p21/waf1/cip1 in colorectal cancer. *International journal of cancer. Journal international du cancer*, 89(1), pp.14–8.

Zong, M., Jia, L. & Li, L., 2013. Expression of novel tumor markers of pancreatic adenocarcinomas in intrahepatic cholangiocarcinomas. *OncoTargets and therapy*, 6, pp.19–23.

Zong, M., Meng, M. & Li, L., 2011. Low Expression of TBX4 Predicts Poor Prognosis in Patients with Stage II Pancreatic Ductal Adenocarcinoma. *International journal of molecular sciences*, 12(8), pp.4953–63.

6. Appendix

6.1. Plasmid Constructs

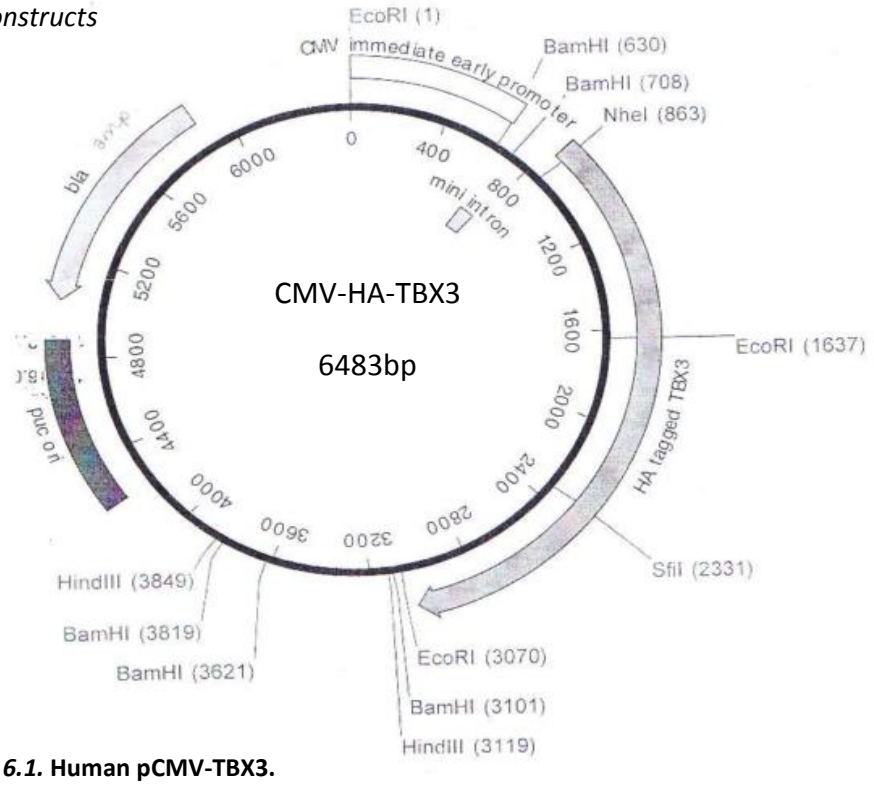

Appendix figure 6.1. **Human pCMV-TBX3.**

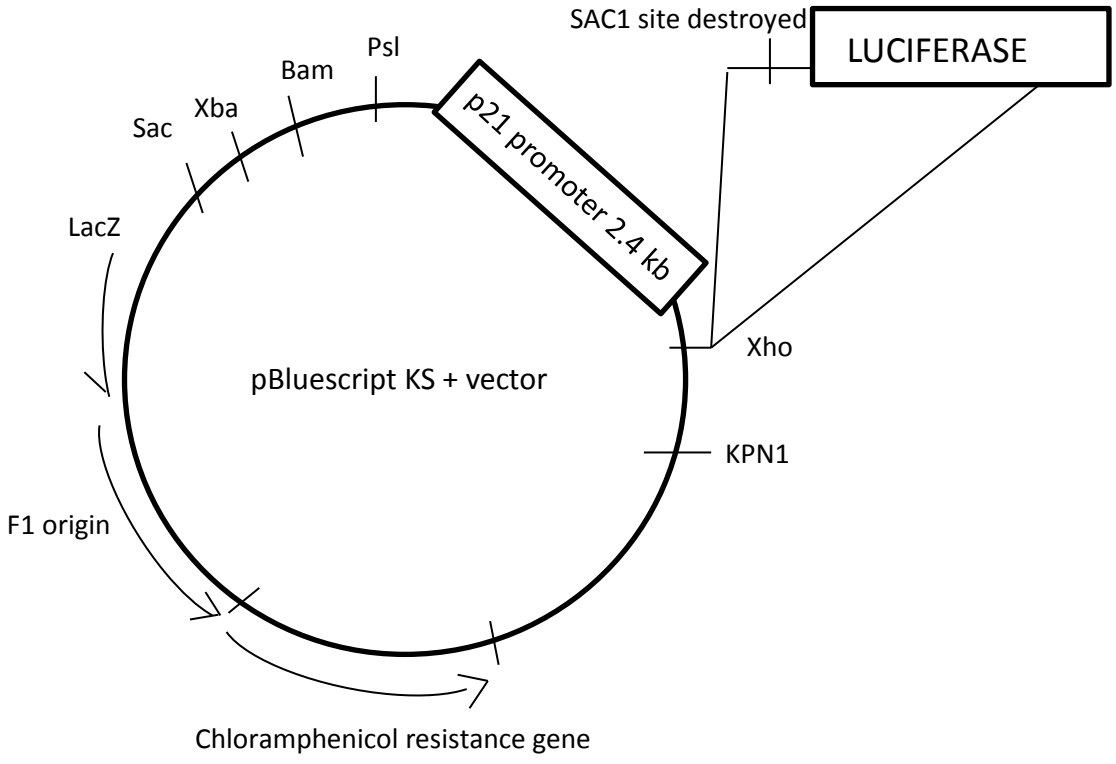

Appendix figure 6.2. **Human p21-luc.**

6.2. *Site-directed mutagenesis, mini-preparation and maxi-preparation to generate pCMV TBX3 S190A/E mutant constructs*

1% Agarose gel
0.5g agarose
50ml 1 X TBE (Tris-Borate-EDTA)
4µl Ethidium Bromide (EthBr)
Heat solution to dissolve the agarose, cool and add the EthBr. Pour gel and allow to set.

Luria Broth (LB)
10g Bacto Tryptone
5g Bacto Yeast
10g Sodium Chloride
Make up to 1L with dH_20 and autoclave

LB Agar
1.5% agar
Add 15g Agar to 1L LB

Ampicillin LB Agar plates
Ampicillin (100µg/ml) is added to LB agar, the solution poured into bacterial dished and allowed to set at room temperature.

6.3. *Cell culture*

Dulbecco's modified Eagle's medium (DMEM)
13.38g DMEM
3.7g $NaHCO_3$
Make up to 1L with sterile dH_2O and adjust pH to 7.4
Filter sterilize (0.22µm) and store at 4°C

Mycoplasma test mounting fluid
20 mM Citric acid
55 mM Na2HPO4.2H2O
50% Glycerol
pH to 5.5 and store at 4°C

6.4. *Protein isolation and western blot analysis*

2 X Boiling Blue: 10ml
1M Tris-HCL ph 6.8
4ml 10% SDS
1ml β-mercaptoethanol
2ml glycerol
1.75ml dH_2O
Pinch of bromophenol blue
Store at -20°C

5 X Protein loading dye
10% glycerol
1% SDS
0.25M Tris-Cl pH 6.8
3mg Bromophenol blue

Sodium Dodecyl Sulphate (SDS)-polyacrylamide gels
Resolving gel:
Acryl-bisacryl-amide mix (30:08) (percentage depending on size of protein of interest)
0.375 M Tris (pH 8.8)
0.1% SDS
0.01% TEMED (tetramethylethylenediamine)
0.1% Ammonium persulphate

Stacking gel:
5% Acryl-bisacryl-amide mix (30:08)
0.192 M Tris (pH6.8)
0.1% SDS
0.01% TEMED
0.1% Ammonium persulphate

Acryl-bisacryl-amide mix (30:08):
29 g acrylamide
1g N,N`-methylenebisacrylamide
Make up to 100 ml, heat at 37°C to dissolve chemicals. Store at 4°C, protected from light

10% Ammonium persulphate (APS)
0.1g ammonium persulphate
Make solution up to 1ml with dH_20
Store at 4^oC

10% Sodium docecyl sulphate (SDS)
100g SDS
Make up to 1L with dH_20, pH to 7.2 and store at room temperature

10 X Running buffer
10g SDS
30g Tris
144g Glycine
pH to 8.3 and make solution up to 1L with dH_20
For use dilute to 1 X (100ml 10X PBS; make up to 1L with dH_20)

10 X Transfer buffer
38g Tris
144g Glycine
Make solution up to 1L with dH_20 and store at 4^oC
For use dilute 1 X (100ml 10 X Transfer Buffer, 200ml Isopropanol and 700ml dH_20)
Store at 4°C

10 X Phosphate Buffer Saline (PBS)
80g NaCl
26.8g $Na_2HPO_4.12H_20$
2g KCl
2.4g KH_2PO_4
Make up to 1L, pH to 6.9 and autoclave
For use dilute to 1 X (100ml 10X PBS; make up to 1L with dH_20)

PBS/Tween:
For membrane washes, add 0.1% Tween to 1X PBS

5% blocking buffer
5% powder milk (w/v)
Make up to 100ml with 1 XPBS/0.1% Tween-20
Store at 4°C

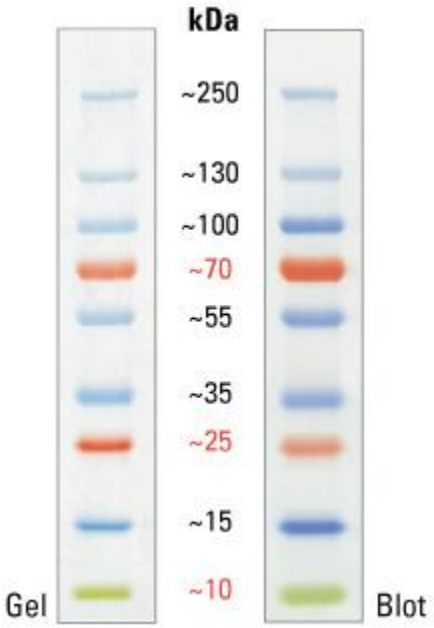

Appendix figure 6.3. **PageRuler Prestained Protein Marker (Fermentas).**

6.5. *Electrophoretic mobility shift assay*

8% polyacrylamide gel
30% acrylamide
10 X TBE
10% APS
TEMED

Cell Buffer A
10mM Hepes, pH 8
1.5mM MgCl2
10mM KCl

0.1% Triton X-100
1mM DTT

Cell Buffer B
20mM Hepes, pH 8
1.5mM MgCl2
420mM NaCl
25% glycerol
0.2mM EDTA

RIPA
150mM NaCl
1% Triton X-100
0.1% SDS
20mM Tris (pH 7.5)
1% deoxycholate

5X incubation buffer
100mM Hepes, pH 7.9
250mM KCl
5mM MgCl2
1mM EDTA, pH 8
20% Ficoll

10 X loading dye
0.25% Bromophenol blue
0.25% xylene cyanol FF
15% Ficoll

Blocking buffer
3% bovine serum albumin
1 X PBS/T (0.1%)

Wash buffer
1 X PBS/T (0.1%)

Equilibration buffer:
1 X PBS

6.6. *ChIP*

NCP Buffer 1
10mMEDTA
0.5mM EGTA
10mM HEPES pH 6.5
0.25% Triton-X

NCP Buffer 2
1mM EDTA
0.5mM EGTA

10mM HEPES pH6.5
200mM NaCl

Lysis buffer
10mM EDTA
50mM TrispH 8.1
1% SDS
0.5% Triton-X
Protease inhibitors were added before use:
1X complete protease inhibitor tablets (Roche, Germany), aprotinin (1µg/ml), pepstatin (1µg/ml), phenylmethanesulphonyl fluoride (PMSF) (0.5mM)

RIPA-IP buffer
2mM EDTA
150mM NaCl
20mM Tris pH 8.1
1% Triton-X
Protease inhibitors were added before use:
1X complete protease inhibitor tablets (Roche, Germany), aprotinin (1µg/ml), pepstatin (1µg/ml), phenylmethanesulphonyl fluoride (PMSF) (0.5mM)

Wash buffer 1
2mM EDTA
20mM Tris-Cl pH 8.1
0.1% SDS
1% Triton X-100
150mM NaCl

Wash buffer 2
2mM EDTA
20mM Tris-Cl pH 8.1
0.1% SDS
1% Triton X-100
500mM NaCl

Wash buffer 3
1mM EDTA
10mM Tris-Cl pH 8.1
250mM LiCl
1% sodium deoxycholate
1% Nonidet P-40

Wash buffer 4
1mM EDTA
10mM Tris-Cl pH 8.1

Extraction buffer
1% SDS
0.1M $NaHCO_3$
Made up with Wash buffer 2

6.7. DNA-affinity immunoblot assay

2 X bead binding and wash buffer
10mM Tris-HCL (pH 7.5)
1mM EDTA
2M NaCl
0.1% Tween-20

EMSA binding buffer
20mM Tris-HCL (pH 7.6)
50mM NaCl
1mM MgCl2
0.2mM EDTA
5% glycerol
0.5mM DTT
2µg poly(dI-dC) per reaction